5-2021

Investigating microbial genes involved in plant colonization and the effects on plant microbiome assembly

David Grant
dgrant13@vols.utk.edu

To the Graduate Council:

I am submitting herewith a thesis written by David Grant entitled "Investigating microbial genes involved in plant colonization and the effects on plant microbiome assembly." I have examined the final electronic copy of this thesis for form and content and recommend that it be accepted in partial fulfillment of the requirements for the degree of Master of Science, with a major in Microbiology.

Sarah Lebeis, Major Professor

We have read this thesis and recommend its acceptance:

Sarah Lebeis, Elizabeth Fozo, Todd Reynolds, Constance Bailey

Accepted for the Council:
Dixie L. Thompson

Vice Provost and Dean of the Graduate School

(Original signatures are on file with official student records.)

Investigating microbial genes involved in plant colonization and the effects on plant microbiome assembly

A Thesis Presented for the
Master of Science
Degree
The University of Tennessee, Knoxville

David L. Grant
May 2021

DEDICATION

To the village of people that it took for me to make it here.

To my family and friends who have been with me every step of the way.

To Madison who has been a source of comfort, support, and balance.

And to God, who made all of this possible and saw me through to the end.

John 6:68

Daniel 3:18

ACKNOWLEDGEMENTS

I am thankful to God, who gave me this opportunity to know and work alongside some amazing people. I thank the people who got me to where I am and who have been so supportive and kind through this process. I think a lot about how I even ended up doing this work, be it a deterministic or stochastic process, and I realize how fortunate I am to have been led here.

I first thank Sarah. There are not enough good things to say about Sarah as a mentor and as a friend. Her kindness, which trumps even her niceness, is an inspiration of how to treat others. She is steadfast and generous with her time, there have been so many instances where I have been overwhelmed and she has been there to help. She is challenging and has the highest level of precision of anyone I know, which is why I consider her such a great scientist. I'm grateful that she let me join her lab as an Undergraduate so that I would find myself here all these years later.

I thank my family and friends, who have always been there for me. While they may have to ask me what it is that I actually do all the time, I'm grateful to have them as a support and to know they have always been behind me. The support from my mother and father, financially and just being supportive has been invaluable.

I thank my coworkers (both past and present) and the people I get the privilege of seeing every day. To Sarah Stuart, Bridget, Alexandra, and Katherine, you guys are the Lebeis lab for me and I could not have picked better people to work alongside.

I'm thankful to my committee members: Liz, Todd, Constance, and Sarah. You were all a huge encouragement, and you made this a good experience. I appreciate the insight you gave me and how you've helped me to grow as a scientist and as a person. I'm glad to have had you all to bug during this process.

And of course, I thank my beautiful Madison. This is generally the point where I get anxious about the future but with you, I don't have to be. I know that you are with me as comfort and support. You are present and strong-willed and have given me so much strength to push through to the end. I love you and I'm grateful that you've been with me through the entirety of this journey.

ABSTRACT

The use of chemical fertilizers and pesticides has had negative impacts on ecological systems and alternatives will be needed to both enhance agricultural production and remediate waste that has accumulated via fertilizer use. A promising alternative to tackle both problems utilizes beneficial organisms in microbial communities associated with plants, which are known as bioinoculants. However, the benefits of bioinoculants are inconsistent in field application and require more research in order to harness them in ways to make them a suitable replacement for chemical fertilizers. Here, I investigate characteristics required to enhance bioinoculant efficiency, including mechanisms required to increase microbial colonization of plants. Specifically using soil-dwelling *Streptomyces* species with Arabidopsis hosts. Also, I investigate means of enhancing bioremediation ability of an aquatic plant, Duckweed, by adding specific duckweed associated bacteria. The goal is to harness microbial potential to a point of suitable replacement for harmful chemical compounds currently used in agriculture and to enhance remediation potential of an aquatic plant organism using microbial inoculum. Thereby, benefiting human population sustainability with clean and effective means for agricultural yield.

TABLE OF CONTENTS

LIST OF TABLES

LIST OF FIGURES

CHAPTER ONE: INTRODUCTION

Microbial Populations and Communities

Microorganisms can be found almost anywhere on Earth where they play key functional roles to support other life within their respective ecosystem [1]. The immense diversity in individual microbial genomes enables certain specificity for environments to be ideal for each specific organism. While some microbes thrive in a warm soil environment, others prefer a cold ocean floor. In each case, the organism's genetic make-up that has developed over time enables the organism to survive in a given niche and the ensuing distribution of microbial life [2]. Generally, the main predictors for an organism's niche are nutrient availability and subsequent metabolism [3]. However, as more and more microorganisms congregate together in their ideal niche, a community, termed microbiome, is created that adds another level of complexity beyond nutrient use. With the presence of other microbes, changes occur in microbial gene expression that can result in cooperative or competitive behavior across members as each organism seeks to enhance its own fitness within the community [4]. These interactions then drive community assembly, causing the ultimate formation of a microbiome. The result is a functional microbiome, which is a key contributor to its ecosystem, including key roles in biochemical nutrient cycling and in decomposition of organic matter [5].

One such system for microbiomes that has been investigated more and more frequently is that which involves host organisms. The collection of microbes that live in a close association with a host organism have far-reaching impacts on host health, across numerous different systems and with varying complexities. For instance, in *Drosophila*, microbiomes can consist of 5-20 species that reside within the fly's gut and effect lifespan and fitness [6, 7]. In the human gut, the microbiome can be upwards of 400 species and aid in digestion and complex carbohydrate breakdown, thus helping to provide nutrients to their host [8, 9]. The composition of these microbiomes can be widely diverse across individuals and can include pathogenic, commensal and beneficial microbial members that drastically impact their respective host's health [10]. In host-microbiome systems, there are two major types of interactions that establish

microbial membership. The first interaction is between the host and the microbes (host-microbiome) and covers the indirect and direct means of control on a host selecting microbial members for its community. The second interaction is between the microbes within the community and how they interact with one another while they inhabit similar niches around the host organism. Both of these interactions are crucial in understanding the complexities within microbial community assembly with a host.

Like the above hosts, plant microbiomes play key functional roles within the plant's health. Within a plant microbiome, there is a collection of beneficial, commensal and pathogenic microbes present that can affect the plant [11]. The benefits that individual microbes can impart to a plant host include stress resistances against drought, heat, soil salinity and aid in phosphate solubilization [12-14]. In return, hosts provide nutrients along with a stable environment and suitable niches for its microbial members to reside [15, 16]. Increasing research has identified that the benefits imparted to a plant host are largely due to microbial members collectively as opposed to individual members [11]. Thus, shifting the focus from individual microbial member recruitment to overall community assembly. To ensure that a microbiome contains beneficial members in their microbiome, plants have numerous systems in place to exert control over assembly. For instance, the plant immune system can shape the microbial community to inhibit pathogenic bacteria from invading [17]. Similarly, plant metabolism can drive community assembly by selecting for specific microbial members based on nutrient availability [16]. However, much is still unknown about the community assembly process that establishes a plant microbiome. Given the impact that a microbiome has on its plant host, it is necessary to untangle the roles of microbial membership and function in the community.

Plant Microbiome Assembly

The plant microbiome is of great interest due to its effects on plant health which is necessary in agriculture and human population sustainability. Individual plant species play host to a vast array of microbial organisms in soil, aquatic, and terrestrial

ecosystems, and the resulting interactions often have large impacts on both the plant host and on the individual microbial member in association. Terrestrial plants are sessile organisms, meaning they are permanently anchored in their spot of germination and are dependent on their environment for nutrients, water, and bacterial inoculum. Likewise, plants are affected by the abiotic and biotic stresses that occur within their environment without the ability to escape. To combat this, plants have developed mechanisms and responses in order to maintain stability even in poor conditions [18]. Many of these responses take advantage of the plant's assembled microbiome that is supplied by water, air, and soil sources [18-20].

As a system, plants are generally divided into two major parts: the above-surface portion (i.e., the phyllosphere) and the below-ground root portion. The below-surface root portion acts as a large reservoir of microbial diversity in terrestrial and aquatic systems [21]. As plant roots grow throughout diverse bulk soil or water sources, they come into contact with numerous unique microbial species. However, the mechanisms behind how these microbes are recruited to a plant host and the ensuing interactions that occur with the community at large are not fully understood. As microbes from different sources accumulate, they begin not only interacting with the plant but also with other microbial members that they come into contact with. Beyond that, there are numerous environmental factors that affect microbial composition, including soil pH, salinity, and water supply [22]. The collection of microbes that ultimately associate within and around a plant's below-ground tissue, the root microbiome, is accordingly a complex web of interactions between both plants and microbes as well as between microbial members. A large area of study has thus emerged to characterize constituents of the root microbiome and its impact on a plant host and to untangle the complex interactions in belowground environments.

The high complexity of interactions between a plant and microbes within a plant system makes it difficult to tease apart individual interactions from one another. On top of that, without knowledge of genetic elements in play between microbes and hosts it is

increasingly difficult to make sense of what interactions are occurring. To help alleviate this issue, studies that investigate the plant microbiome often focus on the flowering plant and model system, *Arabidopsis thaliana* (Arabidopsis). Arabidopsis has many advantages in a controlled laboratory environment, with short generation times, a high number of offspring produced and self-pollination, avoiding an introduction of genetic diversity common in sexual reproduction [23]. In addition, Arabidopsis is a diploid organism that has a small, well-characterized genome with easily accessed tools, datasets, databases, and previously generated mutants [24]. For many of these reasons, Arabidopsis was the first plant to have its microbiome defined using 16S rRNA gene amplicon sequencing studies [25, 26]. Further, immense effort is continually put into developing additional genetic resources and in further characterizing gene functions [27]. Here, I also use the aquatic plant system, *Lemna minor* (Duckweed), in microbiome studies. Duckweed is a monocot, simple and small flowering plant that floats on water surfaces [28]. The aquatic plant grows best in stagnate fresh but can also grow in brackish water environments [29]. Like Arabidopsis, Duckweed reproduces quickly and is well-studied in the literature, with genetic transformation protocols already established [30, 31]. Both systems provide avenues for microbiome research while providing different hosts and implications for research. Therefore, they work as effective models for observing plant-induced root microbiome dynamics and for working phyllosphere and root systems.

Within a below-ground plant root system, there is a gradient of microbial communities that associate with the plant; from the bulk soil or ambient water, which is away from the plant and only minimally affected by any plant-microbe interface, to the rhizosphere, the area directly influenced by plants via alterations in chemistry and exudate profiles, and finally, to within the plant root itself in an area called the endophytic compartment (EC) [25, 32, 33]. Advances in sequencing technology allowed us to obtain a more accurate picture of which microbes are commonly found within these distinct microbiomes. For instance, 16S rRNA gene and internal transcribed spacer (ITS) region amplicon sequencing differentiate bacterial and fungal taxa present

in leaf and root samples [34]. Due to the greater abundance of knowledge of the bacterial members present; their role will be focused on here. Generally, amplicon studies show that along the gradient from bulk soil to the EC, the microbiome membership changes significantly, especially within the EC [25]. The shift in communities is known as the “rhizosphere effect”, and it describes the changes in community structure for both the rhizosphere and EC compared to bulk soil [35]. The rhizosphere effect occurs in numerous plant species and is comparable for taxa between Arabidopsis and other plant species in the EC and is slightly decreased for Arabidopsis in rhizosphere communities [35].

Most taxa found within the plant microbiome fall into four phyla: Actinobacteria, Bacteroidetes, Firmicutes, and Proteobacteria [25, 26]. A majority, over 60%, of the taxa in the Arabidopsis microbiome have cultured representatives to use in laboratory settings [36]. While Actinobacteria are not usually the most abundant taxa in soil and rhizosphere environments, they exhibit increased relative abundance in the EC compared to the external communities [25]. Another example of EC colonizing bacteria are Proteobacteria, which are generally the most abundant phylum in plant tissue but are more variable depending on family level [25]. This prompts investigation into why certain microbes establish themselves in such a close association with plants while other microbes are unable to do so. Specifically, what genes are present within these organisms? Consequently, how might the organisms that possess them subsequently impact the overall microbiome community structure? Highlighting these genes and their functions is important because it allows us to identify which organisms might have the greatest effects on the health of the plant host and the surrounding community structure [22]. Furthermore, by understanding these community dynamics, we can better predict which microbes can establish themselves with the plant. In this way, tuning microbiomes to include beneficial microbes that work synergistically to be more effective at positively enhancing plant health and biomass yield [37, 38].

Applications of Plant Microbiomes in Industry

The use of chemical fertilizers and pesticides has increased since their creation in the 19th and 20th century for large-scale agricultural use [39, 40]. By industrializing agriculture using fertilizers and pesticides, the human population has sustained increasing food requirements and protected crops from disease, including the production and health of required fruits and vegetables necessary in a human diet [39]. The green revolution brought about a dramatic increase in crop production while keeping land use at a sustainable mark using chemical products and advancements [41]. While the benefits to this technology cannot be understated, the use of pesticides and other chemical fertilizers is becoming an increasingly undesirable means of enhancing crop yield.

Due to negative impacts on human and environmental health, it is all the more urgent to find alternative means of increasing crop yields in a safe and efficient way [42]. Similarly, it is important to find ways to remediate current waste build up from current agricultural practices. One such way that is becoming more and more enticing is the use of bioinoculants and bioremediation, as microbial metabolism is capable of providing hosts with important nutrients. Bioinoculants leverage a microbial community in order to produce a desired phenotype within a plant host; for crop yield it would be increased plant growth promotion. However, many bioinoculants today are inconsistent, which suppresses their widespread application [43]. In this way, it is important to better understand the multiple aspects that must be considered when putting together a bioinoculant: the microbes need to be able to persist and survive within the community, they need to be robust colonizers to interact with the plant, and they need to produce the desired phenotype within the plant host (Figure 1.1) [12, 42].

While many growth promoting characteristics of particular microbes have been identified, including auxin production, nitrogen fixation, and phosphate solubilization, it is imperative that these beneficial microbes be able to establish themselves effectively within the plant microbiome [44]. For this reason, organisms possessing genes that

allow them to become endophytic, within plant tissue, are very promising for inclusion in a bioinoculant strains [45]. Also, of equal importance is that the organism is able to adapt and survive within a dynamic community, and perhaps carry some role in community assembly. While an individual microbe can have some effect, the overall community must be considered when creating a viable bioinoculant product. For that reason, it is imperative to identify what genes are growth promoting, what genes help in robust colonization, and the impact that an organism has on the microbial community at large and is impacted by (Figure 1.1). The objective of this thesis is to better understand these complex dynamics and make more efficient the use of bioinoculants for large-scale agricultural purposes. In this way, we aim to reduce fertilizer usage while maintaining agricultural efficiency by studying bioinoculant characteristics in an Arabidopsis system with *Streptomyces* organisms. Also, we look to find ways to alleviate current waste accumulation by investigating the bioremediation of fertilizer pollution using a duckweed system with associated duckweed bacteria. When fertilizers are used too liberally and runoff into aquatic systems, they dump phosphorus and nitrogen into the water [46]. Excess phosphorus and nitrogen can then lead to a dramatic increase in microbial growth, leading to eutrophication and the overgrowth of harmful algae and cyanobacteria that deplete dissolved oxygen in the system [47]. To counter this, Duckweed takes up excess nitrogen and phosphorus which makes it a possible solution to eutrophication caused by fertilizer runoff [48].

Plant-Microbe Interactions

Apart from determining beneficial microbial genes for plant growth, the first key to generating more efficient bioinoculants is determining what genes are associated with robust colonization. A major issue with bioinoculant products is that they often perform inconsistently in field systems, largely due to the lack of knowledge about what genes establish these microbes within the system [49]. Two of the major factors involved in successful colonization are the plant exudates responsible for microbial recruitment and the microbial genes that aid in colonization. As plants fix atmospheric carbon, they secrete significant quantities, upwards of 20-50%, as root exudates that can act as

carbon sources and change the chemical composition of soil, ultimately affecting characteristics of soil and microbial capability to establish within the rhizosphere [50-52]. On the microbial side, microbes within the rhizosphere can alter plant root exudate as noted in a study that showed *Bacillus* strains that induced the exudation of acylsugars from a plant host [50]. Bacteria with mutations in carotenoids and genes with homology to ATP-binding cassette (ABC) transporters show decreased levels of colonization, indicating some potential with specific genes and colonization capability [53]. ABC transporters have been linked to signaling between microbial and plant cells, highlighting a two-way communication between microbial and plant cells [54]. For this research, of utmost interest is what is present on the microbial side that plants are selecting for with root exudates or that is enabling enhanced survival within the system.

There are numerous alterations to plant physiology following microbial colonization [55]. Microbes biosynthesize and release phytohormones and other compounds that can act directly or indirectly on a plant host [56]. Specifically, microbial production of auxins, cytokinins, and N-*acyl*-L-homoserine lactones that can be perceived by plant hosts and act as signaling molecules [56]. In response to a microbial sign, such as phytohormones, microbe-associated molecular patterns, or volatile compounds, plant physiology and exudate composition affected [56]. Furthermore, a subset of microbes that colonize the EC subsequently prime the plant immune system, which effects other microbes within a community, most importantly pathogens. Thus, when a pathogen is introduced into the system, a primed immune system can help aid in an effective plant response to detrimental bacteria [57]. Therefore, of greatest interest are those microbes that can associate within the EC, as they show a great potential for beneficial alterations in plant physiology.

Among microbes with enhanced EC colonization compared to rhizosphere abundances, *Streptomyces* from Actinobacteria show promise for determining gene-specific causes of colonization phenotypes. Initial investigation of *Streptomyces* strains showed significantly different levels of colonization across strain within the genus, with

2-3 log differences in root and seedling colonization [58]. *Streptomyces* are Gram-Positive, filamentous bacteria that are generally found residing in soils and consistently associated with plant hosts. Additionally, members of this taxa can induce plant defense systems while maintaining a symbiotic relationship with the plant host [59]. However, while the relationship between particular *Streptomyces* and plant hosts has been observed, the genetic factors that result in the relationship are not well known. In addition, *Streptomyces* generally boast large metabolic profiles and secondary metabolic products, providing a large genomic repertoire for investigation [60, 61]. Consequently, a deep dive into *Streptomyces* genetics could uncover factors associated with robust colonization and strong plant-microbe relationships.

Of note are pigment producing genes discovered in *Streptomyces* strains that produce melanin. Melanin is a brown-black pigment that results from the enzyme catalyzed oxidation of phenolic compounds, which are compounds present in rhizosphere environments [62-64]. In a rhizosphere environment, phenolic compounds have the ability to induce reactive oxygen species (ROS) and plants may secrete them as exudates against pathogens for defense [65]. Phenolics are also involved in plant development and in plant-microbe signaling [66, 67]. In this way, melanin identifies itself as a potentially beneficial compound in the colonization of plant tissue. Melanin also establishes a direct link in plant-microbe interactions and provides an ideal starting point in genome searching of these organisms.

Beyond *Streptomyces*, there are numerous other plant associated organisms that prompt further investigation into other pigment producing genes that may affect plant root colonization in other isolates present in a synthetic community (SynCom) previously investigated [58]. One of note is a carotenoid produced in a Proteobacteria, *Brevundimonas* sp. 374, which is another robust colonizer when monoinoculated with *Arabidopsis thaliana,* that creates bright orange colonies. Carotenoids are pigments with observed photoprotective and antioxidant capabilities, a function notable in melanin, as well [62, 68, 69]. Furthermore, carotenoid deficient *Pantoea* sp., another Proteobacteria,

show significant decreases in *Arabidopsis thaliana* root colonization that may be linked to rhizosphere survival or in root association [69]. The carotenoid deficient *Pantoea* also showed an altered membrane organization, highlighting its potential indirect role in survival [70]. Between melanin and carotenoid pigments, we observe noteworthy genes as starting places to investigate what genetic elements may be predictors of robust root colonization, thus, helping to support one requirement for efficient bioinoculant use.

Microbe-Microbe Interactions

Beyond genes that play a role in plant root colonization, it is equally important to understand the effect of colonization on subsequent community assembly. As certain isolates associate with a plant host, changes can occur in how the plant host interacts with the environment and with other microbial isolates in the soil [14]. A recent study in plant-growth-promoting-bacteria (PGPB) found that certain rhizobacteria even enhance the association of PGPB with a plant host [71]. Therefore, it is a great resource to the understanding of microbiome research to understand the assembly process. One area of interest is again with the colonization of *Streptomyces* species and how they impact microbiome assembly. For instance, a study on Gray mold in grapevines showed a *Streptomyces'* ability to stimulate the plant's immune system against perceived pathogens, thus indicating some indirect control over community assembly [72]. While *Streptomyces* seem to carry robust colonization capabilities, they also seem to carry a high potential for interacting with other microbial members of a community both by direct and indirect methods. This interaction capability is mostly due to the large metabolic potential of these microorganisms and the impact that *Streptomyces* have in priming plant defenses [72]. However, where these capabilities come from and to what extent the impact the other organisms within the system is largely unknown. The ability of *Streptomyces* to colonize is the first step in their establishment into a community and to have any ability to shape it. There is a gap in our understanding of what mechanisms *Streptomyces* employ either directly or indirectly on other microbial community members to shape the root microbiome.

Beyond Arabidopsis, another system that shows promise in further understanding plant-microbe and microbe-microbe interactions is duckweed and a culture collection of duckweed associated bacteria (DAB). Duckweed microbiomes are taxonomically comparable to Arabidopsis leaf microbiomes, including Proteobacteria, Actinobacteria, Firmicutes, and Bacteroidetes members [73]. The similarity of Duckweed and Arabidopsis microbiomes highlights the comparable nature and connections between the two plant systems [73]. Duckweed is a potential tool for the treatment of wastewater and in fertilizer pollution remediation for its ability to grow quickly and take up phosphorus and nitrogen from the environment, especially in developing countries as a cost-effective approach [48, 74, 75]. However, the efficiency of duckweed largely depends on environmental conditions, many of which are not fully understood [76]. To counter negative environmental conditions, the manipulation of the duckweed microbiome, including many beneficial bacteria, improves efficiency and helps stabilize duckweed productivity in wastewater [77]. Previous work shows the role of indoles, a phytohormone, and similar compounds as active agents in the associations that form between bacteria and duckweed [78]. These compounds show plant growth promoting characteristics, hereby affecting duckweed physiology, and are produced by a number of DAB [78]. By adding different specific DAB to duckweed, it is possible to observe shifts in wastewater microbiomes and duckweed growth. The goal is a system in which changes in microbiota inoculated in duckweed lead to a subsequent decrease in toxic environmental factors and a decrease in harmful pathogenic bacteria found in wastewater. Hence, this system creates the holistic picture of growth promoting microbes with robust colonization and a picture of how they affect community assembly and are affected by community composition. It also provides a means of aiding in environmental bioremediation using an easily acquired organism.

Conclusions

The goal of this work is to advance our understanding of plant root microbiome establishment and the interactions that occur during the assembly process. To do this, I investigated bacterial genes in plant-associated isolates that may impact their

colonization characteristics, specifically pigments. Also, I investigated what affect the colonization of such isolates has on the subsequent colonization of other microbes. Together these studies will define mechanisms for plant-microbe and microbe-microbe interactions during plant microbiome assembly. As Earth's population continues to increase and climate change alters our capability to have sustainable agriculture, it is important to find alternative means of producing higher crop yield. While bioinoculants and growth promoting bacteria are a part of the equation, microbes containing these genes are not necessarily associated with successful plant colonization [15]. For this reason, it is necessary to determine both what genes lead to robust colonization and what genes lead to plant growth promotion so that the coupling of these two things may enhance crop yields. Additionally, it is important to identify community involvement as further predictors because how a potential bioinoculant survives and thrives in an environment will also depend on the community at large and the supporting cast present.

The studies performed here are an important progression in determining what characteristics predict plant colonization and community assembly and provide future avenues in manipulating these characteristics to improve bioinoculant efficiency and agriculture production. Using a controlled plant system that excludes environmental factors that would occur in nature helps to simplify and effectively seek out these answers. Likewise, soil is a very diverse and complex environment that is not easily translated directly into a controlled laboratory setting. Many of the microbes present in soil environments are not culturable in a laboratory setting and cannot be accounted for in controlled experiments. However, understanding the complex issues before us requires teasing apart the multifaceted layers of microbial and plant interactions, and I believe I have done so to push our knowledge forward. By doing so, we equip ourselves to better safeguard plant food production by stimulating growth and protecting plant host health.

My work contributes to our understanding of how high the potential is of microbes in establishing safe and natural alternatives to modern problems. The diversity in microbial organisms is astounding and makes their uses seemingly endless for humans. The use of microbes as a safe and effective way to enhance agricultural yield and bioremediation shows such promise given what we now know and gives hope not only for cleaner operations in the future but also in helping reduce waste of the past. The work that I have done here is important in understanding characteristics necessary for enhanced bioinoculant activity and in the efficacy of bioremediation using plant-microbe systems. More work will need to be done for establishing community level dynamics so that communities may be assembled to optimize beneficial phenotypes to plant hosts.

REFERENCES

1. Prosser, J.I., et al., *The role of ecological theory in microbial ecology.* Nature Reviews Microbiology, 2007. **5**: p. 384-392.
2. Macalady, J.L., et al., *Energy, ecology and the distribution of microbial life.* Philosophical Transactions of the Royal Society B, 2013. **368**(1622).
3. Pereira, F.C. and D. Berry, *Microbial nutrient niches in the gut.* Environmental Microbiology 2017. **19**(4): p. 1366-1378.
4. Freilich, S., et al., *Competitive and cooperative metabolic interactions in bacterial communities.* Nature Communications, 2011. **2**(589).
5. Jiao, S., et al., *Soil microbiomes with distinct assemblies through vertical soil profiles drive the cycling of multiple nutrients in reforested ecosystems.* Microbiomes, 2018. **6**(146).
6. Gould, A.L., et al., *Microbiome interactions shape host fitness.* PNAS, 2018. **115**(51): p. E11951-E11960.
7. Ludington, W.B. and W.W. Ja, *Drosophila as a model for the gut microbiome.* PLOS Pathogens, 2020.
8. Oliphant, K. and E. Allen-Vercoe, *Macronutrient metabolism by the human gut microbiome: major fermentation by-products and their impact on host health.* Microbiome, 2019. **7**(91).
9. Lloyd-Price, J., G. Abu-Ali, and C. Huttenhower, *The healthy human microbiome.* Genome Medicine, 2016. **8**(51).
10. Haque, S.Z. and M. Haque, *The ecological community of commensal, symbiotic, and pathogenic gastrointestinal microorganisms – an appraisal.* Clinical and Experimental Gastroenterology, 2017. **10**: p. 91-103.
11. Song, C., et al., *Beyond Plant Microbiome Composition: Exploiting Microbial Functions and Plant Traits via Integrated Approaches.* 2020. **8**(896).
12. Eida, A., et al., *Genome Insights of the Plant-Growth Promoting Bacterium Cronobacter muytjensii JZ38 With Volatile-Mediated Antagonistic Activity Against Phytophthora infestans.* Frontiers in Microbiology, 2020. **11**(369).

13. Rafi, M.M., M.S. Krishnaveni, and P.B.B.N. Charyulu, *Chapter 17 - Phosphate-Solubilizing Microorganisms and Their Emerging Role in Sustainable Agriculture.* 2019: p. 223-233.
14. Fitzpatrick, C., et al., *Assembly and ecological function of the root microbiome across angiosperm plant species.* PNAS, 2018: p. E1157-E1165.
15. Souza, R.S.C.d., et al., *Genome Sequences of a Plant Beneficial Synthetic Bacterial Community Reveal Genetic Features for Successful Plant Colonization.* Frontiers in Microbiology, 2019. **10**(1779).
16. Trivedi, P., et al., *Plant–microbiome interactions: from community assembly to plant health.* Nature Reviews Microbiology, 2020. **18**: p. 607-621.
17. Teixeria, P.J.P., et al., *Beyond pathogens: microbiota interactions with the plant immune system.* Current Opinion in Microbiology, 2019. **49**: p. 7-17.
18. Žádníková, P., et al., *Strategies of seedlings to overcome their sessile nature: auxin in mobility control.* Frontiers in Plant Science, 2015. **6**(218).
19. Hartman, K. and S.G. Tringle, *Interactions between plants and soil shaping the root microbiome under abiotic stress.* Biochemical Journal, 2019. **476**: p. 2705-2724.
20. Veach, A.M., et al., *Plant Hosts Modify Belowground Microbial Community Response to Extreme Drought.* mSystems, 2020. **5**(3).
21. Maron, P.-A., C. Mougel, and L. Ranjard, *Soil microbial diversity: Methodological strategy, spatial overview and functional interest.* C. R. Biologies, 2011. **334**: p. 403-411.
22. Compant, S., et al., *A review on the plant microbiome: Ecology, functions, and emerging trends in microbial application.* Journal of Advanced Research, 2019. **19**: p. 39-37.
23. Initiative, T.A.G., *Analysis of the genome sequence of the flowering plant Arabidopsis thaliana.* Nature, 2000. **408**: p. 796-815.
24. Goodman, H.M., J.R. Echer, and C. Dean, *The genome of Arabidopsis thaliana.* PNAS, 1995. **92**(24): p. 10831-10835.

25. Lundberg, D.S., et al., *Defining the core Arabidopsis thaliana root microbiome.* Nature, 2012. **488**(7409): p. 86-90.
26. Bulgarelli, D., et al., *Revealing structure and assembly cues for Arabidopsis root-inhabiting bacterial microbiota.* Nature, 2012. **488**: p. 91-95.
27. Bevan, M. and S. Walsh, *The Arabidopsis genome: A foundation for plant research.* Genome Research, 2005. **15**: p. 1632-1642.
28. Hillman, W.S., *The Lemnaceae, or duckweeds: a review of the descriptive and experimental literature.* Botanical Review, 1961. **27**: p. 221-287.
29. Nesan, D., K. Selvabala, and D.C.J. Chieh, *Nutrient uptakes and biochemical composition of Lemna minor in brackish water.* Aquaculture Research, 2020. **51**(9): p. 3563-3570.
30. Laird, R.A. and P.M. Barks, *Skimming the surface: duckweed as a model system in ecology and evolution.* American Journal of Botany, 2018. **105**(12): p. 1962-1966.
31. Yamamoto, Y.T., et al., *Genetic transformation of duckweed Lemna gibba and Lemna minor.* In Vitro Cellular and Developmental Biology-Plant, 2001. **37**: p. 349-353.
32. Moroenyane, I., et al., *Bulk soil bacterial community mediated by plant community in Mediterranean ecosystem, Israel.* Applied Soil Ecology, 2018. **124**: p. 104-109.
33. Berendsen, R.L., C.M.J. Pieterse, and P.A.H.M. Bakker, *The rhizosphere microbiome and plant health.* Trends in Plant Science, 2012. **17**(8).
34. Bergelson, J., J. Mittelstrass, and M.W. Horton, *Characterizing both bacteria and fungi improves understanding of the Arabidopsis root microbiome.* Scientific Reports, 2019. **9**(24).
35. Schneijderberg, M., et al., *Quantitative comparison between the rhizosphere effect of Arabidopsis thaliana and co-occurring plant species with a longer life history.* The ISME Journal, 2020. **14**: p. 2433-2448.
36. Bai, Y., et al., *Functional overlap of the Arabidopsis leaf and root microbiota.* Nature, 2015. **528**: p. 364-369.

37. Trivedi, P., et al., *Tiny Microbes, Big Yields: enhancing food crop production with biological solutions.* microbial biotechnology, 2017. **10**(5): p. 999-1003.
38. Zhang, J., et al., *Harnessing the plant microbiome to promote the growth of agricultural crops.* Microbiological Research, 2021. **245**.
39. Aktar, M.W., D. Sengupta, and A. Chowdhury, *Impact of pesticides use in agriculture: their benefits and hazards.* Interdisciplinary Toxicology, 2009. **2**(1): p. 1-12.
40. Russel, D.A. and G.G. Williams, *History of Chemical Fertilizer Development.* Soil Science of America Journal, 1977. **41**(2): p. 260-265.
41. Pingali, P.L., *Green Revolution: Impacts, limits, and the path ahead.* PNAS, 2012. **109**(31): p. 12302-12308.
42. Romano, I., V. Ventorino, and O. Pepe, *Effectiveness of Plant Beneficial Microbes: Overview of the Methodological Approaches for the Assessment of Root Colonization and Persistence.* Frontiers in Plant Science, 2020. **11**(6).
43. Schütz, L., et al., *Improving Crop Yield and Nutrient Use Efficiency via Biofertilization—A Global Meta-analysis.* Frontiers in Plant Science, 2018. **8**(2204).
44. Bhattacharyya, C., et al., *Evaluation of plant growth promotion properties and induction of antioxidative defense mechanism by tea rhizobacteria of Darjeeling, India.* Scientific Reports, 2020. **10**(15536).
45. Souza, R.d., A. Ambrosini, and L.M.P. Passaglia, *Plant growth-promoting bacteria as inoculants in agricultural soils.* Genetics and Molecular Biology, 2015. **38**(4): p. 401-419.
46. Good, A.G. and P.H. Beatty, *Fertilizing Nature: A Tragedy of Excess in the Commons.* PLOS Biology, 2011. **9**(8).
47. Heisler, J., et al., *Eutrophication and Harmful Algal Blooms: A Scientific Consensus.* Harmful Algae, 2008. **8**(1): p. 3-13.
48. Paterson, J.B., M.A. Camargo-Valero, and A. Baker, *Uncoupling growth from phosphorus uptake in Lemna: Implications for use of duckweed in wastewater*

remediation and P recovery in temperate climates. Food and Energy Security, 2020. **9**.

49. Bonaldi, M., et al., *Colonization of lettuce rhizosphere and roots by tagged Streptomyces.* Frontiers in Microbiology, 2015. **6**(25).
50. Korenblum, E., et al., *Rhizosphere microbiome mediates systemic root metabolite exudation by root-to-root signaling.* PNAS, 2020. **117**(7): p. 3874-3883.
51. Pascale, A., et al., *Modulation of the Root Microbiome by Plant Molecules: The Basis for Targeted Disease Suppression and Plant Growth Promotion.* Frontiers in Plant Science, 2020. **10**(1741).
52. Jeon, J.-S., et al., *Impact of root-associated strains of three Paraburkholderia species on primary and secondary metabolism of Brassica oleracea.* Scientific Reports, 2021. **11**(2781).
53. Matthysse, A.G. and S. McMahan, *Root Colonization by Agrobacterium tumefaciens Is Reduced in cel, attB, attD, and attR Mutants.* Applied and Environmental Microbiology, 1998. **64**(7): p. 2341-2345.
54. Matthysse, A.G., *Conditioned medium promotes the attachment of Agrobacteriumtumefacienstrain NT 1 to carrot ceils.* Protoplamsa, 1994. **183**: p. 131-136.
55. Kandel, S.L., P.M. Joubert, and S.L. Doty, *Bacterial Endophyte Colonization and Distribution within Plants.* Microorganisms, 2017. **5**(77).
56. Ortíz-Castro, R., et al., *The role of microbial signals in plant growth and development.* Plant Signalling and Behavior, 2009. **4**(8): p. 701-712.
57. Liu, H., et al., *Inner Plant Values: Diversity, Colonization and Benefits from Endophytic Bacteria.* Frontiers in Microbiology, 2017. **8**(2552).
58. Lebeis, S.L., et al., *Salicylic acid modulates colonization of the root microbiome by specific bacterial taxa.* Science, 2015. **349**(6250): p. 860-864.
59. Tarkka, M.T., et al., *Plant behavior upon contact with Streptomycetes.* Plant Signalling and Behavior, 2008. **3**(11): p. 917-919.

60. Manteca, A. and J. Sanchez, *Streptomyces Development in Colonies and Soils.* Applied and Environmental Microbiology, 2009. **75**(9): p. 2920-2924.
61. Peng, F., et al., *Insights into Streptomyces spp. isolated from the rhizospheric soil of Panax notoginseng: isolation, antimicrobial activity and biosynthetic potential for polyketides and non-ribosomal peptides.* BMC Microbiology, 2020. **20**(143).
62. El-Naggar, N.E.-A. and S.M. El-Ewasy, *Bioproduction, characterization, anticancer and antioxidant activities of extracellular melanin pigment produced by newly isolated microbial cell factories Streptomyces glaucescens NEAE-H.* Scientific Reports, 2017. **7**.
63. Martinez, L.M., A. Martinez, and G. Gosset, *Production of Melanins With Recombinant Microorganisms.* Frontiers in Bioengineering and Biotechnology, 2019. **7**(285).
64. Iannucci, A., et al., *Plant growth and phenolic compounds in the rhizosphere soil of wild oat (Avena fatua L.).* Frontiers in Plant Science, 2013. **4**(509).
65. Fones, H. and G.M. Preston, *Reactive oxygen and oxidative stress tolerance in plant pathogenic Pseudomonas.* FEMS Microbiology Letters, 2012. **327**: p. 1-8.
66. Mandal, S., D. Chakraborty, and S. Dey, *Phenolic acids act as signaling molecules in plant-microbe symbioses.* Plant Signalling and Behavior, 2010. **5**(4): p. 359-368.
67. Makoi, J.H.J.R. and P.A. Ndakidemi, *Biological, ecological and agronomic significance of plant phenolic compounds in rhizosphere of the symbiotic legumes.* African Journal od Biotechnology, 2007. **6**(12): p. 1358-1368.
68. Billy R. Hammond, J. and L.M. Renzi, *Carotenoids.* Advances in Nutrition, 2013. **4**(4): p. 474-476.
69. Bible, A., et al., *A Carotenoid-Deficient Mutant in Pantoea sp. YR343, a Bacteria Isolated from the Rhizosphere of Populus deltoides, Is Defective in Root Colonization.* Frontiers in Microbiology, 2016. **7**(491): p. 1-15.

70. Kumar, S.V., et al., *A carotenoid-deficient mutant of the plant-associated microbe Pantoea sp. YR343 displays an altered membrane proteome.* Scientific Reports, 2020. **10**(14985).
71. Eckshtain-Levi, N., et al., *Bacterial Community Members Increase Bacillus subtilis Maintenance on the Roots of Arabidopsis thaliana.* Phytobiomes, 2020. **4**: p. 303-313.
72. Vasta-Portugal, P., et al., *How Streptomyces anulatus Primes Grapevine Defenses to Cope with Gray Mold: A Study of the Early Responses of Cell Suspensions.* Frontiers in Plant Science, 2017. **8**(1043).
73. Acosta, K., et al., *Duckweed hosts a taxonomically similar bacterial assemblage as the terrestrial leaf microbiome.* PLOS ONE, 2020.
74. Smith, M.D. and I. Moelyowati, *Duckweed based wastewater treatment (DWWT) design guidlines for hot climates.* Water Science and Technology, 2018. **43**(11): p. 291-299.
75. Iqbal, J., A. Javed, and M.A. Baig, *Growth and nutrient removal efficiency of duckweed (lemna minor) from synthetic and dumpsite leachate under artificial and natural conditions.* PLOS One, 2019.
76. Hashimi, M.A.A.-. and R.A. Joda, *Treatment of Domestic Wastewater Using Duckweed Plant.* Journal of King Saud University - Engineering Sciences, 2010. **22**(1): p. 11-18.
77. Ishizawa, H., et al., *Community dynamics of duckweed-associated bacteria upon inoculation of plant growth-promoting bacteria.* FEMS Microbiology Ecology, 2020. **96**(7).
78. Gilbert, S., et al., *Bacterial Production of Indole Related Compounds Reveals Their Role in Association Between Duckweeds and Endophytes.* Frontiers in Chemistry, 2018. **6**(265).

APPENDIX: FIGURES

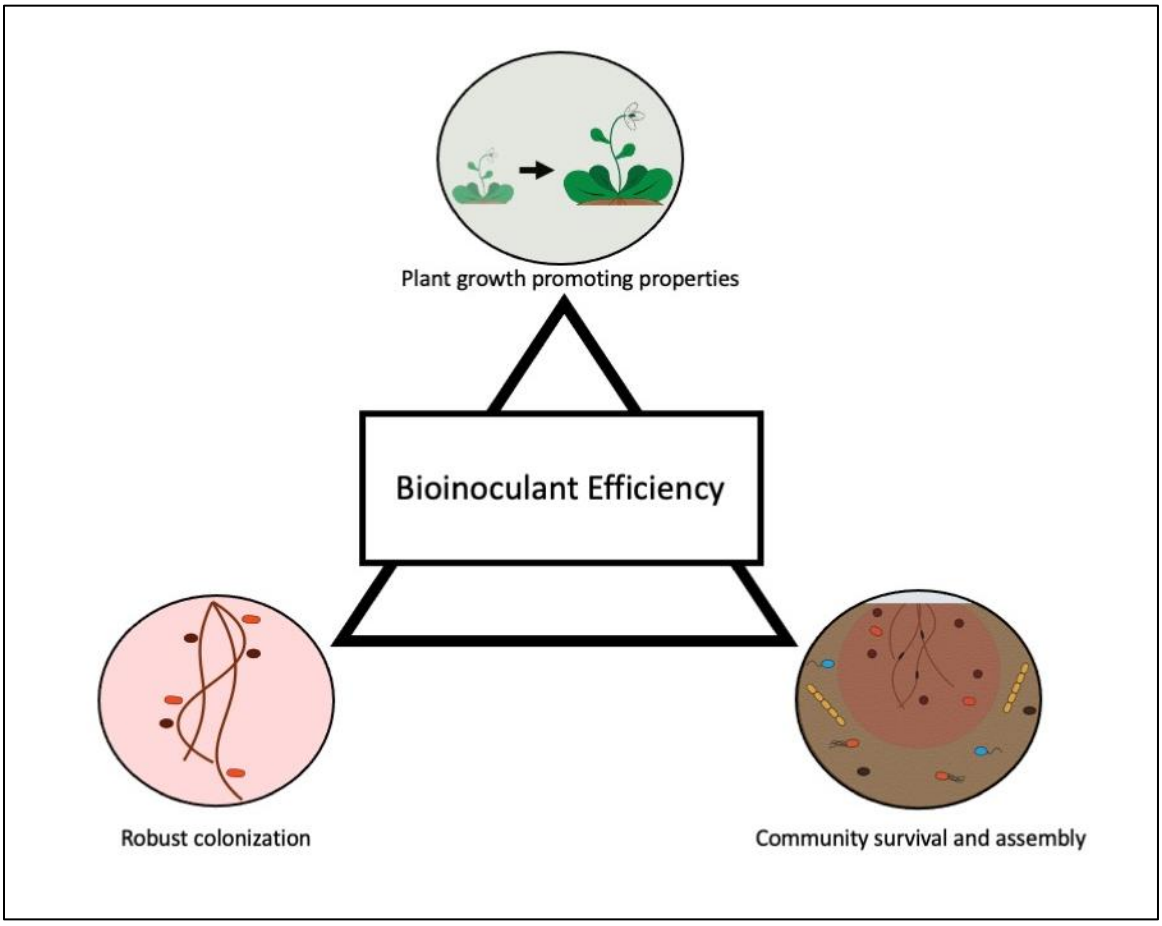

Figure 1. 1:Scheme of microbial attributes that enhance bioinoculant efficiency.

CHAPTER TWO: INVESTIGATING POTENTIAL GENES THAT RESULT IN PIGMENT PRODUCTION TO ENHANCE PLANT COLONIZATION CAPABILITY OF *STREPTOMYCES* AND *BREVUNDIMONAS SP.* OF *ARABIDOPSIS THALIANA*

THIS CHAPTER IS A VERSION OF A PEER-REVIEWED ARTICLE PREVIOUSLY PUBLISHED

Sarah Stuart Chewning, David L. Grant, Bridget S. O'Banion, Alexandra D. Gates, Brandon J. Kennedy, Shawn R. Campagna, and Sarah L. Lebeis. 2019. *Root-Associated* Streptomyces *Isolates Harboring* melC *Genes Demonstrate Enhanced Plant Colonization.* Phytobiomes Journal.

AUTHOR CONTRIBUTIONS

DG, SSC, and SL conceived the experiments. BK performed the melanin-characterizing chemical analysis in the laboratory of SRC. DG performed melanin extraction, tyrosinase assays, phenolic compound experiments, melanin gene expression assays, melanin genetic manipulation experiments, and 374 experiments. SSC performed *Streptomyces* mono-association experiments, phenolic compound experiments and assisted in bioinformatic analysis. SL performed 374 colonization assay. BSO generated and analyzed the phylogenies. ADG and BSO performed mono-associations on related *Streptomyces* isolates and with Salicylic acid. DG, SSC, BSO, BK, and SL analyzed the data. DG, SSC, BSO, and SL wrote the manuscript. DG, SSC, BSO, ADG, and SL revised the manuscript. DG and SL adapted this thesis chapter.

ABSTRACT

Actinobacteria and Proteobacteria assemble into the internal, root endophytic compartment of a wide variety of plants grown in soils worldwide, suggesting their ability to thrive during root microbiome assembly. A previous study found that among four nonpathogenic, root-isolated Actinobacteria in the genus *Streptomyces* (i.e., 303, 299, CL18, and 136), only 303 and 299 colonized endophytic root tissue of the majority of *Arabidopsis thaliana* roots when inoculated with 34 other bacterial isolates. Here we demonstrate that 303 and 299 also colonize significantly more in mono-association with *A. thaliana* seedlings. The genomes of melanin-producing 303 and 299 each contain two copies of the gene encoding tyrosinase (melC2 and melD2), an enzyme necessary for melanin biosynthesis in *Streptomyces* and not found in CL18 and 136. Because tyrosinase oxidizes phenolic compounds and *Streptomyces* colonization of *A. thaliana* appears to be influenced by the phenolic and antimicrobial compound, salicylic acid (SA), we measured direct sensitivity of *Streptomyces* isolates to the phenolic compounds catechol, ferulic acid (FA), and SA *in vitro*. While both 303 and 299 showed higher numbers of surviving colonies than CL18 and 136 in the presence of catechol, only 303 demonstrated a higher number of surviving colonies when isolates were challenged with FA and SA. When seedlings were singly inoculated with a collection of related plant-associated *Streptomyces* isolates, colonization was significantly higher in isolates possessing two tyrosinase gene copies than isolates with either zero or only one gene copy. Additionally, *Brevundimonas sp.*, from the phylum Proteobacteria, shows robust colonization in mono-association with *A. thaliana.* This strain produces a different pigment, a carotenoid, which allowed for investigation on the impacts of 2 different pigments on seedling colonization phenotypes. While no direct impact was provided by the carotenoid pigment, it is interesting to compare the different functionality between both pigments. Overall, we describe a connection between microbes that produce 2 different pigments with increased seedling colonization of nonpathogenic *Streptomyces* and a *Brevundimonas* isolate in *A. thaliana*. We propose tyrosinase activity in *Streptomyces* partially protects against harmful plant-produced phenolic compounds as they transition into an endophytic lifestyle. Alternatively, while the

carotenoid did not seem to impart a survival advantage to the *Brevundimonas sp*., its ability to colonize appears to be specific towards the plant and requires the absences of other organisms in the community.

INTRODUCTION

During plant microbiome assembly, both hosts and microbes drive the complicated and interwoven mechanisms that result in community composition [1]. The microbial members of these communities likely scavenge resources and nutrients from their surroundings [2,3], withstand abiotic and biotic assaults [4,5], and/or act aggressively toward competing microbes [6]. Microbiome assembly is likely influenced by cooperation and competition between microbes vying for niches within the root. Additionally, negotiation of the plant immune system requires specific microbial abilities and potentially host accommodation. Rhizosphere and internal, root endophytic compartment (EC) microbiomes are assembled through plant- specific recruitment of subsets of the soil microbial reservoir, resulting in host-specific microbiome assemblages that are often rich in certain taxa and depleted in others [7,8]. While shifts in community composition may result in a net benefit or cost to the host and other microbes [9], it is still critical to define the finer scale influence of individual microbiome members on host health [1,10]. Understanding incentives for specific host-microbiome establishment will facilitate beneficial community manipulation to improve plant health and growth through defined agricultural practices [5,11].

Deciphering the mechanisms that promote successful colonization of individual microbial strains within a complex microbial inoculum is essential for the development of successful biological products to improve plant health. Among taxa that are found commonly associated with plant hosts, Actinobacteria and Proteobacteria are often abundant. Within Actinobacteria, members of the Streptomycetaceae family are consistently enriched within the roots of various plant species compared with surrounding soil inoculum and are regarded for their high metabolic potential [12–19]. Additionally, while Proteobacteria are variable in colonization depending on family-level, they are among the most abundant taxa found in plant tissue with members of the Caulobacteraceae showing EC enrichment in *A. thaliana* [15]. Ultimately, investigating these two bacterial families specifically provides us with the opportunity to identify novel

molecular mechanisms that contribute to their colonization success and their establishment in root microbiome environments.

Strains of *Streptomyces* can have a range of interactions with a plant host from pathogenic to beneficial. For instance, while *Streptomyces scabiei* and *S. ipomoeae* are plant pathogens [20], most other strains are nonpathogenic and consistent root microbiome members. Many *Streptomyces* contribute to agriculturally important traits, such as drought resistance, improved plant growth promotion, and disease resistance through biocontrol capabilities [18,21,22]. However, it is still necessary to tease apart unique mechanisms that facilitate *Streptomyces* root colonization. Here we define *Streptomyces* strain-specific mechanisms that might potentiate survival advantages during root microbiome assembly.

Proteobacteria is a very diverse phylum with high variability across its bacterial members with the ability to colonize a wide range of hosts [23]. It includes mammalian pathogenic bacteria, including strains of *Salmonella, Pseudomonas,* and *Campylobacter* that have defined effects on mammalian hosts [23]. Many of the organisms from these genera can also colonize plants and can be introduced via fertilizer inoculation, including *Salmonella* and *Pseudomonas* strains [24,25]. Among the Proteobacteria families that are consistently found associated with plants, *Brevundimonas spp*. show interest due to their growth enhancing and colonizing capability [19,26]. While all of their effects on a plant host may not be well known, they are an ideal organism for understanding microbiome establishment due to their consistency in associating with a plant host. They also provide a representative organism from Proteobacteria, which have similarity to Actinobacteria. This similarity was noted in a recent study with maize roots that showed both Actinobacteria and Proteobacteria taxa were most affected by benzoxazinoids, secondary metabolites from plants that can regulate plant-microbe signaling and plant defense signaling [27]. In this way, Proteobacteria provide another avenue for investigating potential genes involved in enhanced root microbiome survival and plant association.

Previous experiments inoculated axenic *Arabidopsis thaliana* seedlings with a synthetic community (SynCom) of 38 taxonomically diverse bacterial isolates, which included four isolates in the actinobacterial genus *Streptomyces*. Colonization of 6- to 8-week-old *A. thaliana* roots differed between these four *Streptomyces* isolates [28]. Specifically, two *Streptomyces* isolates, 303 and 299, were found with significantly greater abundance in the root EC than in inoculum and were thus indicated as "EC-enriched," while the other two, CL18 and 136 were not [28]. Root EC colonization by these strains was influenced by salicylic acid (SA), a phenolic compound, which inhibits microbial growth [29,30], acts as a plant defense phytohormone [31,32], and is measurable in root tissue, seedlings, and exudates [8,28,33,34]. Isolate 136 colonized significantly better in pad4 plants, which are unable to trigger SA accumulation, while 303 displayed significantly increased levels of root colonization in plants sprayed with exogenous SA [28]. Thus, *Streptomyces* colonization appears to be influenced by at least one phenolic compound present in the root–soil interface. However, it was unclear if SA influence was direct or indirect, acting through the plant immune system.

Here, we explore distinct phenotypic and genomic characteristics of these four nonpathogenic, *A. thaliana* root-associated *Streptomyces* strains. While recent studies established that plant-associated *Streptomyces* do not use SA as a carbon source during colonization [35], here we test the hypothesis that SA and other phenolic compounds in the root/soil interface provide selective pressure during root microbiome community assembly. We investigate the strain-specific kinetics and products of tyrosinase, an enzyme present in the two root EC- enriched strains, 303 and 299, but not CL18 or 136. Further, we suggest that inhibiting this enzyme negatively influences protection conferred to 299 and 303 against phenolic compounds during seedling colonization. These studies present a unique opportunity to elucidate microbial determinants of seedling colonization for root-associated strains within a single genus.

Streptomyces fall within the phylum Actinobacteria, a taxonomic group with vast and varied metabolic potential [36]. We propose that one beneficial product for plant-associated *Streptomyces* strains during colonization is melanin, a pigment ranging in color from tan to black, which is also produced by other bacterial taxa, fungi, plants, insects, and mammals [37–41]. In bacteria, the polymer is produced in various forms including eumelanin, which is produced during tyrosinase oxidation and is black-brown, pheomelanin, which is yellow-red and produced via cysteinylation of dihy-droxyphenylalanine (DOPA), and the less studied allomelanin [42]. These melanins can shuttle electrons or act as final electron acceptors [42]. While function and synthesis vary by organism, melanins are generally hypothesized to provide protection from stresses such as reactive oxygen species, antibiotics, and antimicrobial peptides [39,43,44], thereby providing a potential survival advantage [45]. In the root pathogen *S. scabies*, mutants that lose melanin production exhibit decreased virulence, although this phenotype often co-occurred with decreased production of the virulence factor thaxtomin A [46]. Therefore, it remains unclear what role melanin might play during root colonization with nonpathogenic *Streptomyces*.

The extracellular production of melanin in *Streptomyces* is frequently observed and conferred by the *melC* operon, which contains two genes: *melC1* and *melC2*. *melC2* encodes a tyrosinase enzyme critical for oxidizing compounds at multiple steps during melanin production from tyrosine[47–49]. *melC1* encodes a helper protein that adds the required copper ions for tyrosinase function and contains a secretion signal that facilitates the exporting of both MelC1 and MelC2 proteins into the extracellular space, where the MelC2 enzyme participates in melanin production[50,51]. A previous study discovered that a collection of melanin producing *Streptomyces* isolates contained two predicted copies of the *melC* operon, each containing the two required genes [44]. The second copy of the operon (termed *melD*) resulted in an intracellular enzyme and phenolic compounds oxidation within the cell [44]. While *melD* was observed in strains without *melC*, the opposite was not true [44]. Yang and Chen observed that strains with

only *melD* lacked melanin production, confirming that *melC* confers extracellular melanin production [44].

Here we describe that *Streptomyces* isolates 303 and 299, which are both capable of producing melanin also possess a predicted *melC* and a predicted *melD* operon and exhibit increased resistance to phenolic compounds. The experimental system we use allows us to determine the potential survival advantage of *mel*-harboring isolates via hypothesized protective tyrosinase or melanin activities to enhance the opportunity to colonize plants, which we test on four *Streptomyces* strains isolated from a different plant host species. Advancing our understanding of how *Streptomyces* spp. colonize *A. thaliana* will provide future opportunities to understand their activities in root microbiomes and determine if they manipulate microbiome composition to improve plant health, growth, and ultimately yield.

In the same 38-member SynCom experiment as above, fifteen Proteobacteria were inoculated on *A. thaliana,* and a Proteobacteria, *Brevundimonas sp. 374* that showed higher colonization levels around 10^8 CFU/g. Interestingly, 374 also showed an orange pigment production on media that has been associated with plant colonization in a the majority of plants [28]. Carotenoids are pigments found in plant and bacterial species that have vital roles in plant health with roles in photosynthesis and photoprotection [52]. Like melanin pigments, carotenoids have antioxidant effects and confer UV resistance to organisms [43,53]. Therefore, we predict both pigment types provide a survival advantage to their organisms during host colonization. Recent studies investigating a root-associated Pantoea strain, another Proteobacteria, that produces a carotenoid found that a disruption in the pigment producing genes, mainly genes *crtY* and *crtB*, resulted in a decrease in plant root colonization [54]. Furthermore, a follow-up study showed that the deficient mutant also had altered membrane functionality, resulting in defects with IAA secretion and motility [55]. Highlighting the importance of carotenoid pigments in bacterial survival. However, the functionality of a carotenoid in

the root context is not well understood and requires further investigation to determine if it is a good gene marker for enhanced root colonization.

Using different organisms with a diverse range of metabolic potential to investigate factors responsible for EC colonization helps to narrow down potential markers for plant colonization. *Streptomyces* isolates that colonize plant roots well, even in SynCom, provide a large reservoir of genes to investigate and a large number of microbe-microbe interactions to consider. Conversely, a *Brevundimonas* strain with a smaller secondary metabolic potential that only colonizes well in mono-inoculation helps to provide a smaller reservoir to investigate genes involved in direct plant-microbe association. Melanin and carotenoid pigments found in these organisms each provide a way of uncovering the role of pigments in plant root colonization and in identifying genes associated with increased colonization. In this way, mining each organism's metabolic potential for explanations to observed plant colonization phenotypes to better understand how microbes associate and establish with a plant host.

MATERIALS AND METHODS

Strain culture preparation

Streptomyces isolates were grown in lysogeny broth (LB) [56] at 30°C with shaking at 150 rpm for 4 to 7 days. Cultures were vortexed vigorously for 5 s and beaten with 3 mm glass beads for 2.5 min to disrupt bacterial aggregates. A spectrophotometer measured the optical density at 600 nm (OD600) and cultures were normalized to an OD600 of 0.01. One hundred microliters of all normalized isolate resuspensions were plated on LB solid medium, incubated at 28°C for 4 to 7 days, and colony forming units (CFUs) were counted. Inoculum ranged from 1×10^2 to 3×10^4 CFU/ml. LB medium was used for initial inoculation of many of our assays due to the consistent size of flocculants and pigment production that two of our *Streptomyces* strains made on solid and in liquid media that made it possible to differentiate the isolates from one another (Figure 2.1A). Additionally, because it is a rich medium, we

could easily detect contamination with other faster growing bacteria. *Brevundimonas* sp. 374 was grown up in LB at 30°C with shaking at 150 rpm for 1-2 days. On plate media, 374 makes a noticeable bright orange pigment while it is not obvious in liquid media and requires pelleting cells down to see orange pigment on cells. 374 cultures were also normalized to an OD600 of 0.01 with inoculum ranges resembling the higher limit of *Streptomyces*, at 3 x 10^4 CFU/ml.

Melanin pigment extraction

For *Streptomyces* strains, pigment extraction from bacterial strains was adapted from Drewnowska et al. [57]. Specifically, 200 ml of cultures of 303, 299, CL18, and 136 was split between four 50-ml sterile conical tubes each and centrifuged for 15 min at 3,200 × g. Supernatants of each isolate were transferred to two 100-ml glass bottles. The pH of the supernatants was adjusted to 2.0 via addition of 1 M HCl. Samples were incubated at room temperature for 1 week in the dark. Following incubation, the acidified supernatants were boiled in the glass bottles for 1 h. Cooled supernatants from each isolate were transferred to four 50-ml conical tubes and centrifuged for 15 min at 3,200 × g. After supernatants were removed, 303, 299, and CL18 had approximately a 1-ml pellet remaining in each tube while 136 had no evident pellet. Pellets from each isolate were resuspended and combined into a single 15-ml tube per isolate. The three tubes were then centrifuged again for 7 min at 3,200 × g and supernatants were discarded. Pellets were washed and centrifuged for 7 min at 3,200 × g three times in 15 ml of 0.1M HCl and a final time in 15 ml of water. After each wash, supernatants were discarded. After washing, 10 ml of absolute ethanol was added to each of the 15-ml tubes containing the pellets and resuspended. The tubes were placed in a boiling water bath for 10 min and then incubated at room temperature for 1 day. Following incubation, the suspensions were centrifuged for 7 min at 3,200 × g and the supernatant was discarded. The pellets were washed twice with absolute ethanol and centrifuged for 7 min at 3,200 × g between washings. After the second wash, the pellets were allowed to air dry. The pellets for 303 and 299 cultures were brown while the pellet from CL18 culture was orange.

Liquid-chromatography mass spectrometry (LC-MS)

Pigment pellets were digested following the protocol established by Ito and Wakamatsu [58]. Briefly, approximately 1-mg portions of the dried pigments were weighed and transferred to glass vials (4 dr) for digestion. The solid samples were suspended in 100 ml of high-performance liquid chromatography (HPLC)-grade H2O, which was sonicated for 2 min to increase dispersion of pigments in the aqueous solution and centrifuged at 4,000 rpm to correct for the splashing that occurred during sonication. To the suspension of pigment in H_2O, 30 ml of 30% H_2O_2 and 375 ml of 1 M K_2CO_3 were added. The vials were capped and secured on an orbital shaker set to 200 rpm to digest at room temperature for about 20 h. After digestion, excess peroxide was destroyed with the addition of 50 ml of 10% Na_2SO_3 and each sample was acidified with 140 ml of 6 N HCl. These digested, quenched, and acidified samples were centrifuged at 13,000 rpm for 5 min to pelletize any undigested melanin, and then 300 ml of supernatant was transferred into autosampler vials for chemical analysis. The LC-MS analyses were performed on an UltiMate 3000 UHPLC system coupled to an Exactive Plus Orbitrap mass spectrometer (Thermo Scientific, Pittsburgh, PA). Separations were performed on an Accucore HILIC LC column (150 × 2.1 mm; 2.6 mm particle size, Thermo Scientific) kept at 25°C. For each analysis, 10 ml of sample was injected onto the LC column and the chromatographic method employed used 0.1% formic acid in ACN and 0.1% formic acid in H2O as mobile phases A and B. The chromatographic conditions were as follows: 0 min, 80% A; 10 min, 80% A; 10.1 min, 100% A; 20 min, 80% A; 25 min, 80% A; with a constant flow rate of 200 ml/ min. The high-resolution mass spectrometric (HRMS) experiments were all conducted in negative ion mode using an electrospray ionization (ESI) source. The ESI parameters used were a spray voltage of −4.0 kV, an aux gas flow rate of 8 units, sheath gas flow rate of 25 units, sweep gas set to 3 units, and capillary temperature set to 32°C. The mass spectrometer scanned a mass range of 120 to 1,800 m/z with a resolution of 140,000, an automatic gain control (AGC) target of 3.0×10^6, and maximum injection time of 200ms. The HRMS data were analyzed and processed using the MAVEN [59] software and

processed to generate bar graphs (data not shown). Extracted ion chromatograms were generated in MAVEN [59] with an extraction window of 5 ppm.

Seed sterilization and germination

For all seedling experiments, Col-0 accession *A. thaliana* plants were used. All seeds were surface sterilized in 70% ethanol with 0.1% Triton X-100 for 1 min, 10% household bleach with 0.1% Triton X-100 for 15 min, and three washes with sterile distilled water. Seeds were stratified for at least 3 days in the dark at 4°C and subsequently germinated at 24°C with 16 h of light for 6 to 8 days on agar plates containing half- strength (2.22 g/liter) Murashige & Skoog (MS) vitamins, 1% sucrose, and 1% Phytoagar (Bioworld).

Plant colonization experiments

To inoculate plates, 150 µl of individual isolate resuspensions at OD 0.01 was spread on prepared quarter-strength MS square agar plates (150 mm × 150 mm) with no sucrose. For colonization experiments with SA, 100 µl of isolate resuspensions was spread on quarter-strength MS square agar plates (100 mm × 100 mm) with no sucrose and 0.1 mM SA, which did not influence seedling survival after 14 days. Plates were allowed to dry and four to five sterile seedlings were aseptically transferred onto each plate with flame-sterilized tweezers. Plates were sealed with Parafilm M Laboratory Film and randomly stacked vertically in open wire trays, which were grown at 24°C with 16 h of light for 14 to 15 days. Every 2 days, root length was observed, phenotype was assessed, and plates were shuffled. After 14 to 15 days, the seedlings from each plate were aseptically harvested and pooled in sterile previously weighed 1.5-ml centrifuge tubes. Tubes were weighed again after tissue was added to determine seedling biomass. To quantify internal levels of colonization, roots were rinsed and vortexed 5 s three times with sterile distilled water to determine combined level of colonization for internal and tightly attached external bacteria. For homogenization of weighed seedlings, a combination of sterile garnet and 3 mm glass beads were aseptically transferred to tubes containing the pooled, surface sterilized whole seedlings, 1 ml of

sterile phosphate buffered saline was then added to each tube, and samples were homogenized in a 2010 Geno/ Grinder at 1,500 rpm for 5 min. From homogenized tissue, 100 µl was spread on LB plates and incubated at 28°C for 4 to 7 days. CFUs were counted and recorded. For experiments in pots, 64 ml of sterile calcined clay (Pro's Choice Rapid Dry) in three-inch square pots was inoculated with 49 ml normalized culture suspended in half strength MS buffered with sterile 2-(N-morpholino) ethane- sulfonic acid (MES). Six-day-old seedlings were aseptically transferred to inoculated pots. An additional 1 ml of suspended inoculum was applied directly to seedling roots to bury them in the calcined clay. Plants were watered every 2 to 3 days from the top with sterile distilled water and grown in growth chambers (Percival, model AR41L3C8) with 10 h of light at 22°C and 14 h of dark at 18°C. Beginning at 6 weeks of growth, plants were aseptically harvested when inflorescence began to emerge. Whole plants were submerged in 25 ml of sterile harvesting phosphate buffer with 0.01% Silwet (Lehle Seeds) and vortexed vigorously for 10 s. Roots and rosettes were separated with sterile forceps and transferred to sterile centrifuge tubes and weighed to measure biomass (Figure 2.2).

Pangenomic visualization

Genomes for strains 303, OV320, 299, OV308, CL18, YR375, 136, OK210, and *Streptomyces scabiei 87.22* (Tables 2.1 and 2.2) were downloaded from Joint Genome Institute (JGI) Integrated Microbial Genomes & Microbiomes (IMG/M) expert review (ER) system [60]. Genomes were mined using JGI IMG/M ER query tools and Anvi'o v2.1.0 (a platform used to analyze and visualize genomic data) [61]. Pangenomic analysis was performed with Anvi'o, as outlined by Eren et al. [61]. Homologs were identified using similarity searches through NCBIs BLASTP and protein clusters were resolved with the MCL algorithm (inflation parameter 6) [62] using the minbit scoring method (score 0.5). Annotations were done with clusters of orthologous groups (COG) [63]. Manual "binning" of protein clusters shared between subsets of genomes facilitated identification of group-specific gene clusters. Analyses resulted in a visual

representation of the pangenome and a database of protein family annotations from the COG database [63].

Phylogenetic trees and identification of mel *operons*

A concatenated alignment of the amino acid sequences of five housekeeping genes (*trpB*, *gyrB*, *rpoB*, *atpD*, and *recA*) from nine plant-associated *Streptomyces* strains and one *Kitasatospora* strain, which represents another genus in the family Streptomycetaceae, was used to build a maximum likelihood (RAxML v7.2.8) phylogenetic tree using 100 bootstrap replicates [64]. Alignment, using MAFFT v7.017 [65], was performed in Geneious version R7 [64]and tree building was done using RAxML-HPC Black Box (version 8.2.10) through the CIPRES Science Gateway V. 3.3 [66]. Melanin genes (*melC1* (SCAB85691), *melC2* (SCAB85681), *melD1* (SCAB59231), and *melD2* (SCAB59241)) from *S. scabiei 87.22* identified by [44] were used as queries for NCBI BLASTP searches to identify melanin genes in all strains [44]. Alignment (MAFFT v7.394) [65] of amino acid sequences of the *melC2*, *melD2*, *melC1*, and *melD1* genes from six *Streptomyces* strains was used to build a Maximum Likelihood tree using RAxML-HPC Black Box (version 8.2.10) through CIPRES Science Gateway V. 3.3 (for the tyrosinase tree) [66] or RAxML v7.2.8 through Geneious version R7 (for cofactor tree). Housekeeping and *mel* trees were visualized in iTOL [67]. Among the nine *Streptomyces* that we included in our analysis, six encoded at least one *mel* operon. All six strains encoded the *melD* genes, whereas only five strains encoded the *melC* genes (Figure 2.3C and D).

Tyrosinase assay

Enzymatic oxidation of L-3,4-dihydroxy- phenylalanine (L-DOPA) by tyrosinase was monitored spectrophotometrically [68] using the BioTek Synergy Multi-Detection Microplate Reader. Synthesis of Dopachrome was monitored at an absorbance of 475 nm. To prepare the assay, liquid cultures of each Streptomyces isolate were grown in 100 ml standard glucose-minimal salts medium with Tiger's Milk at 30°C with shaking for 5 to 7 days, according to Kieser et al. [71]. Approximately 20 ml of each culture was

harvested and split between two 15-ml conical tubes, which were centrifuged for 7 min at 3,200 × g. Supernatants were collected and kept on ice while pellets were resuspended and washed with 10 ml of 0.1 M sodium phosphate (pH 6.8). Resuspended cells were then centrifuged for 7 min at 3,200 × g and supernatants were discarded. Following resuspension of cell pellets in 10 ml of 0.1 M sodium phosphate (pH 6.8), suspensions were moved to 100 µm silica bead tubes (Ops Diagnostics 100-100-01) and a 1× treatment of protease inhibitor cocktail (VWR M222-1ML) was added. Tubes were bead beaten for 10 min at 1,560 rpm and were treated with lysozyme using 40 µl of a 100 mg/ml stock and incubated for 30 min at 37°C. Cells were then centrifuged for 3 min at 13,000 × g and supernatants were collected, which was considered the cell extract fraction. Supernatants were treated with 70% ammonium sulfate ($(NH_4)_2SO_4$) and incubated on ice until dissolved. After dissolution, extracellular protein extracts were centrifuged at 4°C for 30 min at 3,200 × g. Supernatants were discarded, and protein pellets were resuspended in 2.5 ml of 0.1 M sodium phosphate. To remove the salt from the protein pellets, samples were applied to PD 10 desalting columns and allowed to pass through via gravity. Before application, columns were washed with four applications of 0.1 M sodium phosphate (pH 6.8). After desalting, total protein concentrations were determined via the microtiter Bio-Rad protein assay. Samples were normalized by protein concentration to 1,000 µg/ml and loaded into 96-well microtiter plates, which included the following: 100 µl of cell extract or extracellular extract all resuspended in 0.1 M sodium phosphate, 100 µl of 6.8 mM L- DOPA, and with or without 5 mM of a tyrosinase inhibitor kojic acid (KA) [69]. For 299 supernatant protein extractions, 6 mM $CuSO_4$ was also added to the reaction to observe activity. KA is known to inhibit the enzymatic activity of tyrosinase[69,70]. KA has been shown to have a competitive inhibitory effect on monophenolase activity via copper chelation. Additionally, KA is known to have a mixed inhibitory effect on dephenolase activity of tyrosinase and likely inhibits tyrosinase via copper chelation at the enzyme's active site [70]. Controls included three replicates of wells without protein containing combinations of 0.1 M sodium phosphate, L-DOPA, and 5 mM KA. A tyrosinase standard was also run using lyophilized powder from Spectrum Chemical Group and 25,000 U (25 mg) of

enzyme was diluted in 0.1 M sodium phosphate buffer (pH 6.8) and subsequent standards were prepared in a range from 1 to 15 activity units for reads (Figure 5). Absorbance at 475 nm was measured every minute for 3 to 11 h.

Phenolic compound challenges on agar

To determine strain resistance to phenolic compounds, standard glucose-minimal salts medium (MM) was prepared with the addition of 0.01 g of $CuSO_4$ and 100 ml of phosphate buffer (NaH_2PO_4 at 138 g/liter and Na_2HPO_4 at 142 g/liter) per liter. Filter sterilized phenolic com- pounds were added to cooled, autoclaved media at concentrations of either 0, 0.125, 0.5, 1, or 5 mM for salicylate (salicylic acid, SA), catechol, and ferulate (ferulic acid, FA). Twenty-five milliliters of phenol-containing agar was pipetted or poured onto petri dishes. Once solid, 100 µl of *Streptomyces* strains 299, 303, CL18, and 136 standardized to OD600 of 0.01 (described previously) and diluted 1:10 was pipetted onto solidified plates and spread with sterile beads (CFU range: 4×10^3 to 4×10^4). Plates were incubated at 30°C and checked daily for CFU formation. CFUs were counted after 4 to 7 days of incubation and recorded.

SA challenge in liquid media

Liquid cultures of each isolate were first prepared as described above with the exception of growth medium type. Cultures were grown in liquid MM [71] with $CuSO_4$ rather than solid LB. A spectrophotometer measured the optical density at 600 nm (OD600) and cultures were normalized to an OD600 of 0.1. To inoculate flasks, 100 µl of all normalized isolate resuspensions was added to sterile 125-ml flasks containing 75 ml of MM and concentrations of either 0.0- or 0.5-mM SA. These concentrations were chosen based on results from solid media as well as previous findings from Lebeis et al. [28]. In addition, a separate complete set of flasks was inoculated exactly as described, with the addition of 1.5 mM KA. Three replicate cultures were prepared. Erlenmeyer flasks were incubated at 30°C with shaking at 125 rpm for 6 days. After the 6-day incubation, biomass was collected via 10 s vacuum filtration of each 75-ml culture on 0.2 µm filter paper. Filters were allowed to dry overnight. Three filter paper controls with

filtered liquid media only were weighed, and biomass for each sample was calculated based on the average mass of the control filter paper subtracted from the filter paper with *Streptomyces* biomass.

Tyrosinase gene expression of 303 and 299 in seedlings

Axenic, Col-0 6- to 7-day-old seedlings were left sterile or inoculated with 303 and 299 as described above and grown for 10 days. At 10 days, individual plants were placed in bead tubes containing 100 µm silica, 4 mm silica, and 1.7 mm zirconium beads (Ops Diagnostics 4000-100-28). For positive controls, in vitro 25 ml of 303 and 299 cultures grown in LB for 6 days were spun down and placed in bead tubes containing 100 µm silica beads (Ops Diagnostics 100-100-02). One milliliter of TRIzol reagent was added to each tube, and samples were homogenized in a 2010 Geno/Grinder for 10 min at 1,560 rpm. After homogenization, tubes were centrifuged at 12,000 × g for 5 min and the supernatant was transferred to a new microcentrifuge tube. To each tube, 200 µl of Chloroform was added, and samples were incubated for 15 min at 4°C. Phase separation was performed by centrifugation at 12,000 × g for 5 min at 4°C. The upper aqueous phase was removed, and the RNA was cleaned using the RNA Clean and Concentrator kit for TRIzol clean-up (Zymo R1015). RNA was converted to cDNA using Quantabio qScript (95048-025) and PCRs were performed using 303 and 299 *melC* specific primers to amplify a 665-bp (303) and 525-bp (299) range inside each isolate's respective *melC* operon using the SnapGene program. Strain 303MelCFwd primer (CAGTCGGTGTCGAAGGT GTAGTG) and 303MelCRev_01205 (CACCGTTCCCCTTCCTTCC TGC) were used for 303. Strain 299MelCFwd primer (CCGCCGTCCTGGAGCTGAAG) and 299MelCRev primer (CATGGACCCGGTTGTGCAGGTTGAC) were used for 299. PCR conditions for 303 were 3 min at 95°C, 40 cycles of 30s at 95°C, 30s at 64°C, and 1min at 72°C followed by 5min at 72°C. PCR conditions for 299 were 3 min at 95°C, 30 cycles of 30s at 95°C, 30s at 60°C, and 1min at 72°C followed by 5min at 72°C. Following the PCRs, a 1% agarose gel electrophoresis was performed to verify that a 665-bp product was specifically amplified for 303 and a 525-bp product was amplified for 299.

Streptomyces *electroporation*

Streptomyces electroporation was adapted from Pigac et al. [72]. Mycelia were grown up flasks of either 25mL of LB broth at 30°C with 1% glycine or 0.5mg/mL lysozyme. After 2-4 days, mycelia were washed three times with 25mL ice col 15% glycerol. After washes, mycelia were resuspended in 2mL of electroporation buffer (30% PEG 1000, 10% glycerol, 6.5% sucrose). To electroporate, 1ul of desired plasmid was added to 80ul of resuspended mycelia. The sample was then transferred to a 2mm electroporation cuvette and given a 2kV electric pulse. Cells were immediately suspended in 0.75mL of ice-cold LB. Cells were then incubated for 3 hours at 30°C.

Alternatively, *Streptomyces* spores were electroporated using methods adapted from Tyurin et al. [73]. Fresh spores were grown in 25mL LB with 25mg/mL $MgCl_2$ and incubated at 30°C for 2 hours. Cells were harvested and washed twice with 25mL 10% sucrose. Cells were then resuspended in 2mL of electroporation buffer described above. Electroporation was performed the same as above for spores and mycelia.

Streptomyces *conjugation*

Conjugation was adapted from Flett et al. [74]. The common *Streptomyces* donor strain, *Escherichia coli* strain ET12567, was used in conjugation experiments. ET12567 was grown in 25mL of LB with 25ug/ml chloramphenicol at 37°C overnight. Cells were then diluted 1:100 the following day and grown up to mid log (OD_{600} = 0.4-0.6). ET12567 cells were washed with 25mL of LB and resuspended in a final volume of 0.1mL. *Streptomyces* spores were placed in 500ul of 2xYT (16g Tryptone, 10g Yeast Extract, 5g NaCl, 1L dH_2O) media and heat shocked at 50°C for 10 minutes. After cooling, spores were added to ET12567 at a 0.5mL:0.5mL volume ratio and mixed. The mix was then plated on mannitol soya flour medium (20g Mannitol, 20g Soya flour, 20g agar, 1L dH_2O) with 10mM $MgCl_2$ and incubated at 30°C for 20 hours. An antibiotic overlay of 1mL with 0.5mg nalidixic acid and 1mg apramycin was then added and plates were again incubated at 30°C.

Streptomyces *plasmid extraction*

Plasmids were extracted from *Streptomyces* strains using the Qiagen plasmid kit (ref. 12123) with modifications. Mycelia were grown up at 30°C for 4-6 days before cells were spun down and resuspended in 8mL lysozyme buffer (50mM Tris-HCl, 10mM EDTA, 4mg/mL lysozyme). Cells were incubated at 37°C for 30 minutes before continuing the kit protocol.

Tyrosinase mutant generation experiments

Numerous avenues were pursued in order to generate a 303 mutant in *melC* and *melD* to create a tyrosinase-deficient mutant. First, a standard CRISPR approach was taken, using the pCRISPR plasmid and inserting a 20bp spacer sequence gRNA for mid-way into both *melC* and *melD* genes. The plasmid was generated but unable to insert into 303 cells using electroporation or conjugation methods using the conjugation donor *Escherichia coli* strain ET12567.

The second approach utilized a *Streptomyces* specific CRISPR system using the plasmid pCRISPomyces-2 on the novel 303 strain. For this plasmid, a construct was made with gRNAs for *melC* and *melD* genes in order to knock out each gene separately. Each gRNA was a 20bp sequence inside the target gene. The gRNAs were inserted into the pCRISPomyces-2 vector using Golden Gate Assembly. *E. coli* plasmids were extracted using Promega Wizard Plus SV Minipreps (ref. A1330). Complementary 1kb sequences upstream and downstream of the target genes were included to act as repair templates homologous recombination upon gene deletion. After plasmid assembly, conjugation with ET12567 and electroporation techniques were used in an attempt to insert the plasmid into the novel *Streptomyces* 303 strain. However, while the plasmids were sequenced and verified, they were unable to be inserted into the novel strain as noted by the lack of any colonies recovered.

To test plasmid insertion into a novel *Streptomyces* strain, a model organism *Streptomyces lividans* was obtained that included the plasmid pIJ702. *S. lividans* has

the *melD* operon in its chromosome while the other, *melC*, is in the plasmid pIJ702. Plasmid extraction and purification was performed using as described above to isolate pIJ702. Plasmid uptake into novel strains CL18 and 136 was attempted in order to supply a single *mel* operon for observance of phenotypic changes in plant association. However, the plasmid was not able to be inserted into either strain using conjugation and electroporation techniques as noted by the lack of colonies.

The model organism, *Streptomyces lividans* TK24 was investigated for understanding *Streptomyces* genetics as it is widely used in genetic manipulation. TK24 has only one tyrosinase gene, *melD*, so that gene was subsequently focused on for deletion. Using the same pCRISPomyces-2 system as above a construct was made with a gRNA sequence of 20bp within the gene and with a repair template of 1kb upstream and downstream of the gene to aid in successful gene deletion. Both the construct and the pIJ702 plasmid from above were sequence, verified, and attempted to be inserted into TK24 using electroporation and conjugation methods. Only pIJ702 was successfully conjugated into TK24 using conjugation, other methods were unsuccessful at introducing DNA into a *Streptomyces*.

374 secondary metabolite investigation

The genome for *Brevundimonas sp. 374* was downloaded from JGI and uploaded to AntiSMASH using default settings (KnownClusterBlast, ActiveSiteFinder, and SubClusterBlast) [75,76]. AntiSMASH uses profile Hidden Markov Models of genes to identify gene clusters of secondary metabolites. Two Biosynthetic gene clusters (BGCs) were identified within the genome for investigation.

Nutrient effects on 374 carotenoid production

374 was grown on minimal M9 media with different carbon sources to test the effect of nutrient composition on carotenoid production. 50mL M9 agar (BD ref. 248510) with $MgSO_4$ was supplemented with 5mL of 50% solutions of either lactose, glycerol,

sucrose and glucose. 374 was then spread onto plates with 100ul of a 0.1 OD solution and incubated at 30°C for 2-5 days to observe changes in orange pigmentation.

Carotenoid gene expression of 374 in seedlings

Identified carotenoid genes *crtY* and *crtB* were investigated for expression *in planta*. Following the methods performed for 303 tyrosinase expression, 374 *crtY* and *crtB* gene primers were created to capture segments of both genes. Seedlings were prepared as described above and transferred to square MS plates. Isolate 374 was inoculated onto seedlings at an OD 0.01, and plates were incubated vertically for 7 days. Following incubation, RNA was extracted as above and converted to cDNA. *crtY* and *crtB* primers were used to amplify carotenoid genes and show expression of them within plant samples.

Transposon mutagenesis

Mutant library generation was performed using *E. coli* strain EZ193, with plasmid pEZ16, which was a gift from the Zinser lab at the University of Tennessee Microbiology Department. The protocol was performed following the protocol by Katherine Moccia [87]. The donor EZ913 was struck on LB agar with 75uL of 100mM DAP (diaminopimelic acid) along with 30ug/L chloramphenicol. Plates were incubated for 24 hours at 37°C. A *Brevundimonas* sp 374-166 strain tagged with mCherry was struck on LB and incubated for 24 hours at 30°C. After incubation, EZ913 and 374-166 were conjugated as lawns together on LB with DAP in a 1:1 concentration and incubated for 24 hours at 30°C. Then, 2mL of LB liquid was added to the plate and isolates were then scraped gently off the plate and transferred to a microcentrifuge tube. Dilutions were made and plated on LB with chloramphenicol plates and freezer stocks were made in 50% glycerol and frozen at -80°C.

Mutant screening and 16S sequencing

Mutants were screened for growth on antibiotic plates and altered orange pigmentation. Colonies that were to be white or a faint orange were picked, struck onto

new LB with chloramphenicol plates, and incubated in LB broth with chloramphenicol for 24 hours at 30°C. After liquid growth, DNA extraction was performed using Qiagen DNeasy UltraClean Microbial Kit (ref. 12224-250). 16S sequencing was performed using 338F and 806R primers to verify 374-166 identity.

374-166 mutant colonization assay

Arabidopsis seedlings were prepared as described above. *Brevundimonas* sp. 374-166 wild type (WT) and mutants were inoculated in LB with chloramphenicol for 24 hours at 30°C on the sixth day of seedling germination. Mutants included a white colony, two faint orange colonies, and a normal orange mutant. Following the 7-day germination period, 374-166 WT and mutants were normalized to an OD600 of 0.01 and spread onto square MS plates 100mm x 100mm. Seedlings were then transferred to square MS plates and incubated vertically on a diurnal cycle. After incubation, plants were harvested as described above and plated on LB plates to perform CFU counts. 374 WT and an orange mutant were used as controls in colonization assay.

Statistical analysis

LC-MS ion counts, seedling colonization, phenolic compound challenge, culture biomass, and plant biomass results were statistically analyzed with Prism version 7.0a for Mac (GraphPad Software, La Jolla, CA, https://www.graphpad.com). Two-way ANOVA with Dunnett's multiple comparisons were used for LC-MS peak ion counts. For seedling colonization, culture biomass, and plant biomass results, a Kruskal-Wallis with Dunn's multiple comparisons was used. For phenolic compound challenge, a two-way ANOVA with a Fisher's LSD was used to determine differences between strains at each phenolic compound concentration.

RESULTS

Melanin production is associated with root-enriched Streptomyces *isolates*

When *A. thaliana* was inoculated with a defined bacterial community of isolates and grown for 6 to 8 weeks, two *Streptomyces* isolates, 299 and 303, displayed

enriched root endophytic compartment colonization while another two, CL18 and 136, did not [28]. Strikingly, 299 and 303 cultures of liquid and solid media developed distinct pigmentation *in vitro*, which never appear in CL18 or 136 cultures (Figure 2.1A). Pigment produced by strain 299 was delayed and lighter in color than that produced by 303 (Figure 2.1A). The brown/black color suggested the potential production of a melanin pigment.

Pigments produced by cultures of 303, 299, and CL18 was extracted from spent liquid media. No pigment pellet resulted from extraction performed on spent 136 liquid cultures. LC-MS analysis of pigments extracted from 299 and 303 indicated molecular similarity to a synthetic melanin standard by the presence of two distinct melanin degradation products (pyrrole-2,3-dicarboxylic acid (PDCA) and pyrrole-2,3,5-tricarboxylic acid (PTCA) [58], while the CL18 samples were not significantly different than the blank sample controls (Figure 2.1B). Overall, our findings suggest that 299 and 303 produce an extracellular melanin in vitro, while CL18 and 136 do not.

***Seedling colonization is* Streptomyces *strain specific*.**

In a mixed bacterial community, our two melanin-producing strains 299 and 303 were significantly more abundant in mature roots than in inoculum, while our nonproducing strains CL18 and 136 were not [28]. Thus, to determine if colonization differences are observed earlier and distinguish influences of mixed bacterial communities from individual strain capabilities, *Streptomyces* isolates 299, 303, CL18, and 136 were screened for their ability to colonize *A. thaliana* seedlings as the sole inoculum for 14 days (Figure 2.1C). After 2 weeks, seedlings were colonized with significantly higher concentrations of isolates 299 and 303 than 136, whereas CL18 colonization was not significantly different from any other isolate in this mono-association (Figure 2.1C). Importantly, plants growing in mono-association with these strains show no signs of pathology or change in biomass even after 6 to 8 weeks of growth with *Streptomyces* colonization, indicating that they are not pathogens or growth promoting strains under these conditions (Figure 2.2). Thus, in addition to increased

root colonization of mature plants when competing with other bacteria [28], 299 and 303 colonize seedlings better than 136, while CL18 is not significantly different from the other *Streptomyces* (Figure 2.1C).

Genomes of melanin-producing strains contain genes essential for melanin production

To reveal genetic similarities among *Streptomyces* strains with higher plant colonization, we decided to compare the genomes of 303, 299, CL18, and 136 with a selection of plant-associated *Streptomyces* isolates. For this analysis, we added four additional *Streptomyces* strains isolated from Poplar trees. We also included the plant pathogen *S. scabiei 87.22* in this comparison for its robust colonization of *A. thaliana* roots and melanin pigment production. *S. scabiei 87.22* proved more closely related to 299 and 303 than CL18 or 136 (Figure 2.3A), although none of our strains are pathogens. Besides the genome of *S. scabiei 87.22*, which is complete, all genomes were estimated to be >99% complete by Anvi'o identification of four sets of bacterial single- copy gene collections [61]. Our genome comparison revealed that 303, 299, and *S. scabiei 87.22* had larger genomes with 1,500 to 3,000 additional genes than CL18 and 136, leaving room for exploration of genes and potential gene products involved in plant association (Figure 2.3B). Among the four additional plant- isolated *Streptomyces* from Poplar trees, three had remarkably high genome identity (>93% ANI) with 303, 299, or 136 (Figure 2.3B, Table 2.3). We next performed a pangenomic analysis of the nine *Streptomyces* strains to investigate conserved and unique genes across their whole genomes. Among genes present in 303, 299, and *S. scabiei*, but absent in CL18 and 136 were those responsible for melanin production, providing us with the opportunity to explore a potential link between the abilities of microbes to survive oxidative stress and colonize plants.

BLASTP searches for genes encoding tyrosinase enzymes, which are known to be required for *Streptomyces* melanin production, returned two copies in the genomes of 303, OV320, 299, OV308, and *S. scabiei*, and a single copy in the genome of YR375

(Figure 2.3C). Directly, upstream of each tyrosinase is its annotated cofactor encoding the helper protein (Figure 2.3D) responsible for copper ion addition to tyrosinase allowing enzymatic function [44]. Because we found multiple copies of the genes encoding tyrosinases and their cofactors, we searched for the presence of distinct *melC* and *melD* operons in our select Streptomyces genomes to suggest potential distinguishable extracellular and intracellular tyrosinases [44]. Phylogenetic trees of tyrosinase genes and helper genes cluster into two groups with a single represented *mel* homolog gene from *S. scabiei* present in each (Figure 2.3C and D). Further, the predicted *melC1* and *melC2* genes were contiguous within each genome, which was also true for the predicted *melD1* and *melD2* genes. Components of the melanin operon were not identified in the genomes of CL18 or 136. Therefore, our genome comparisons identify two distinct *mel* operons in the genomes of melanin-producing strains 303 and 299.

Enzyme kinetics differentiate tyrosinase activity between* Streptomyces *strains

While extracellular melanin production was observed in 303 and 299 in vitro cultures, it was unclear what the potential activity of a second tyrosinase/cofactor pair might confer. We next sought to determine if 299 and 303 did indeed produce both functional intracellular and extracellular tyrosinases by performing an enzymatic activity assay on whole cell extracts and culture supernatants of all four isolates. Whole cell (intracellular) and supernatant (extracellular) protein extracts from all four strains were combined with tyrosinase substrate L-DOPA, and enzymatic activities were observed by dopachrome production. While strain 303 showed enzymatic activity in the extracellular and intracellular protein extracts, the enzymatic activity in the whole cell protein extract was lower (Figure 2.4A). Interestingly, the tyrosinase activity demonstrated in 303 intracellular (whole cell) and extracellular protein extract could be inhibited by the copper chelation activity of KA *in vitro* (Figure 2.4A). Extracellular 299 tyrosinase activity required exogenous $CuSO_4$ to observe activity and was slower compared with 303 extracellular tyrosinase (Figure 2.4B), corresponding to delayed pigment production *in vitro* (Figure 2.1A). Intracellular 299 tyrosinase activity was similar in dynamics to

intracellular 303 and extra- cellular 299 tyrosinases (Figure 2.4B). Finally, intracellular and extracellular tyrosinase activity in 299 could not be inhibited with KA (Figure 2.4B). Under similar conditions, we did not detect an enzymatic activity in CL18 or 136 cultures (Figure 2.5). Together, our results suggest that while 299 and 303 both produce melanin, the tyrosinase required for its production has different activity and susceptibility to tyrosinase inhibitors in the two strains (Figure 2.4).

Survival and growth in the presence of phenolic compounds is improved in enriched colonizers

Microorganisms living close to and within plant roots must contend with root exudates, potentially including phenolic compounds such as SA and FA, which inhibit *Streptomyces* growth [44]. SA is measurable in *A. thaliana* roots and seedlings while both SA and FA are present in root exudates of *A. thaliana* and *Avena barbata* [8,28,33]. To determine if melanin-producing *Streptomyces* isolates have greater tolerance to these phenolic compounds, we counted surviving colonies of all isolates on solid MM containing varying concentrations of catechol, SA, and FA (Figure 2.6). As seen in Figure 2.6A, catechol challenge resulted in significantly more colonies for 303 and 299 than CL18 and 136 at 0.125 and 0.25 mM concentrations. When challenged with FA, a lignin degradation product at concentrations of 0.125, 0.5, and 1 mM, 303 grew significantly better than all other strains (Figure 2.6B)[77]. At concentrations of 0.125, 0.25, and 0.5 mM SA, 303 grew significantly better than 299, CL18, and 136 (Figure 2.6C). Therefore, *Streptomyces* isolates with two functional copies of tyrosinase are more resistant against phenolic compounds than isolates with no tyrosinases.

Isolate 303 also encodes enzymes in a *Streptomyces* SA degradation pathway while similar genes were not found in the genomes of 299, CL18, and 136 [28]. To determine if the increased resistance to SA on solid medium was due to increased growth of 303, or increased protection from SA, we added the tyrosinase inhibitor KA liquid minimal medium with SA and measured biomass accumulation after 6 days of growth. Biomass comparisons of 303 indicated that SA addition does not increase

growth (Figure 2.6D), suggesting that 303 does not have increased growth under these *in vitro* conditions, but rather is protected from SA.

Influence of SA and tyrosinase on seedling colonization

Our *in vitro* assays demonstrate that SA directly prevents *Streptomyces* colony formation (Figure 2.6A to C). To determine if SA negatively influences *Streptomyces* isolate seedling colonization, 0.1 mM SA was added to seedlings during a 14-day colonization experiment. Isolates 303 and 299, which have functional tyrosinases, were still able to significantly colonize seedlings (Figure 2.7A). However, CL18, which does not have a functional tyrosinase, did not colonize significantly higher than the no bacteria control (Figure 2.7A). To establish that *Streptomyces* tyrosinase was expressed and could therefore potentially protect microbes from SA during colonization, we performed RT-PCR on *A. thaliana* seedlings 10 days after inoculation with 303 using 303 *melC2* specific primers. Thus, we were able to demonstrate expression in 303 inoculated seedlings, which could not be detected in uninoculated seedlings controls (Figure 2.8). Together, we see that when SA is applied to seedlings during colonization, 303 and 299 with their functional MelC and MelD maintain their colonization patterns, while CL18 and 136 do not.

In genome comparison of nine selected *Streptomyces* isolates, we determined that several isolates from Poplar trees in Oregon shared a high degree of identity with our strains (Figure 2.3B). We found that OV320 and OV308 also produced melanin in vitro, had two identified copies of tyrosinase in their genomes, and exhibited similar intracellular tyrosinase activity to 303 and 299 (Figure 2.9). OK210 did not produce melanin *in vitro* and did not encode any tyrosinase in its genome. When *A. thaliana* seedlings were grown with these isolates for 14 days, we observed that OV320 and OV308 colonized significantly better than OK210 (Figure 2.7B), as predicted from their closely related strains 303, 299, and 136 (Figure 2.3B). The level of colonization when SA was added to these mono-associations with seedlings was also similar to their close relatives with OV320 and OV308 maintaining significant colonization, despite SA

presence. Further, as with 136, OK210 is not significantly different from OV320 and OV308 under these stressful colonization conditions (Figure 2.7C). Finally, we also colonized seedlings with strain YR375, which was isolated from a Poplar tree in North Carolina. This strain sporadically made melanin *in vitro* and only encoded a single tyrosinase gene, which fell in the same clade as *melD* (Figure 2.3C). Because *melD* is the predicted intracellular copy of tyrosinase in *S. scabiei* [44], we suspect the sporadic melanin production observed occurred when cells lysed during *in vitro* growth. We observed sporadic colonization with this isolate, which was significantly lower than OV320 and OV308, but not significantly different from the no bacteria control or OK210 (Figure 2.7B). When we investigated gene clusters shared within the genomes of 303, OV320, 299, OV308, and *S. scabiei*, but not YR375, CL18, 136, or OK210, we observed that the second copy of the *mel* operon, which encodes the extracellular MelC tyrosinase was exclusively shared by those strains with significantly higher colonization of *A. thaliana* seedlings, even when SA was present.

374 shows enhanced plant association in mono-association

Colony forming units for *Brevundimonas sp.* 374 inoculated on axenic Arabidopsis plants showed enhanced colonization relative to other strains studied in mono-association. Colonization numbers exceed the colonization capability of 303 and 299 *Streptomyces* strains and indicate some level of increased root association capability upwards of 10^8 CFU/g (Figure 2.10). While there are no major changes in biomass or root morphology, 374 does give a look into what genes provide enhanced colonization and highlights the need for research into the organism's genome.

374 genomic investigation reveals pigment producing carotenoid genes

Genome investigation into isolate 374 showed 2 Biosynthetic Gene Clusters (BGCs) that encode predicted secondary metabolites within the organism: a bacteriocin and a terpene annotated with phytoene and lycopene genes. The terpene genes showed homology with known carotenoid pigments produced by many bacterial and plant organisms, which was supported by a bright orange pigment when the isolate is

grown on nutrient rich media. Within the BGC, there are two core biosynthetic genes: a lycopene cyclase that transcribes a protein with homology to known CrtY, and a phytoene synthase family protein with homology to protein CrtB. Therefore, for these experiments the genes within 374 will be identified by their discovered counterparts as *crtY* and *crtB*. The predicted carotenoid operon with core genes is depicted in Figure 2.11.

***Carbon source affects carotenoid production of 374* in vitro**

To detect the effect of carbon source on 374 carotenoid production, M9 media was supplemented with different carbon sources, with and without $CaCl_2$ and with and without casamino acids. When amino acids were added to the media, regardless of carbon source, bright orange cells were observed indicating the presence of the carotenoid pigment (Table 2.4). However, in media supplemented with $CaCl_2$ but without amino acids, 374 produced visibly white colonies on plate media depending on carbon source (Table 2.4). Plates supplemented with glycerol, lactose, and sucrose all appeared white while glucose and fructose both produced orange colonies (Table 2.4). In this way, carotenoid production likely depends on carbon source availability as a way to increase or decrease overall carotenoid production.

***Carotenoid expression detected* in vivo**

To test the ability of 374 to produce the carotenoid *in vivo* with a plant host, RT-PCR was performed on axenic Arabidopsis inoculated with 374. Amplification was observed for both *crtY* and *crtB* genes, indicating that while 374 is colonizing the plant host, it is the expression of both of these genes involved in carotenoid production. This experiment was performed at 4-day and 7-day timepoints, with expression observed at both times (data not shown). Therefore, expression appears at multiple times throughout the colonization process of 374 with Arabidopsis.

Carotenoid production does not impact colonization of 374 with Arabidopsis

Following mutant generation of 374-166, about 5,000 mutants were screened for signs of pigment deficiency. Pigment mutants, ranging from a faint orange to white colonies, were verified with 16S sequencing and subsequently colonized with Arabidopsis to test impacts on colonization with visually deficient pigment production. Isolates' DNA was extracted after the colonization assay as well and further verified using 16S rRNA gene sequencing to ensure isolates were *Brevundimonas* strains. Across each mutant and Wild-Type (WT), there was no significant difference between colonization numbers across isolates (Figure 2.12). To further verify these results, the operon will need to be sequenced to locate the where the transposon insertion site is or arbitrary PCR performed to detect which specific genes were impacted. Thus, indicating no major effect of pigment production on colonization capability. While this contradicts the carotenoid deficient Pantoea sp. YR343 with decreased colonization capability, it may reflect the importance of carotenoid-producing mechanisms behind pigment production, as opposed to the pigment itself. Furthermore, it may be explained by the difference in carotenoid operons between the organisms. Also, this experiment used a fluorescent light in the growth chamber, while one with UV may highlight the benefit of the carotenoid production more favorably. However, this result is in line with a different *Pantoea* sp. R4, in which the carotenoid mutant did not show a difference in colonization phenotype [87].

DISCUSSION

Streptomyces species and select Proteobacteria are capable of colonizing the roots of a wide variety of plant species [12–16,19,28] in geographically and geologically diverse soils [78], emphasizing the need to understand their assembly into the root microbiome. Select *Streptomyces* strains have been identified as plant growth promoting and even disease suppressive [18], highlighting their potential applications in agriculture. Although microbial activities associated with root colonization for more predominant taxa, including Proteobacteria, have been elucidated, specific functions involved in root microbiome assembly mechanisms for less abundant microbes, such as *Streptomyces* are largely unexplored [18,21,79,80]. Here, we begin to investigate a set

of plant-associated *Streptomyces* isolates and a Proteobacteria isolate and identify genes in each that may influence early stages of colonization in seedlings.

Based on our ability to distinguish *Streptomyces* strains by degree of root and seedling colonization, we hypothesized that genomic differences would explain strain variation. Our comparative genomic analyses suggest distinct differences between *Streptomyces* isolates. These findings highlight that functional conclusions based on genus- level abundance from 16S rRNA gene amplicon studies inadequately capture the organisms' potential, as previously described for plant- associated *Pseudomonas* strains [81]. Further, including the plant pathogen *S. scabiei* 87.22 in our genomic comparisons revealed shared genetic factors contributing to increased seedling colonization in our nonpathogenic, melanin- producing *Streptomyces* isolates. Interestingly, Beausejour and Beaulieu [46] found that *S. scabies* virulence and colonization was reduced in mutants that lost the ability to make melanin. Beyond their role in melanin production, the tyrosinase enzymes encoded by *Streptomyces* are capable of oxidizing various phenolic compounds, including SA and FA, into their quinone form [44]. The data we present here using phenolic compounds previously shown to induce ROS production suggest that plant-associated strains living on or near roots with multiple tyrosinases may better resist phenolic root exudates during colonization[29,82].

Although SA is not assimilated by *Streptomyces* during *A. thaliana* colonization, it does influence *Streptomyces* assembly into a mature root microbiome through the immune responses or direct antimicrobial activity [28,35]. In SA-containing inoculated liquid medium, KA did not significantly influence 303 biomass accumulation, suggesting that there are other mechanisms to alleviate SA-induced stress, such as the previously identified SA degradation pathway in 303 or other tyrosinase products [28]. Taken together, our genomic, *in vitro*, and in *vivo* findings emphasize that 299 and 303 tyrosinases have differential enzyme coding sequences, substrates, and products, supporting strain-specific SA-induced oxidative stress survival adaptations. A critical

next step is defining the role of melanin and/or MelC tyrosinase is the generation of a targeted mutant strain. Further, such phenolic compounds are likely just one of many potential selective pressures imposed by the plant host.

Beyond tyrosinases and melanin-pigment producing genes in *Streptomyces*, carotenoid pigment producing genes in a Proteobacteria shows promise in enhancing plant root association. Here, a Proteobacteria, *Brevundimonas sp. 374*, shows colonization numbers near the ability of *Streptomyces* strains 303 and 299 in mono-association. The genes responsible for the pigment production, *crtY* and *crtB*, are both expressed during root colonization. While it is not definitively known what advantage the pigment is bestowing on the microbe, it may be a role similar to that seen in *Streptomyces* strains carrying melanin-producing genes due to the similarity in enzyme function. 374-166 mutants that were generated via transposon insertion were used to colonize Arabidopsis to see if pigment production impacted colonization (Figure 2.12). These mutants, while white, still require arbitrary PCR and verification of insert location. While there does not appear to be an impact of overall pigment production on plant colonization, there may be other genes involved in the process of pigment production at work. Investigation into a pigment deficient *Pantoea* showed the lack of carotenoid caused membrane physiology changes, lower IAA secretion, and increased sensitivity to ROS with a decrease in plant colonization [55]. Carotenoids have been linked to antioxidant capability and in plant health, highlighting their useful not only to plants but to human populations [83]. Increasing carotenoid production in plants and in food provides a great nutritional benefit to humans and in malnourished countries [83]. There is still much unknown about carotenoid functionality and importance in microbial communities. Therefore, studying carotenoids in this system provides a dual benefit of understanding plant association with microbes and in beneficial microbially produced compounds.

Previous studies established that genomes of plant-associated bacteria were larger than the genomes of non-plant-associated bacteria[84], which might contain a

number of genes to aid in the transition of living in bulk soil to within plant tissue. Likewise, we found that the *Streptomyces* isolates that colonize plants better have larger genomes coding for a wide range of potential functions. We chose to focus on *mel* genes based on a clear in vitro phenotype, widespread occurrence in environmental *Streptomyces* isolates, and the potential links to mitigating oxidative stress. Our data suggest that during plant colonization, melanin- producing strains are protected against phenolic compounds commonly found in the root-soil interface during colonization [8,33,34,77,85,86]. Likewise, this may be a similar effect seen in a Proteobacteria strain that harbors carotenoid-producing genes. Although our four additional plant-associated *Streptomyces* strains (OV320, OV308, YR375, and OK210) were isolated from trees in Oregon and North Carolina, their colonization patterns of *A. thaliana* seedlings correlate with their number of tyrosinase gene copies with significantly higher colonization in those isolates that contain *melC*, not just *melD*. Previous studies noted that *melD* was more common than *melC* among environmental *Streptomyces* [44]. The impact of this finding is particularly interesting given that melanins are produced by a range of other soil-isolated fungi and bacteria [37,42,57]. Understanding this new context for melanin production advances our understanding of the complex process of root microbiome assembly and manipulation.

As we seek new strategies to tackle the challenges of climate change-induced crop decline, we look toward the potential of the plant microbiome. Recently, plant drought resistance bacterial community studies identified Actinobacteria and more specifically *Streptomyces* as root enriched in drought conditions [21,22]. Similarly, Proteobacteria are seen commonly root enriched even though they are more variable between taxa [13,28]. In order to more fully understand microbial capabilities in a microbiome, additional strain- level genomic and *in situ* studies are essential. Thus, we suggest the power of linking taxonomic identification and abundances to distinct strain gene comparisons and product exploration. Together our findings provide opportunities for harnessing the power of *Streptomyces* to improve plant health and more broadly enhance agricultural applications and crop productivity. Similarly, these findings

advance our understanding of what microbial genes are responsible for enhanced root association and provide direction in the discovery of other potential genes of interest.

ACKNOWLEDGEMENTS

Thank you to current and former members of the Lebeis laboratory for useful discussions, especially Katherine Moccia, Caleb Whitley, Lizzy Denison, and Jake Massey. The *Streptomyces* stains were originally isolated in the laboratories of Jeffery Dangl at the University of North Carolina and Dale Pelletier at Oak Ridge National Laboratory. The chemical analysis of melanin was performed at the Biological and Small Molecule Mass Spectrometry Core at the University of Tennessee.

REFERENCES

1. Coyte, K.Z., Schluter, J., and Foster, K.R. (2015). The ecology of the microbiome: Networks, competition, and stability. Science *350*, 663–666.
2. Hibbing, M.E., Fuqua, C., Parsek, M.R., and Peterson, S.B. (2010). Bacterial competition: surviving and thriving in the microbial jungle. Nat. Rev. Microbiol. *8*, 15–25.
3. Wei, Z., Yang, T., Friman, V.-P., Xu, Y., Shen, Q., and Jousset, A. (2015). Trophic network architecture of root-associated bacterial communities determines pathogen invasion and plant health. Nat. Commun. *6*, 8413.
4. Jousset, A., Schulz, W., Scheu, S., and Eisenhauer, N. (2011). Intraspecific genotypic richness and relatedness predict the invasibility of microbial communities. ISME J. *5*, 1108–1114.
5. Lareen, A., Burton, F., and Schäfer, P. (2016). Plant root-microbe communication in shaping root microbiomes. Plant Mol. Biol. *90*, 575–587.
6. Fiegna, F., and Velicer, G.J. (2005). Exploitative and hierarchical antagonism in a cooperative bacterium. PLoS Biol. *3*, e370.
7. Sasse, J., Martinoia, E., and Northen, T. (2018). Feed Your Friends: Do Plant Exudates Shape the Root Microbiome? Trends Plant Sci. *23*, 25–41.
8. Zhalnina, K., Louie, K.B., Hao, Z., Mansoori, N., da Rocha, U.N., Shi, S., Cho, H., Karaoz, U., Loqué, D., Bowen, B.P., *et al.* (2018). Dynamic root exudate chemistry and microbial substrate preferences drive patterns in rhizosphere microbial community assembly. Nature Microbiology *3*, 470–480. Available at: http://dx.doi.org/10.1038/s41564-018-0129-3.
9. Lakshmanan, V., Selvaraj, G., and Bais, H.P. (2014). Functional soil microbiome: belowground solutions to an aboveground problem. Plant Physiol. *166*, 689–700.
10. van der Heijden, M.G.A., and Hartmann, M. (2016). Networking in the Plant Microbiome. PLoS Biol. *14*, e1002378.
11. Sheth, R.U., Cabral, V., Chen, S.P., and Wang, H.H. (2016). Manipulating Bacterial Communities by in situ Microbiome Engineering. Trends Genet. *32*, 189–200.
12. Bonaldi, M., Chen, X., Kunova, A., Pizzatti, C., Saracchi, M., and Cortesi, P. (2015).

Colonization of lettuce rhizosphere and roots by tagged Streptomyces. Front. Microbiol. *6*, 25.

13. Bulgarelli, D., Rott, M., Schlaeppi, K., Ver Loren van Themaat, E., Ahmadinejad, N., Assenza, F., Rauf, P., Huettel, B., Reinhardt, R., Schmelzer, E., *et al.* (2012). Revealing structure and assembly cues for Arabidopsis root-inhabiting bacterial microbiota. Nature *488*, 91–95.
14. Edwards, J., Johnson, C., Santos-Medellín, C., Lurie, E., Podishetty, N.K., Bhatnagar, S., Eisen, J.A., and Sundaresan, V. (2015). Structure, variation, and assembly of the root-associated microbiomes of rice. Proc. Natl. Acad. Sci. U. S. A. *112*, E911–20.
15. Lundberg, D.S., Lebeis, S.L., Paredes, S.H., Yourstone, S., Gehring, J., Malfatti, S., Tremblay, J., Engelbrektson, A., Kunin, V., Rio, T.G. del, *et al.* (2012). Defining the core Arabidopsis thaliana root microbiome. Nature *488*, 86–90.
16. Peiffer, J.A., Spor, A., Koren, O., Jin, Z., Tringe, S.G., Dangl, J.L., Buckler, E.S., and Ley, R.E. (2013). Diversity and heritability of the maize rhizosphere microbiome under field conditions. Proc. Natl. Acad. Sci. U. S. A. *110*, 6548–6553.
17. Seipke, R.F., Kaltenpoth, M., and Hutchings, M.I. (2012). Streptomyces as symbionts: an emerging and widespread theme? FEMS Microbiol. Rev. *36*, 862–876.
18. Viaene, T., Langendries, S., Beirinckx, S., Maes, M., and Goormachtig, S. (2016). Streptomyces as a plant's best friend? FEMS Microbiol. Ecol. *92*. Available at: http://dx.doi.org/10.1093/femsec/fiw119.
19. Yeoh, Y.K., Paungfoo-Lonhienne, C., Dennis, P.G., Robinson, N., Ragan, M.A., Schmidt, S., and Hugenholtz, P. (2016). The core root microbiome of sugarcanes cultivated under varying nitrogen fertilizer application. Environ. Microbiol. *18*, 1338–1351.
20. Bignell, D.R.D., Fyans, J.K., and Cheng, Z. (2014). Phytotoxins produced by plant pathogenic Streptomyces species. J. Appl. Microbiol. *116*, 223–235.
21. Fitzpatrick, C.R., Copeland, J., Wang, P.W., Guttman, D.S., Kotanen, P.M., and Johnson, M.T.J. (2018). Assembly and ecological function of the root microbiome

across angiosperm plant species. Proc. Natl. Acad. Sci. U. S. A. *115*, E1157–E1165.

22. Xu, S., Huang, S., Luan, Z., Chen, T., Wei, Y., Xing, M., Li, Y., Du, C., Wang, B., Zheng, F., *et al.* (2018). Farnesoid X receptor is essential for the survival of renal medullary collecting duct cells under hypertonic stress. Proc. Natl. Acad. Sci. U. S. A. *115*, 5600–5605.
23. Moon, C.D., Young, W., Maclean, P.H., Cookson, A.L., and Bermingham, E.N. (2018). Metagenomic insights into the roles of Proteobacteria in the gastrointestinal microbiomes of healthy dogs and cats. Microbiologyopen *7*, e00677.
24. Hofmann, A., Fischer, D., Hartmann, A., and Schmid, M. (2014). Colonization of plants by human pathogenic bacteria in the course of organic vegetable production. Frontiers in Microbiology *5*. Available at: http://dx.doi.org/10.3389/fmicb.2014.00191.
25. Walker, T.S., Bais, H.P., Déziel, E., Schweizer, H.P., Rahme, L.G., Fall, R., and Vivanco, J.M. (2004). Pseudomonas aeruginosa-plant root interactions. Pathogenicity, biofilm formation, and root exudation. Plant Physiol. *134*, 320–331.
26. Naqqash, T., Imran, A., Hameed, S., Shahid, M., Majeed, A., Iqbal, J., Hanif, M.K., Ejaz, S., and Malik, K.A. (2020). First report of diazotrophic Brevundimonas spp. as growth enhancer and root colonizer of potato. Scientific Reports *10*. Available at: http://dx.doi.org/10.1038/s41598-020-69782-6.
27. Hu, L., Robert, C.A.M., Cadot, S., Zhang, X., Ye, M., Li, B., Manzo, D., Chervet, N., Steinger, T., van der Heijden, M.G.A., *et al.* (2018). Root exudate metabolites drive plant-soil feedbacks on growth and defense by shaping the rhizosphere microbiota. Nature Communications *9*. Available at: http://dx.doi.org/10.1038/s41467-018-05122-7.
28. Lebeis, S.L., Paredes, S.H., Lundberg, D.S., Breakfield, N., Gehring, J., McDonald, M., Malfatti, S., del Rio, T.G., Jones, C.D., Tringe, S.G., *et al.* (2015). Salicylic acid modulates colonization of the root microbiome by specific bacterial taxa. Science *349*, 860–864. Available at: http://dx.doi.org/10.1126/science.aaa8764.
29. Bosund, I., Tilander, K., Åselius, J., Refn, S., and Westin, G. (1960). The

Bacteriostatic Action of Benzoic and Salicylic Acids. II. The Effect on Acetate Metabolism. Acta Chemica Scandinavica *14*, 111–125. Available at: http://dx.doi.org/10.3891/acta.chem.scand.14-0111.

30. Yang, L., Li, B., Zheng, X.-Y., Li, J., Yang, M., Dong, X., He, G., An, C., and Deng, X.W. (2015). Salicylic acid biosynthesis is enhanced and contributes to increased biotrophic pathogen resistance in Arabidopsis hybrids. Nat. Commun. *6*, 7309.
31. Rivas-San Vicente, M., and Plasencia, J. (2011). Salicylic acid beyond defence: its role in plant growth and development. J. Exp. Bot. *62*, 3321–3338.
32. Studham, M.E., and MacIntosh, G.C. (2012). Phytohormone signaling pathway analysis method for comparing hormone responses in plant-pest interactions. BMC Res. Notes *5*, 392.
33. Chaparro, J.M., Badri, D.V., Bakker, M.G., Sugiyama, A., Manter, D.K., and Vivanco, J.M. (2013). Root exudation of phytochemicals in Arabidopsis follows specific patterns that are developmentally programmed and correlate with soil microbial functions. PLoS One *8*, e55731.
34. Strehmel, N., Böttcher, C., Schmidt, S., and Scheel, D. (2014). Profiling of secondary metabolites in root exudates of Arabidopsis thaliana. Phytochemistry *108*, 35–46.
35. Worsley, S.F., Macey, M.C., Newitt, J.T., Patrick, E., Yu, D.W., Wilkinson, B., Murrell, C., and Hutchings, M.I. (2019). Investigating the role of exudates in recruiting Streptomyces bacteria to the Arabidopsis thaliana root microbiome. bioRxiv 532309.
36. Barka, E.A., Vatsa, P., Sanchez, L., Gaveau-Vaillant, N., Jacquard, C., Meier-Kolthoff, J.P., Klenk, H.-P., Clément, C., Ouhdouch, Y., and van Wezel, G.P. (2016). Taxonomy, Physiology, and Natural Products of Actinobacteria. Microbiol. Mol. Biol. Rev. *80*, 1–43.
37. Eisenman, H.C., and Casadevall, A. (2012). Synthesis and assembly of fungal melanin. Appl. Microbiol. Biotechnol. *93*, 931–940.
38. Emami, S.A., Yazdian-Robati, R., Sadeghi, M., Baharara, J., Amini, E., Salek, F., and Tayarani-Najaran, Z. (2017). Inhibitory effects of different fractions of Nepeta

satureioides on melanin synthesis through reducing oxidative stress. Res. Pharm. Sci. *12*, 160–167.

39. Manivasagan, P., Venkatesan, J., Sivakumar, K., and Kim, S.-K. (2013). Actinobacterial melanins: current status and perspective for the future. World J. Microbiol. Biotechnol. *29*, 1737–1750.
40. Valverde, P., Healy, E., Jackson, I., Rees, J.L., and Thody, A.J. (1995). Variants of the melanocyte–stimulating hormone receptor gene are associated with red hair and fair skin in humans. Nat. Genet. *11*, 328–330.
41. Zhang, L., Martin, A., Perry, M.W., van der Burg, K.R.L., Matsuoka, Y., Monteiro, A., and Reed, R.D. (2017). Genetic Basis of Melanin Pigmentation in Butterfly Wings. Genetics *205*, 1537–1550.
42. Plonka, P.M., and Grabacka, M. (2006). Melanin synthesis in microorganisms--biotechnological and medical aspects. Acta Biochim. Pol. *53*, 429–443.
43. Brenner, M., and Hearing, V.J. (2008). The protective role of melanin against UV damage in human skin. Photochem. Photobiol. *84*, 539–549.
44. Yang, H.-Y., and Chen, C.W. (2009). Extracellular and intracellular polyphenol oxidases cause opposite effects on sensitivity of Streptomyces to phenolics: a case of double-edged sword. PLoS One *4*, e7462.
45. Nosanchuk, J.D., and Casadevall, A. (2003). The contribution of melanin to microbial pathogenesis. Cell. Microbiol. *5*, 203–223.
46. Beauséjour, J., and Beaulieu, C. (2004). Characterization of Streptomyces scabies mutants deficient in melanin biosynthesis. Can. J. Microbiol. *50*, 705–709.
47. Bernan, V., Filpula, D., Herber, W., Bibb, M., and Katz, E. (1985). The nucleotide sequence of the tyrosinase gene from Streptomyces antibioticus and characterization of the gene product. Gene *37*, 101–110.
48. Katz, E., Thompson, C.J., and Hopwood, D.A. (1983). Cloning and expression of the tyrosinase gene from Streptomyces antibioticus in Streptomyces lividans. J. Gen. Microbiol. *129*, 2703–2714.
49. Lee, Y.H., Chen, B.F., Wu, S.Y., Leu, W.M., Lin, J.J., Chen, C.W., and Lo, S.C. (1988). A trans-acting gene is required for the phenotypic expression of a

tyrosinase gene in Streptomyces. Gene *65*, 71–81.

50. Chen, L.Y., Leu, W.M., Wang, K.T., and Lee, Y.H. (1992). Copper transfer and activation of the Streptomyces apotyrosinase are mediated through a complex formation between apotyrosinase and its trans-activator MelC1. Journal of Biological Chemistry *267*, 20100–20107. Available at: http://dx.doi.org/10.1016/s0021-9258(19)88671-4.
51. Leu, W.M., Chen, L.Y., Liaw, L.L., and Lee, Y.H. (1992). Secretion of the Streptomyces tyrosinase is mediated through its trans-activator protein, MelC1. J. Biol. Chem. *267*, 20108–20113.
52. Sun, T., Yuan, H., Cao, H., Yazdani, M., Tadmor, Y., and Li, L. (2018). Carotenoid Metabolism in Plants: The Role of Plastids. Mol. Plant *11*, 58–74.
53. Reis-Mansur, M.C.P.P., Cardoso-Rurr, J.S., Silva, J.V.M.A., de Souza, G.R., Cardoso, V. da S., Mansoldo, F.R.P., Pinheiro, Y., Schultz, J., Lopez Balottin, L.B., da Silva, A.J.R., *et al.* (2019). Carotenoids from UV-resistant Antarctic Microbacterium sp. LEMMJ01. Sci. Rep. *9*, 9554.
54. Bible, A.N., Fletcher, S.J., Pelletier, D.A., Schadt, C.W., Jawdy, S.S., Weston, D.J., Engle, N.L., Tschaplinski, T., Masyuko, R., Polisetti, S., *et al.* (2016). A Carotenoid-Deficient Mutant in Pantoea sp. YR343, a Bacteria Isolated from the Rhizosphere of Populus deltoides, Is Defective in Root Colonization. Front. Microbiol. *7*, 491.
55. Vijaya Kumar, S., Abraham, P.E., Hurst, G.B., Chourey, K., Bible, A.N., Hettich, R.L., Doktycz, M.J., and Morrell-Falvey, J.L. (2020). A carotenoid-deficient mutant of the plant-associated microbe Pantoea sp. YR343 displays an altered membrane proteome. Sci. Rep. *10*, 14985.
56. Bertani, G. (1951). Studies on lysogenesis. I. The mode of phage liberation by lysogenic Escherichia coli. J. Bacteriol. *62*, 293–300.
57. Drewnowska, J.M., Zambrzycka, M., Kalska-Szostko, B., Fiedoruk, K., and Swiecicka, I. (2015). Melanin-Like Pigment Synthesis by Soil Bacillus weihenstephanensis Isolates from Northeastern Poland. PLoS One *10*, e0125428.
58. Ito, S., and Wakamatsu, K. (1998). Chemical degradation of melanins: application to identification of dopamine-melanin. Pigment Cell Res. *11*, 120–126.

59. Clasquin, M.F., Melamud, E., and Rabinowitz, J.D. (2012). LC-MS data processing with MAVEN: a metabolomic analysis and visualization engine. Curr. Protoc. Bioinformatics *Chapter 14*, Unit14.11.
60. Chen, I.-M.A., Markowitz, V.M., Chu, K., Palaniappan, K., Szeto, E., Pillay, M., Ratner, A., Huang, J., Andersen, E., Huntemann, M., *et al.* (2017). IMG/M: integrated genome and metagenome comparative data analysis system. Nucleic Acids Res. *45*, D507–D516.
61. Eren, A.M., Murat Eren, A., Esen, Ö.C., Quince, C., Vineis, J.H., Morrison, H.G., Sogin, M.L., and Delmont, T.O. (2015). Anvi'o: an advanced analysis and visualization platform for 'omics data. PeerJ *3*, e1319. Available at: http://dx.doi.org/10.7717/peerj.1319.
62. Enright, A.J., Van Dongen, S., and Ouzounis, C.A. (2002). An efficient algorithm for large-scale detection of protein families. Nucleic Acids Res. *30*, 1575–1584.
63. Galperin, M.Y., Makarova, K.S., Wolf, Y.I., and Koonin, E.V. (2015). Expanded microbial genome coverage and improved protein family annotation in the COG database. Nucleic Acids Res. *43*, D261–9.
64. Kearse, M., Moir, R., Wilson, A., Stones-Havas, S., Cheung, M., Sturrock, S., Buxton, S., Cooper, A., Markowitz, S., Duran, C., *et al.* (2012). Geneious Basic: an integrated and extendable desktop software platform for the organization and analysis of sequence data. Bioinformatics *28*, 1647–1649.
65. Katoh, K., Misawa, K., Kuma, K.-I., and Miyata, T. (2002). MAFFT: a novel method for rapid multiple sequence alignment based on fast Fourier transform. Nucleic Acids Res. *30*, 3059–3066.
66. Miller, M.A., Pfeiffer, W., and Schwartz, T. (2010). Creating the CIPRES Science Gateway for inference of large phylogenetic trees. 2010 Gateway Computing Environments Workshop (GCE). Available at: http://dx.doi.org/10.1109/gce.2010.5676129.
67. Ciccarelli, F.D., Doerks, T., von Mering, C., Creevey, C.J., Snel, B., and Bork, P. (2006). Toward automatic reconstruction of a highly resolved tree of life. Science *311*, 1283–1287.

68. Claus, H., and Decker, H. (2006). Bacterial tyrosinases. Syst. Appl. Microbiol. *29*, 3–14.
69. Chen, J.S., Wei, C.I., and Marshall, M.R. (1991). Inhibition mechanism of kojic acid on polyphenol oxidase. J. Agric. Food Chem. *39*, 1897–1901.
70. Chang, T.-S. (2009). An updated review of tyrosinase inhibitors. Int. J. Mol. Sci. *10*, 2440–2475.
71. Kieser, T., Bibb, M.J., Buttner, M.J., Chater, K.F., Hopwood, D.A., and Others (2000). Practical streptomyces genetics (John Innes Foundation Norwich).
72. Pigac, J., and Schrempf, H. (1995). A Simple and Rapid Method of Transformation of Streptomyces rimosus R6 and Other Streptomycetes by Electroporation. Appl. Environ. Microbiol. *61*, 352–356.
73. Tyurin, M., Starodubtseva, L., Kudryavtseva, H., Voeykova, T., and Livshits, V. (1995). Electrotransformation of germinating spores of Streptomyces spp. Biotechnol. Tech. *9*, 737–740.
74. Flett, F., Mersinias, V., and Smith, C.P. (1997). High efficiency intergeneric conjugal transfer of plasmid DNA from Escherichia coli to methyl DNA-restricting streptomycetes. FEMS Microbiol. Lett. *155*, 223–229.
75. Blin, K., Shaw, S., Steinke, K., Villebro, R., Ziemert, N., Lee, S.Y., Medema, M.H., and Weber, T. (2019). antiSMASH 5.0: updates to the secondary metabolite genome mining pipeline. Nucleic Acids Res. *47*, W81–W87.
76. Grigoriev, I.V., Nordberg, H., Shabalov, I., Aerts, A., Cantor, M., Goodstein, D., Kuo, A., Minovitsky, S., Nikitin, R., Ohm, R.A., *et al.* (2012). The genome portal of the Department of Energy Joint Genome Institute. Nucleic Acids Res. *40*, D26–32.
77. Kirby, R. (2005). Actinomycetes and Lignin Degradation. Adv. Appl. Microbiol. *58C*, 125–168.
78. Choudoir, M.J., Doroghazi, J.R., and Buckley, D.H. (2016). Latitude delineates patterns of biogeography in terrestrial Streptomyces. Environ. Microbiol. *18*, 4931–4945.
79. Jones, S.E., Ho, L., Rees, C.A., Hill, J.E., Nodwell, J.R., and Elliot, M.A. (2017). Streptomyces exploration is triggered by fungal interactions and volatile signals.

Elife *6*. Available at: http://dx.doi.org/10.7554/eLife.21738.

80. Yandigeri, M.S., Meena, K.K., Singh, D., Malviya, N., Singh, D.P., Solanki, M.K., Yadav, A.K., and Arora, D.K. (2012). Drought-tolerant endophytic actinobacteria promote growth of wheat (Triticum aestivum) under water stress conditions. Plant Growth Regul. *68*, 411–420.
81. Blakney, A.J.C., and Patten, C.L. (2011). A plant growth-promoting pseudomonad is closely related to the Pseudomonas syringae complex of plant pathogens. FEMS Microbiol. Ecol. *77*, 546–557.
82. Cheng, A.-X., Gou, J.-Y., Yu, X.-H., Yang, H., Fang, X., Chen, X.-Y., and Liu, C.-J. (2013). Characterization and ectopic expression of a populus hydroxyacid hydroxycinnamoyltransferase. Mol. Plant *6*, 1889–1903.
83. Alós, E., Rodrigo, M.J., and Zacarias, L. (2016). Manipulation of Carotenoid Content in Plants to Improve Human Health. Subcell. Biochem. *79*, 311–343.
84. Levy, A., Salas Gonzalez, I., Mittelviefhaus, M., Clingenpeel, S., Herrera Paredes, S., Miao, J., Wang, K., Devescovi, G., Stillman, K., Monteiro, F., *et al.* (2017). Genomic features of bacterial adaptation to plants. Nat. Genet. *50*, 138–150.
85. Bakker, M.G., Manter, D.K., Sheflin, A.M., Weir, T.L., and Vivanco, J.M. (2012). Harnessing the rhizosphere microbiome through plant breeding and agricultural management. Plant Soil *360*, 1–13.
86. Hartmann, A., Schmid, M., van Tuinen, D., and Berg, G. (2009). Plant-driven selection of microbes. Plant Soil *321*, 235–257.
87. Moccia, K., *More than the sum of their parts: Building a framework for understanding host-microbe interactions in Medicago sativa*, in *Microbiology*. 2020, University of Tennessee Knoxville.

APPENDIX: TABLES

Table 2. 1: This table provides a link between the Streptomyces strains that were used in these experiments.

Also, the identification numbers for the permanent draft genomes on IMG/ER (https://img.jgi.doe.gov/mer/).

Strain Abbreviation	Strain name	IMG Genome ID	Figure references
303	*Streptomyces sp.* 303MFCol5.2	2521172626	1,2,3,4,5
299	*Streptomyces canus* 299MFChir4.1	2521172643	1,2,3,4,5
CL18	*Streptomyces sp.*UNC401CLCol	2563366515	1,2,3,4,5
136	*Streptomyces sp.* 136MFCol5.1	2636416059	1,2,3,4,5
S. scabiei 87.22	*Streptomyces scabiei* 87.22	646564576	2
OV320	Actinobacteria bacterium OV320	2634166429	2 and 5
OV308	*Streptomyces mirabilis* OV308	2582581313	2 and 5
YR375	*Streptomyces sp.* YR375	2615840635	2 and 5
OK210	*Streptomyces sp.* OK210	2615840540	2 and 5

Table 2. 2 *Streptomyces'* genome investigation reveals divergent properties and biosynthetic product predictions.

Genome features include estimated size, GC content, number of scaffolds in the permanent draft genome, estimated gene numbers, the number of predicted copies of the *mel* operon, and if isolates produce a brown pigment in standard glucose-minimal salts liquid medium with Tiger's Milk, an amino acid cocktail with excess tyrosine. Y* indicates that YR375 occasionally produces a brown pigment in this medium while the other *Streptomyces* strains with *mel* operons consistently make a brown pigment. Each genome was estimated to be >99% complete by Anvi'o identification of four sets of bacterial single-copy gene collections.

Streptomyces Isolate	Genome Size (MB)	G+C Content	Scaffolds	Protein Coding Genes	Total Genes	*mel* operon copies	Pigment production
S. scabiei 87.22	10.2 MB	71%	1	8746	8841	2	Y
303	9.5 MB	71%	77	8387	8480	2	Y
OV320	10.1MB	71%	38	9082	9183	2	Y
299	10.5 MB	70%	116	9620	9710	2	Y
OV308	10.0MB	71%	81	9025	9126	2	Y
YR375	9.1MB	71%	122	7683	7795	1	Y*
CL18	7.3 MB	72%	49	6591	6677	0	N
136	7.8 MB	70%	31	6905	6991	0	N
OK210	8.1MB	70%	34	7183	7222	0	N

Table 2. 3: Average nucleotide identity and alignment fraction for plant-associated Streptomyces strains.

The level of average nucleotide identity (ANI) between isolates are shown above the grey diagonal line (darker shades of blue = higher shared identity, white =lower shared identity). The fraction of the genome that aligns between the isolates are shown below the grey diagonal line (darker shades of red = higher shared identity), white = lower shared identity. Because species are defined by ANI>96.5% and AF>60%, strains with common symbols are considered the same species (Varghese et al. 2015).

	OV308	299	303 ^	OV320 ^	YR375	CL18	136 *	OK210 *	
OK210 *	80.09	79.94	80.29	80.29	80.395	80.375	99.75		OK210 *
136 *	80.08	79.975	80.305	80.315	80.395	80.39		0.92	136 *
CL18	83.605	83.44	83.58	83.665	83.975		0.505	0.5	CL18
YR375	85.1	85.07	89.845	89.925		0.525	0.465	0.455	YR375
OV320 ^	85.145	84.965	97.385		0.62	0.56	0.48	0.465	OV320 ^
303 ^	84.93	84.865		0.845	0.635	0.575	0.495	0.485	303 ^
299	93.145		0.595	0.58	0.545	0.56	0.48	0.475	299
OV308		0.72	0.62	0.61	0.555	0.56	0.48	0.475	OV308
	OV308	299	303 ^	OV320 ^	YR375	CL18	136	OK210 *	

Table 2. 4: Changes in 374 pigment phenotype on minimal M9 media supplemented with different carbon sources and nutrients.

Carbon Source	M9 Only	M9 + CaCl2	M9 + Casamino acids	M9 + CaCl2 + Casamino acids
Glucose	Orange	Orange	Orange	Orange
Glycerol	No Growth	White	Orange	Orange
Lactose	No Growth	White	Orange	Orange
Fructose	No Growth	Orange	Orange	Orange
Sucrose	No Growth	White	Orange	Orange

APPENDIX: FIGURES

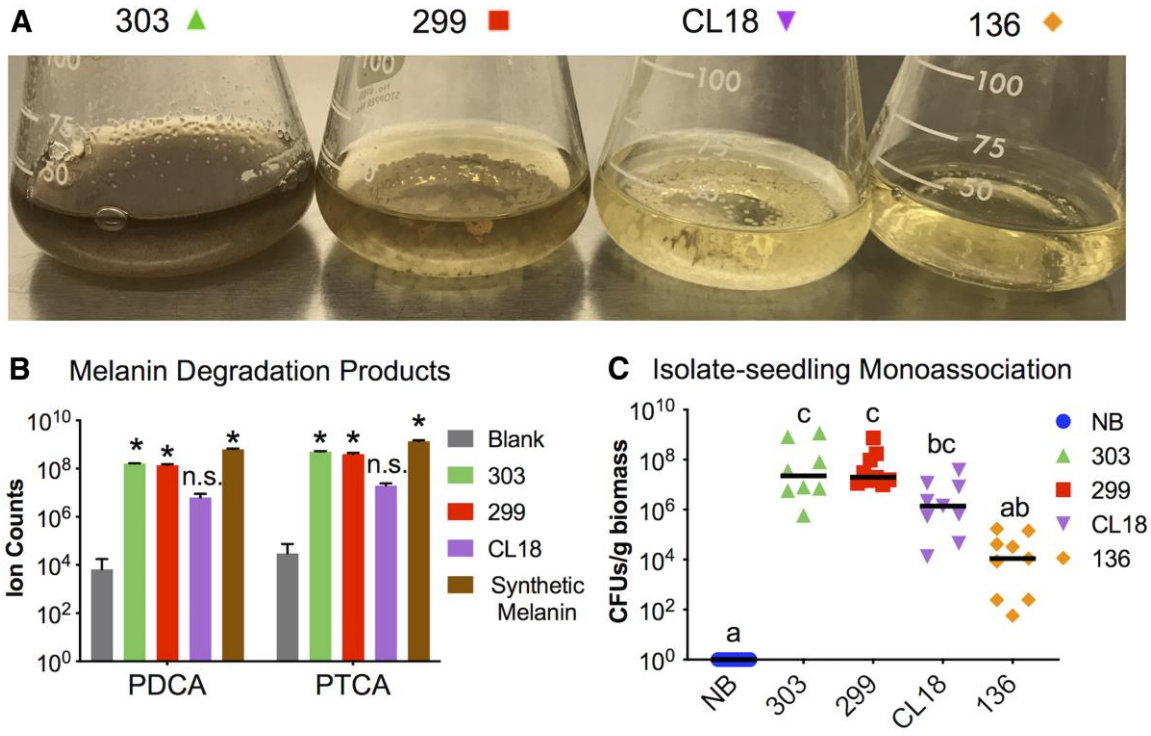

Figure 2. 1: *Streptomyces* strains 303 and 299 produce a pigment consistent with synthetic melanin.

A, Strains 303 (far left) and 299 (middle left) liquid cultures produce an extracellular pigment in lysogeny broth medium. B, Liquid chromatography-mass spectrometry of pigmented bacterial extracts indicate degradation components consistent with melanin (gray bars, n = 13), 303 extracts (green bars, n = 3), 299 extracts (red bars, n = 3), CL18 extracts (purple bars, n = 3), and synthetic melanin control (brown bars, n = 3). Ion counts normalized to mass digested means are displayed with standard deviation indicated by error bars. * Indicates significantly different from the blank controls ($P < 0.0001$), two-way analysis of variance with Dunnett's multiple comparison test. C, Axenic 7 day-old Col-0, wild-type seedlings were singly inoculated with each Streptomyces isolate (no bacteria control [NB, blue circles], 303 [green triangles], 299 [red squares], CL18 [purple triangles], or 136 [orange diamonds], n = 6 to 9) and grown for 14 days when seedling colonization level was determined. Different letters indicate statistical differences using a Kruskal-Wallis with Dunn's multiple comparison.

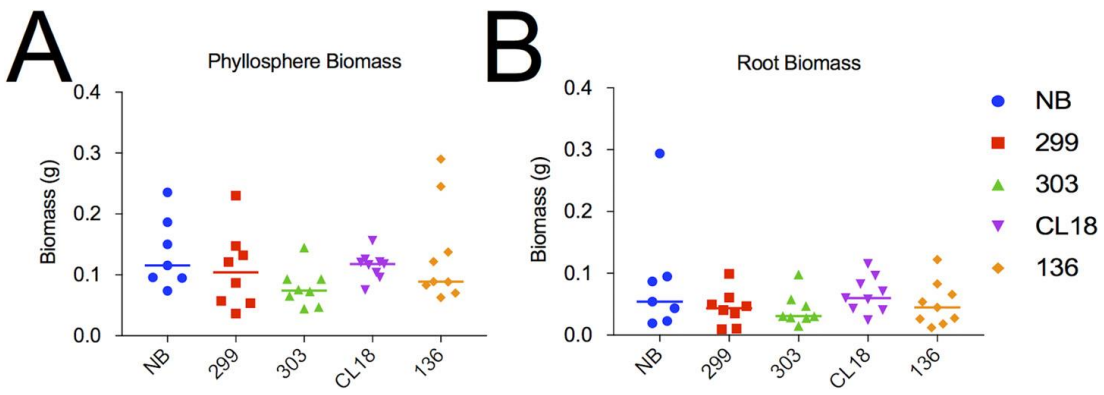

Figure 2. 2: *Streptomyces* strains do not alter *Arabidopsis thaliana* biomass. Biomass of phyllosphere (A) and roots (B) from plants inoculated with a single Streptomyces isolate (no bacteria control (NB, blue circles), 299 (red squares), 303 (green triangles), CL18 (purple triangles), 136 (orange diamonds)) grown for 8 weeks in pots with MES buffered MS medium was measured and did not significantly differ (n=7-10) by Kruskal- Wallis with a Dunn's multiple comparison.

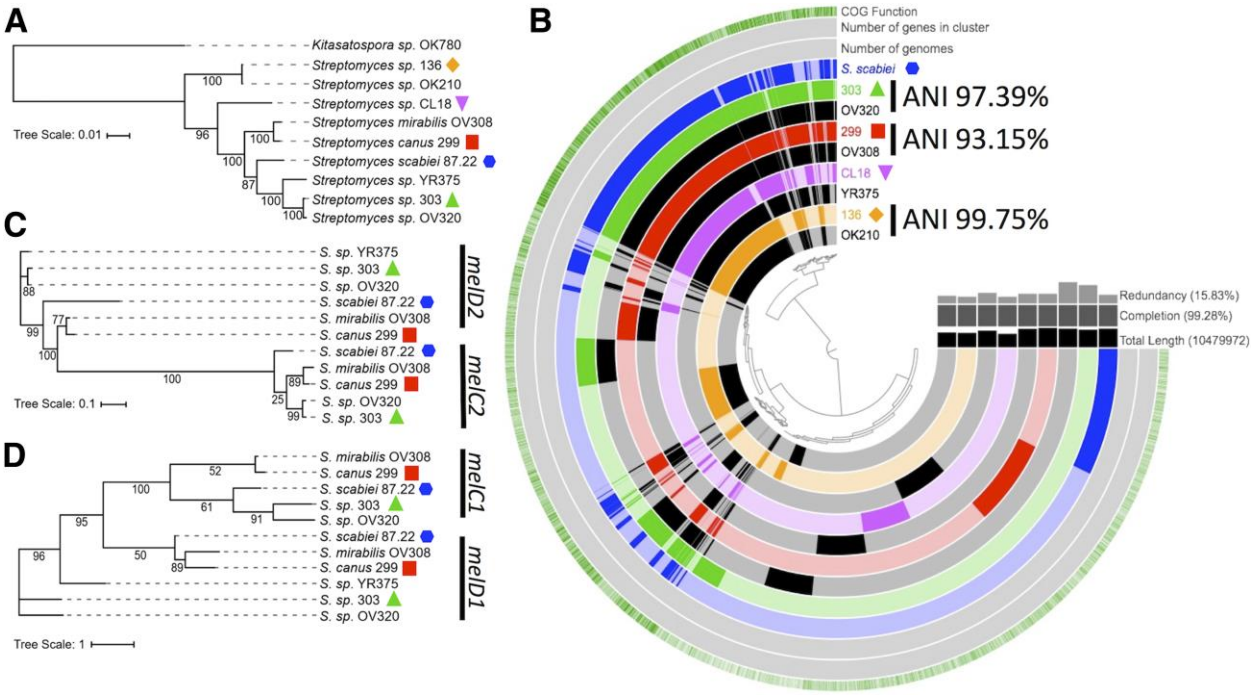

Figure 2. 3: Phylogenetic and pangenomic comparison of *Streptomyces* spp. indicate distinct phylogeny and overlapping genes consistent with melanin production.

Phylogenetic and pangenomic comparison of Streptomyces spp. indicate distinct phylogeny and overlapping genes consistent with melanin production. A, Phylogenetic tree built using a concatenated alignment of amino acid sequences for housekeeping genes trpB, gyrB, rpoB, atpD, and recA from nine Streptomyces strains and one outgroup (Kitasatospora sp. OK780) (maximum likelihood, bootstrap consensus values based on 100 iterations). B, Pangenomic comparison of nine Streptomyces isolates, including 136 (orange), CL18 (purple), 299 (red), 303 (green), and S. scabiei (blue). Maximum likelihood trees built using amino acid alignments of C, tyrosinase genes and D, tyrosinase helper genes from six pigment-producing Streptomyces reveal distinct clades that separate with a S. scabiei single annotated gene (melC1, melC2, melD1, and melD2) falling into each clade (bootstrap consensus values based on 100 iterations).

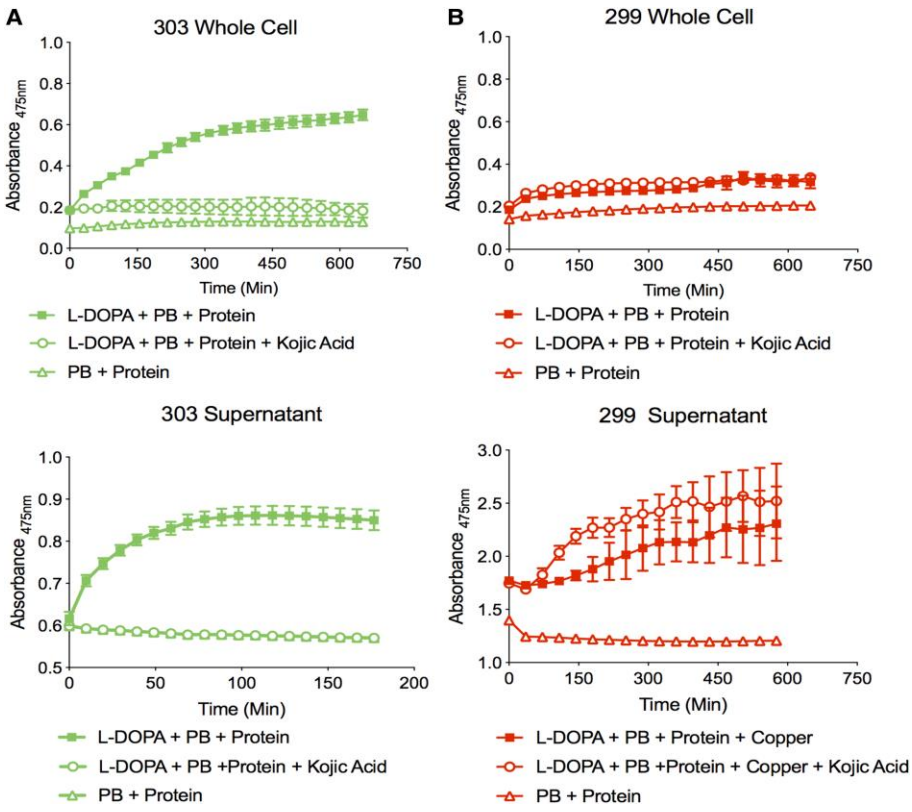

Figure 2. 4: Strain-specific tyrosinase activity in intracellular and extracellular protein extracts from 303 and 299 in vitro cultures.

Dopachrome production was measured by absorbance at 475 nm for three replicate cell pellet (top panels) and supernatant (bottom panels) protein extracts from A, 303 and B, 299, which were normalized by protein concentration following the addition of phosphate buffer alone (open triangles), phosphate buffer and L-DOPA (closed squares), or phosphate buffer, L-DOPA, and kojic acid (open circles). For 299 supernatant, 6 mM $CuSO_4$ was added to observe activity. The mean and standard deviation is displayed for each graph.

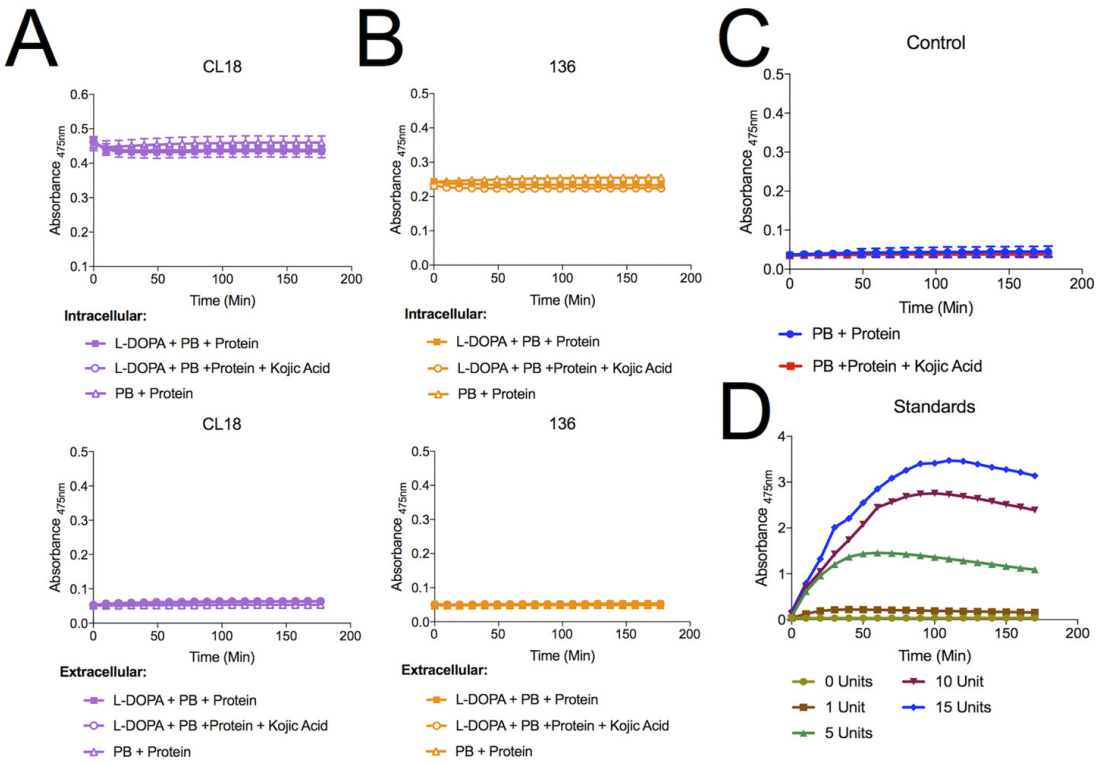

Figure 2. 5: Strain-specific tyrosinase activity in intracellular and extracellular protein extracts from CL18, 136, and tyrosinase control.

(A-B) Dopachrome production was measured by absorbance at 475 nm for 3 replicates for cell pellet (top panels) and supernatant (bottom panels) protein extracts from CL18 (A) and 136 (B) following the addition of phosphate buffer alone (open triangles), phosphate buffer and L-DOPA (closed squares), or phosphate buffer, L-DOPA, and kojic acid (open circles). (C) Phosphate buffer with isolate protein extracts alone and with kojic acid were used as negative controls. (D) Increasing amounts (0 units (green), 1 unit (brown), 5 units (green), 10 units (red), and 15 units (blue)) of purified tyrosinase were added to phosphate buffer and L-DOPA as a positive control for the tyrosinase assay. The mean and standard deviation is displayed for each graph.

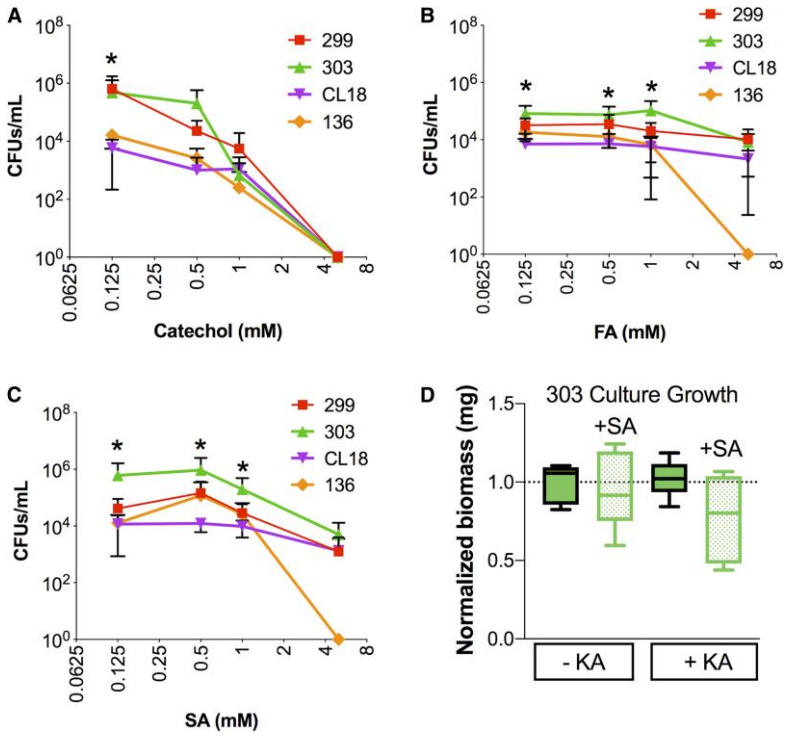

Figure 2. 6: Phenolic compound tolerance differs between *Streptomyces* isolate. Strains (303, green; 299, red; CL18, purple; and 136, orange) were grown on solid minimal media containing the indicated concentrations of A, catechol, B, ferulic acid (FA), or C, salicylic acid (SA). In A, * indicates 303 and 299 are significantly greater than CL18 and 136 according to two-way analysis of variance (ANOVA) and Fisher's least significant difference (LSD) (n = 6 to 9, $P < 0.05$). In B, * indicates 303 is significantly higher than 299, CL18, and 136 according to two-way ANOVA and Fisher's LSD, (n = 6 to 9, $P < 0.05$). In C, * indicates 303 is greater than 299, CL18, and 136 according to two-way ANOVA and Fisher's LSD (n = 6 to 9, $P < 0.05$). D, Biomass of 75 ml of liquid culture grown for 6 days in buffered minimal medium with (patterned green) and without (solid green) kojic acid (KA) with and without the addition of 0.5 mM SA. The average biomass of the no KA, no SA control was used to normalize the biomass values between experiments, which was run twice in triplicate, with no significant differences found, using a Kruskal-Wallis with Dunn's multiple comparison.

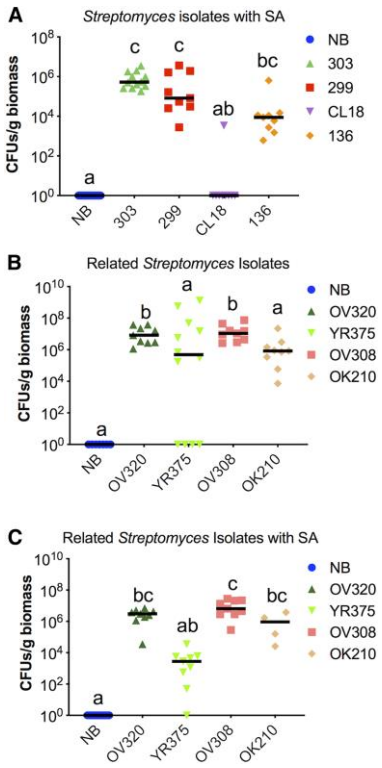

Figure 2. 7: Differential colonization of *Arabidopsis thaliana* seedlings by *Streptomyces* isolates with the application of salicylic acid (SA).

A, Axenic 6- to 7-day-old Col-0 wild-type seedlings were singly inoculated with each *Streptomyces* isolate (no bacteria control [NB, blue circles], 303 [green triangles], 299 [red squares], CL18 [purple triangles], 136 [orange diamonds], *n* = 9 to 12) and grown with 0.1 mM SA. After 14 days, plants were rinsed and seedling colonization level was determined. Different letters indicate statistical differences using a Kruskal-Wallis with Dunn's multiple comparison. B and C, Axenic 6- to 7-day-old Col-0 wild-type seedlings were singly inoculated with four plant-associated *Streptomyces* isolates with genetic similarity to 303, 299, and 136 (no bacteria control [NB, blue circles], OV320 [dark green triangles], YR375 [light green triangles], OV308 [light red squares], and OK210 [dark orange diamonds], *n* = 4 to 12) and grown for 14 days B, without SA or C, with 0.1 mM SA when rinsed seedling colonization level was determined. Different letters with b and c indicate statistical differences using a Kruskal-Wallis with Dunn's multiple comparison.

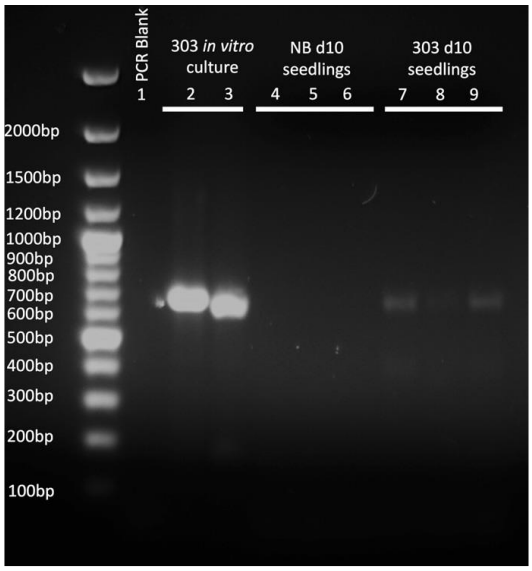

Figure 2. 8: *Streptomyces* sp. 303 melC2 expression in *A. thaliana* seedlings. Axenic 6 day-old Col-0, wild-type seedlings were singly inoculated with *Streptomyces* sp. 303 and grown for 10 days along with no bacteria (NB) before RNA was extracted from 1-2 seedlings and cDNA was generated. Agarose gel shows the results for a PCR reaction using primers specific to the 303 melC2 gene. Following the 100bp ladder each lane contains: Lane 1: PCR blank negative control; Lanes 2-3: cDNA generated from 303 grown in standard glucose-minimal salts liquid medium with Tiger's Milk (an amino acid cocktail with excess tyrosine); Lanes 4-6: cDNA generated from seedlings with no bacterial inoculation; and Lanes 7-9: cDNA generated from seedlings inoculated with 303.

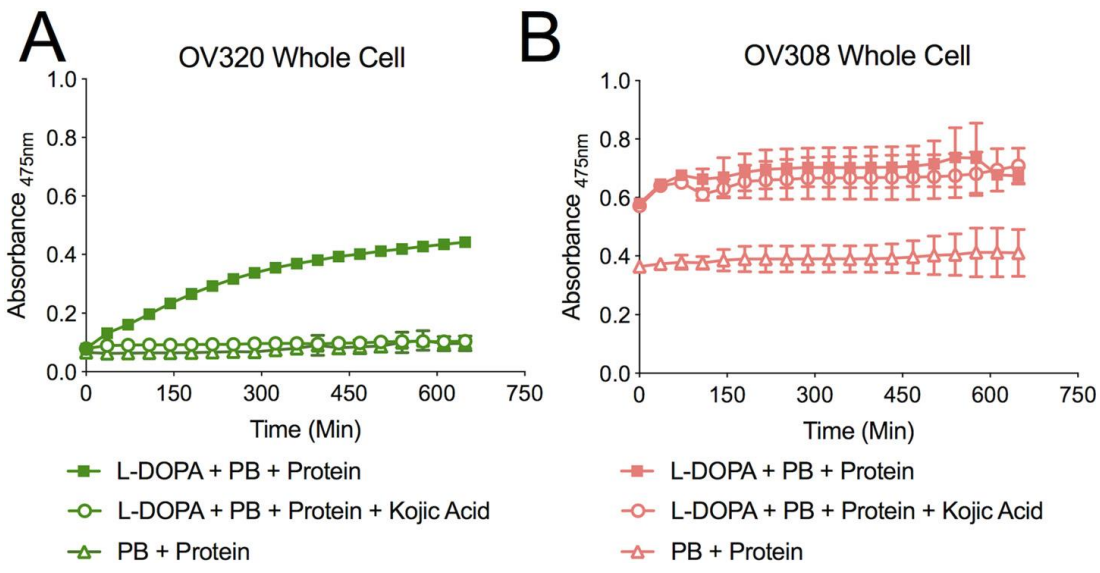

Figure 2. 9: Strain-specific tyrosinase activity in intracellular and extracellular protein extracts from OV320 and OV308 in vitro cultures.

(A-B) Dopachrome production was measured by absorbance at 475 nm for 3 replicates for protein extracts from OV320 (A) and OV308 (B) cell pellets, which were normalized by protein concentration following the addition of phosphate buffer alone (open triangles), phosphate buffer and L- DOPA (closed squares), or phosphate buffer, L-DOPA, and kojic acid (open circles). The mean and standard deviation is displayed.

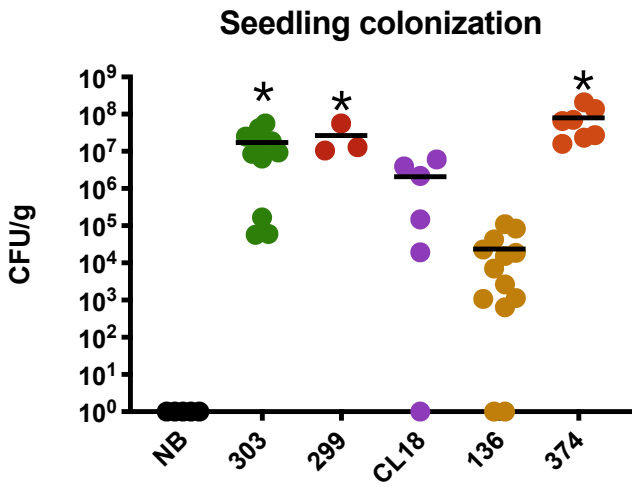

Figure 2. 10: *Brevundimonas* sp. 374 (orange) colonization numbers (CFU/g) of axenic Arabidopsis seedlings after 7-days.

374 is compared to the No Bacteria control (NB, black) and *Streptomyces* strains 303 (green), 299 (red), CL18 (purple), and 136 (yellow) (n=7-12). Asterisk (*) denotes statistical significance of isolate compared to NB control using Kruskal-Wallis with Dunn's multiple comparison.

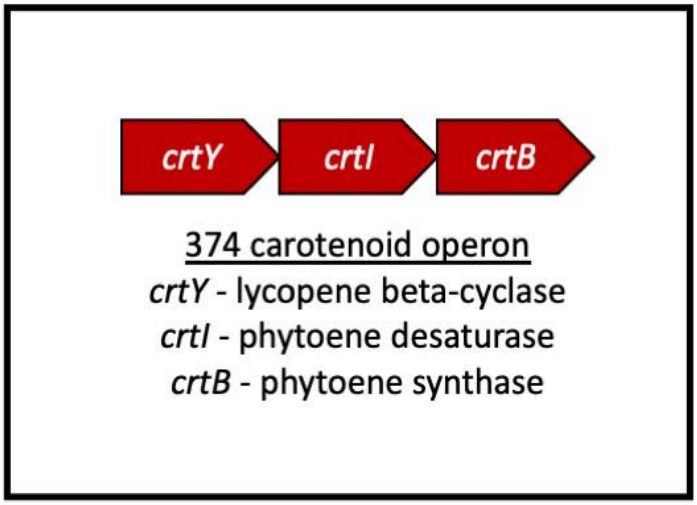

Figure 2. 11:Predicted carotenoid operon in *Brevundimonas* sp. 374.

Generated using antiSMASH. Core biosynthetic genes are outlined here with predicted function of the operon.

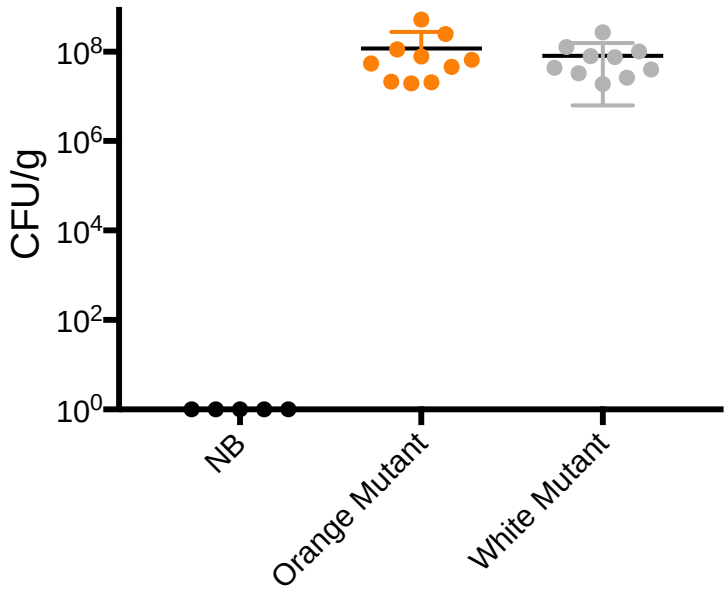

Figure 2. 12: Colonization numbers (CFU/g) of an orange and white mutant of 374-166 colonized with axenic Arabidopsis.

Mutants were generated viz transposon mutagenesis. Kruskal-Wallis test with post hoc Dunn's multiple comparisons used for statistical analysis. No significant difference between mutant types. Only significance between mutants and no bacteria control (n=5-10).

CHAPTER THREE: *STREPTOMYCES* STRAINS INDUCE UNIQUE ROOT EXUDATES THAT INFLUENCE ASSEMBLY OF BACTERIAL TAXA INTO *ARABIDOPSIS THALIANA* ROOT MICROBIOMES

A VERSION OF THIS CHAPTERS IS UNDER REVIEW FOR PUBLICATION

David L. Grant, Sarah Stuart Chewning, Bridget S. O'Banion, Alexandra D. Gates, Andrew J. Willems, Jonathan Dickey, Sara Howard, James A. Fordyce, and Sarah L. Lebeis

AUTHOR CONTRIBUTIONS

DG and SL designed and performed the exudate composition experiment. DG performed metabolite extractions. SH performed the metabolomics. SSC and SL designed the two-step inoculation experiment, SSC and DG performed the experiment. Metabolic modeling and metabolomic PCoA was performed by BSO. QIIME2 analysis to generate ASVs and UniFrac was performed by AW. Indicator species analysis was performed by ADG. Statistical analysis of Hill numbers to determine differences in alpha diversity between the treatment groups in the two-step inoculation experiment were performed by JD and DG. Figures were generated by DG, SSC, BSO, and SL. DG, SSC, and SL wrote the manuscript. DG, SL, SSC, BSO, ADG, AW, JD, and JF revised the manuscript.

ABSTRACT

Although the advent of 16S rRNA gene amplicon sequencing has revealed common microbiome membership, it remains unclear how microbial metabolism influences community assembly. Here, we explore the chemical shifts in root exudate composition following colonization by four *Streptomyces* isolates. We also explore how these changes might subsequently impact root microbiome assembly using comparative genomics and *in vitro* co-culture. Metabolites in the plant-microbe interface might be altered through microbial utilization of root exudates, influence on plant physiology, or biosynthesis of new compounds. *Streptomyces* are metabolically productive, ubiquitous soil-dwelling organisms known to inhabit the internal root tissue of a wide variety of plants. We establish that *Streptomyces* inoculation alters the *Arabidopsis thaliana* (Arabidopsis) root exudate profile with some metabolites disappearing while others appear to be produced by either the plant or the bacterium. When Arabidopsis seedlings are initially inoculated with a single *Streptomyces* isolate, we find differences in the bacterial community acquired from low diversity subsequent inocula. However, we do not observe *Streptomyces* influence in the resulting microbiome composition when a complex microbial supernatant from a soil slurry is inoculated onto seedlings. Overall, our findings confirm *Streptomyces* as consistent members of root microbiomes and suggest their subtle influence over root microbiome community composition. Understanding assembly processes of plant microbiomes is pivotal for improving crop physiology and overall plant health. While several factors are associated with alterations in plant microbiome composition, the impact of individual microbiome members on both the plant host and the total microbial community is less well defined. Here, we examine how specific *Streptomyces* strains impact seedling root exudate profiles and the resulting mature Arabidopsis root microbiome composition. We inoculate seedlings with microbial communities of different complexities and sources to determine the strength of the *Streptomyces* influence. Although complex soil inoculum remains the primary driver of mature root microbiomes, these studies reveal that commensal *Streptomyces* strains appear to exert both positive and negative effects on high and low abundance taxa

assembled into root microbiomes. Such knowledge has the potential to aid the translation of science into the development of agricultural products.

INTRODUCTION

Due to the sessile nature of plants, the microbial inocula for their microbiomes are introduced via their surrounding soil, water, and air environments (1) with soil serving as the primary inoculum for host plants, particularly in their below-ground tissues (2). The selection process by which microbes from inocula join and are maintained in plant microbiomes is mediated by both plant-microbe and microbe-microbe interactions (3), with the resulting microbial assemblages significantly influencing host health and growth (4). Here, we untangle these interactions by combining metabolomics and comparative genomics with amplicon sequencing data to shed light on potential mechanisms that drive root microbial community assembly in *Arabidopsis thaliana* (Arabidopsis).

Amplicon sequencing surveys of 16S rRNA genes from root microbiome studies suggest common members across a variety of plant species belong to four dominant phyla: Actinobacteria, Bacteroidetes, Firmicutes, and Proteobacteria (5–10). This consistency is remarkable considering the vast diversity of the soil inoculia in which roots reside (11, 12). Among Actinobacteria, *Streptomyces spp*. commonly display increased abundance in roots compared to the surrounding soil for a wide range of plant hosts (5, 6, 13). The metabolic capabilities of select *Streptomyces* strains contribute to host health through their role in disease suppressive soils (14, 15), drought tolerance (16), and in plant growth-promoting potential (17). Further, their secondary metabolites possess distinct biocontrol capabilities (17) that allude to root microbiome sculpting potential, suggesting their activities in the root microbiome may exceed their abundance. Even between *Streptomyces* strains, root and seedling colonization of Arabidopsis varies but is connected to plant genotype and bacterial tyrosinase gene copy number (18, 19). We hypothesized that *Streptomyces* strains could alter root exudates, directly or indirectly, when they are initially inoculated on Arabidopsis seedlings to ultimately influence mature root microbiome composition.

Within a complex soil inoculum, there are several factors that influence plant microbiome community assembly, including the host immune system (18), host pathogen infection (20), nutrient availability (21–23), salt concentration (24), and water availability (10). To provide tractable and reproducible findings, large collections of cultured representatives of plant microbiomes provide researchers with the tools to test hypotheses generated from large amplicon sequencing, metagenomics, and metatranscriptomic studies (25, 26). The combination of bacterial cultured representatives into synthetic communities (SynComs) (27) provides a critical middle ground in complexity between single strain inoculation and highly complex microbial communities found in nature (28). Plant microbiome studies using bacterial SynComs revealed keystone species in maize and Arabidopsis (8, 29), as well as distinct nutrient influence on individual members during alfalfa microbiome assembly (23). Here, we initially inoculated Arabidopsis plants with one of four *Streptomyces* strains and subsequently inoculated with an 11-member bacterial SynCom or supernatant from a soil slurry (SoilSup). Plants were grown in open air to allow any microbes present in the air of a shared reach-in plant growth chamber to colonize for 6-8 weeks. This experimental design allowed us to examine how each of the microbial sources contributes to membership of the root microbiome. Our results establish if inoculation with a single bacterial strain can impact the trajectory of community assembly from air and soil inoculation species pools by altering the plant exudate composition and overall metabolic profile.

MATERIALS AND METHODS

Seed sterilization and germination

For all experiments, we used Col-0 accession of *Arabidopsis thaliana* (Arabidopsis) plants. All seeds were surface sterilized via treatment in 70% ethanol with 0.1% Triton-X100 for 1 minute, 10% household bleach with 0.1% Triton-X100 for 15 minutes, and three washes with sterile distilled water. Seeds were stratified for 3 days in the dark at 4^{o}C and subsequently germinated at 24^{o}C with 18 hours of light for 6-7 days

on agar plates containing half strength (2.22g/L) Murashige & Skoog (MS) vitamins (MP Biomedicals), 1% sucrose, and 1% Phytoagar (Bioworld).

Culture preparations

Streptomyces isolates were grown in Lysogeny Broth (LB) at 30^{o}C with shaking at 150 rpm for 4-7 days. Cultures were vortexed and beaten at 1500rpm with 3mm sterile, glass beads in the tubes for 3.5 minutes to disrupt bacterial aggregates using a Geno/Grinder SPEX Sample Prep. All other isolates were grown in LB at 30^{o}C with shaking at 150 rpm for 1-2 days. A spectrophotometer measured the optical density at 600nm (OD_{600}), and individual cultures were normalized to an OD_{600} of 0.01.

Streptomyces *inoculation of Arabidopsis seedlings*

For inoculation of seedings, 100µL of each *Streptomyces* isolate resuspension was spread on 100 mm x 100 mm square plates containing ¼ strength MS square agar plates with no sucrose. An additional 100µL of all normalized isolate resuspensions were plated on LB and incubated at 28^{o}C for 4-7 days to quantify colony forming units (CFUs). Inoculum ranged from $1x10^{2}$ to $3x10^{4}$ CFU/mL. Inoculated plates, as well as no bacteria controls, were allowed to dry and 4-5 seedlings were aseptically transferred onto each plate with flame-sterilized tweezers. Plates were sealed with Parafilm® M Laboratory Film and randomly stacked vertically in open wire trays, which were grown at 24 ^{o}C with 18 hours of light for 7 days. Every two days, root length was observed and plates were shuffled (Figure 3.1A, B). After 7 days, seedlings were harvested to determine colonization levels were determined for each isolate (Figure 3.2A).

Metabolic modeling

Genomes of the four *Streptomyces* isolates 299, 303, CL18, and 136 were downloaded from JGI IMG/M ER (30). Metabolic modeling and flux balance analysis (FBA) was performed using applications in the DOE KBase (May 2020 versions of applications) (31). The genomes were imported into KBase and annotated using RASTtk with the 'Annotate Microbial Genome' App. Annotated genomes were then run through the 'Build Metabolic Model' application, using a custom made glucose minimal media for

gapfilling (0.5g L-asparagine, 0.5g K_2HPO_4, 0.2g $MgSO_4$ $7H_2O$, 0.01g $FeSO_4$ $7H_2O$, 10g glucose) and the Gram-positive template for reconstruction. A secondary gapfilling ('Gapfill Metabolic Model' App) was then performed on all four models using a custom made media representing MS medium. The beta version of both the 'Build Metabolic Model' and 'Gapfill Metabolic Model' applications were used because at the time of analysis (May 2020), the beta version was corrected for ATP flux errors present in the released version. The resulting metabolic models were then run through the 'Run Flux Balance Analysis' app using the MS medium from the prior gapfilling step. The resulting compounds and reactions list for each FBA was downloaded and compared outside of the KBase system (data not shown). Comparisons between isolates were done using the 'uptake' and 'min_uptake' columns.

Preparation of culture media and root exudate samples

Seedlings were prepared as described above for sterilization and germination. *Streptomyces* isolates (i.e., 299, 303, CL18, and 136) were grown for 4-6 days and prepared as described above. We also included seedlings inoculated with an unrelated proteobacteria *Brevundimonas sp.* 374 as an additional control. In 12-well plates, 2mL of ¼ MS with no sucrose was added to each well along with 15-20 Arabidopsis seedlings. No plant controls were also prepared with only ¼ MS with no sucrose. After 24 hours, the liquid from the 6-well plates was collected and vacuum centrifuged to evaporate liquid as controls for both plant and no plant control samples.

Isolates were added to remaining wells to an OD of 0.01. Five replicates were performed for each isolate (299, 303, CL18, 136, and 374), as well as no bacteria (NB) controls for plant and no plant samples. Seedlings were grown for 6 days with 18 hours of light and shaking inside the growth chambers. Tissue was harvested, snap frozen in liquid nitrogen, and stored at -80^{o}C. Liquid samples were collected and vacuum centrifuged until all liquid was evaporated. Dried samples were processed by the Biological and Small Molecule Mass Spectrometry Core at the University of Tennessee, Knoxville.

Metabolite samples were extracted with a solution of 20:40:40 water/methanol/ acetonitrile with 0.1M formic acid following the procedure previously reported (32). After extraction, samples were dried under a stream of nitrogen and then were reconstituted in ultra-pure water and prepared to be run on an ultra high-pressure chromatography Dionex LC system. A Phenomonex Synergi Hydro PR (100 mm x 2.0 mm, 2.5 µm pore size, Phenomonex, Torrance, CA) was utilized to separate the extracted metabolites. The untargeted metabolomics method, adapted from Lu *et al.* (32), was run for 26 minutes with the applied multi step gradient. The mobile phases used to separate the analytes were A) 97:3 water/methanol with 11mM tributylamine and 15 mM acetic acid; and B) methanol at a flow rate of 0.2 mL/minute. The gradient was run as follows: 0 minutes, 0% B; 5 minutes, 20% B; 13 minutes, 55% B; 15.5 minutes, 95% B; 19 minutes, 0% B; 25 minutes, 0% B. Samples were analyzed utilizing electrospray ionization (ESI) probe attached to an Exactive Plus Oribtrap Mass Spectrometer (Thermo Fisher Scientific, Waltham, MA) and was operated in negative mode with a scan range from 72 to 1,2000 m/z and a resolution of 140,000. The raw files were converted to mzML then processed using Metabolomic Analysis and Visualization Engine (MAVEN) where metabolites were chosen based on peaks shape and signal-to-noise-ratio. Data from MAVEN was normalized by weight (data not shown). Normalized ion counts were then converted to relative abundances for each sample and used as input for Principal Coordinate Analyses (PCoAs). PCoAs were performed in the PAST software (version 3.25, (33)) using Euclidean distances and a transformation exponent of 2. The resulting distance matrix was exported and visualized in Graphpad Prism (version 8, GraphPad Software, La Jolla California USA, www.graphpad.com).

Colorimetric auxin assay

Auxin production was determined as described by *Szkop* et al. with some modification (34). *Streptomyces* isolates were grown from spore stocks inoculated in 25mL of LB broth. After a 4-6 day incubation at 30^{o}C, *Streptomyces* cultures were bead beaten with 3mm glass beads and inoculated into 10 mL LB with 1% Tryptophan added. Cultures were incubated at 30^{o}C with shaking at 150 rpm for 2-3 days. After incubation,

cells were removed from culture by centrifugation at 4,000 x *g* for 10 minutes. After centrifugation, 1mL of supernatant was removed from each tube and incubated with 2mL of Salkowski reagent (35% H_2SO_4 and 10mmol $FeCl_3$) in the dark at room temperature for 30 minutes. Following incubation, 100µL of each supernatant mixture or uninoculated medium was added to a clear, flat-bottom 96-well plate and absorbance was measured at l = 540nm for each sample (Figure 3.1C).

Genome comparison and biosynthetic gene cluster identification

To perform comparative genomics, all genomes (i.e., 299, 303, CL18, 136, 2, 374, 181, 40, 50, and CL11) were downloaded from JGI IMG/M ER (30). Genomes were mined using JGI IMG/M ER query tools and the antibiotics and Secondary Metabolites Analysis Shell (antiSMASH, v5), with default options selected (i.e., KnownClusterBlast, ActiveSiteFinder, and SubClusterBlast) (35). AntiSMASH utilizes profile Hidden Markov Models of genes to identify all gene clusters encoding potential secondary metabolites from all known chemical classes. Gene clusters were generated from complete IMG fasta nucleic acid sequences of genomes from these isolates (Table 3.2).

Co-culture microbe-microbe interactions

Streptomyces isolates were grown as described above in LB. After 4-7 days of incubation, 2mL of each *Streptomyces* culture were taken and beaten with 3mm glass beads for 2.5 minutes using the Geno/Grinder SPEX Sample Prep. OD_{600} was measured using a spectrophotometer and cultures were normalized to an OD_{600} of 0.1. Co-culture assays were adapted from Vargas-Bautista *et. al* (36) and performed on LB, 1/10th LB, or M9 (ref. BD 248510) minimal salts with glucose (11.28g/L 5X M9 + 0.2mL 1M $MgSO_4$ + 20mL of 10% casamino acids (BD 223120) + 20mL of 20% glucose for 1L). Using a multichannel pipette to evenly place culture spots 1 cm apart from each other, three 15µL spots of each non-*Streptomyces* challenge isolate were plated perpendicular to two 15µL spots of *Streptomyces* isolates on the agar plate surface. The plate was then incubated overnight at 28°C. Colony formation was monitored every 3 days for 9 days. Challenge strains were selected to pick a representative from each of the other three major plant

microbiome phyla (i.e., Bacteroidetes, Firmicutes, and Proteobacteria) with sequenced genomes and previous SynCom inclusion (18, 22, 37, 38).

Synthetic community (SynCom) selection and preparation

To build our SynCom, we began by including each of the 6 isolates used in the *in vitro* co-culture experiment. We also decided to include in our SynCom two isolates with previously demonstrated low seedling colonization, *Escherichia coli* DH5a and *Deinococcus sp.* TN56 (18, 23), an additional *Burkholderia* (*Burkholderia sp.* TN8), an additional *Pseudomonas* (*Pseudomonas sp.* TN19), and an additional Firmicutes strain (*Bacillus sp.* A415) (Table 3.3). These additions allowed us to distinguish species-level differences in colonization beyond patterns set by genus or phylum. The SynCom inoculum was created by growing each member in liquid LB, normalizing to an OD_{600} of 0.01, and creating a mixed inoculum containing 1mL of each member. Freezer stocks of this SynCom were created by combining 200µL of the mixed bacterial community with 200µL 80% glycerol, then snap freezing in liquid nitrogen, and storing them at -80^{o}C. Prior to seedling inoculation, a frozen stock was thawed, centrifuged, and resuspended in LB for growth at 30^{o}C with shaking at 150 rpm for 2 days. This incubation allowed isolates to be actively growing at the time of their inoculation. After 2 days, the mixed culture was normalized to an OD_{600} of 0.01 in MES (5mL of 0.5M 2-(N-morpholino) ethanesulfonic acid buffered to pH 5.7 with KOH + 1.11g MS Salts + 0.5mL 1000X Gamborg's B5 Vitamins) buffer and inoculated onto seedlings as described below.

Wild soil slurry supernatant (SoilSup) preparation

Wild soils were collected from Oak Ridge National Laboratory and an aliquot was prepared by filling a sterile centrifuge tube to 20mL. 100mL of water was added to an autoclave bottle with a stir bar and sterilized. To generate the soil supernatant (SoilSup) inoculum, the aliquot of wild soil was added to the water and allowed to stir uninterrupted for 1.5 hours. The soil slurry was removed from the magnetic stir plate and allowed to settle for 1-2 minutes. 250µL of the resulting supernatant liquid above the sediment was collected and added to sterile freezer stock tubes with 250µL 60% glycerol, snap frozen

in liquid nitrogen, and stored at -80°C. The day of inoculation, freezer stocks of SoilSup were thawed and centrifuged at 13,000 *x g* for 1 minute. Glycerol-containing freezer stock medium was removed and the SoilSup pellet was resuspended in 2mL sterile water. OD_{600} was measured using a spectrophotometer and SoilSup inoculum was normalized in ¼ MS buffered with sterile MES to an OD_{600} of 0.01. Resuspensions were then used as subsequent inoculum as described below.

Two-step seedling inoculation, plant growth, and tissue harvest

Arabidopsis seedlings were grown on sterile or single *Streptomyces* strain inoculated ¼ MS plates as described above. Following 7 days of vertical growth, Arabidopsis seedlings were aseptically transferred to individual three-inch square pots with 64 mL of sterile calcined clay (Pro's Choice Rapid Dry). Pots contained 50mL of either: 1) uninoculated ¼ MS buffered with MES (NB), 2) our 11-member SynCom in ¼ MS buffered with MES (SynCom), or 3) soil supernatant in ¼ MS buffered with MES (SoilSup). All pots were grown in open air, allowing for microbes in the ambient air of the reach-in growth chambers to be assembled into the root microbiome communities.

Plants were watered every 2-3 days from the top with sterile, distilled water and grown open-air in growth chambers (Percival, model: AR41L3C8) with 10 hours of light at 22°C and 14 hours of dark at 18°C to prolong flowering and extend the period of vegatative growth. After 6-8 weeks of growth, plants were aseptically harvested when inflorescence began to emerge. Whole plants were submerged in 25mL of sterile harvesting phosphate buffer (6.33g of $NaH_2PO_4*H_2O$, 16.5g of $Na_2HPO_4*H_2O$) with 0.01% Silwet (Lehle Seeds) and vortexed vigorously for 10 seconds. Roots and rosettes were separated with sterile forceps and transferred to sterile centrifuge tubes and weighed. Roots were rinsed three times with sterile distilled water and snap-frozen in liquid nitrogen. Frozen roots were lyophilized overnight (LABCONCO FreeZone 6 catalog number 7753020; drying chamber: short clear chamber with valves, catalog number 7318802). After lyophilizing, roots were homogenized via bead beating in the

Geno/Grinder SPEX Sample Prep with sterile 3mm glass beads or garnet beads for 2.5 minutes.

DNA extraction and 16S rRNA gene amplicon sequencing

DNA was extracted from homogenized plant roots using the Mo Bio PowerSoil kit (now a Qiagen product, DNeasy Powersoil Kit 12888-100). DNA concentration was quantified with the Quant-iT PicoGreen dsDNA Assay Kit and fluorospectrometer. Polymerase chain reaction (PCR) was performed in triplicate and with a negative control to ensure absence of contamination. A mixture of two peptide nucleic acid (PNA) blockers, which bind to plant host plastid and mitochondrial 16S rRNA genes (i.e., pPNA and mPNA from PNABio), were used to minimize amplification of host DNA. The University of Tennessee, Knoxville Genomics Core performed library preparation using the Illumina preparation kit and sequenced the samples. Based on previous findings of high-quality reads, 16S rRNA gene barcoded V3-V4 Illumina primer sets with Illumina adapters were utilized for PCR reactions (39) and sequenced by Illumina MiSeq® pyrosequencing. Index PCR reactions used Nextera XT forward and reverse index primers. A 600-cycle flow cell was used with paired-end reads at length 275bp. Raw sequences were deposited in the Sequence Read Archive under Bioproject accession number PRJNA693844**.**

Amplicon sequence variant (ASV) analysis in QIIME2

The *in silico* tool used to perform the 16S rRNA gene microbial analysis was QIIME 2. QIIME 2 is an open source, extensible, and decentralized microbiome analysis package with a focus on data and analysis transparency (40) (www.qiime2.org). Data files were imported into the .qza file format using the QIIME tools import command. The software package FastQC was used to visualize the quality metrics of the sequences and determine the appropriate places to trim and truncate the reads in order to ensure the highest quality reads. Based on quality plots, each read was trimmed from the 5’ end by 15 base pairs and truncated to 250 bp. To perform trimming and truncating, the QIIME DADA2 (41) denoise-paired command was run and two tables were generated: an Amplicon Sequence Variant (ASV) table and a representative sequences table (42). The

QIIME alignment MAFFT and mask commands were used to perform a multiple sequence alignment and to mask highly variable regions found. The QIIME phylogeny FASTREE and midpoint root command were used to create a mid-point rooted phylogeny. The QIIME phylogeny midpoint-root command was run to create a mid-point rooted phylogenetic tree. The QIIME diversity core-metrics-phylogenetic command was carried out with a uniform sampling depth of 2,000, allowing inclusion of 98% of samples, which generated beta diversity metrics as well as plotting capabilities (e.g., weighted UniFrac and principal coordinate analysis). To infer taxonomy, a Naïve-Bayesian classifier was generated with SILVA V132, a 16S rRNA gene reference database (43). This classifier was then trained against reference ASVs with the QIIME feature-classifier fit-classifier-naive-bayes command. Taxonomy was built using the QIIME feature-classifier classify-sklearn command on the representative sequences file. Although mitochondrial and plastid PNA blocker were used in the amplicon library preparation, plant reads remained, and thus these ASVs were manually removed. PCR blanks were run for quality control. These samples generated less than 100 reads each, which were subtracted from ASV counts in the read table. Samples ranged in read depth from 88,375 reads to 109,765 reads (Table 3.4).

Statistical analyses

Results for Figures 3.1, 3.2, 3.7 and 3.9 were statistically analyzed with Prism version 8.0 for Mac (GraphPad Software, La Jolla California USA, www.graphpad.com). Differences in *Streptomyces* CFU from seedlings were detected by Kruskal-Wallis test with post hoc Dunn's multiple comparisons as previously performed (19). For Figure 3.2C, the discovery of which metabolites differ from the NB controls was performed by using an unpaired *t*-test for each inoculated sample type followed by a two-stage Benjamini, Krieger, and Yekutili False Discovery Rate procedure (results in Table 3.1). For Figure 3.5, a Hill numbers approach for understanding microbiome diversity (44, 45) was used to discern differences in alpha diversity amongst inoculation treatments (46). For read counts in Figures 3.7B, 3.7C, 3.9B, and 3.9C, 1-way ANOVA with *post hoc* Tukey's multiple comparisons were performed. Indicator species analysis was run using the

relative abundances of ASVs found in at least 3 samples from plants inoculated with SynCom or SoilSup inocula, as well as NB plants using the R package indicspecies with 50,000 permutations (47).This analysis determined ASVs associated with specific pretreatments and post treatments using a point biserial correlation coefficient.

RESULTS

Differential Streptomyces *isolate seedling colonization*

Streptomyces colonize the root systems of a variety of plants with several strains able to produce compounds that influence plant health and microbial growth (7, 17, 48). We hypothesized that different *Streptomyces* isolates would differentially shape the chemical landscape surrounding root systems by altering plant physiology, and by extension, root microbiome assembly. To test this hypothesis, we performed 1 week plant-microbe colonization assays of Arabidopsis seedlings inoculated with each of four *Streptomyces* strains (i.e., 299, 303, CL18, and 136) to reveal distinct root morphology (Figure 3.1A, B), levels of colonization (Figure 3.2A), and root exudate profiles (Figure 3.2B, 1C, 3.3A). Our four *Streptomyces* isolates differentially colonized Arabidopsis when they were the sole seedling inoculant for two weeks on solid medium (19), as well as when they were all included in a 38-member mixed bacterial community growing in calcined clay in pots for 6-8 weeks (18). In these 1-week experiments, we observe similar results to the previous experimental designs, with 299 and 303 colonizing to a significantly higher degree than 136, and CL18 indistinguishable from any of the other isolates (Figure 3.2A).

Predicted and detected metabolites present during Streptomyces *colonization*

Genomic comparisons revealed that *Streptomyces* strains with higher Arabidopsis colonization *(*i.e., 299 and 303) have larger genomes and a greater percentage of genes predicted to be involved in biosynthetic gene clusters (BGCs) than those that did not (i.e., CL18 and 136) (Table 3.2). To explore the metabolic potential of each *Streptomyces* isolate, we performed metabolic modeling and flux balance analysis (FBA) using the DOE KBase environment. The majority of predicted compounds and reactions in FBAs

simulated on MS medium, which was used for colonization experiments, were shared between all 4 *Streptomyces* isolates (Figure 3.3B, C). FBAs for isolates 299 and 303, which consistently colonize Arabidopsis at the highest levels (Figure 3.2A), found that only 2-3% of predicted compounds and 6-8% of predicted reactions were uniquely shared by these isolates (Figure 3.3B, C). In order to determine which predicted differential metabolites and reactions might be relevant to our seedling colonization system, we performed metabolomics on roots exudates harvested from inoculated seedlings.

To explore differences in root exudation following *Streptomyces* inoculation, we performed untargeted metabolomics on Arabidopsis seedlings after 7 days of inoculation, as well as uninoculated plants and no plant controls (Figure3.3A). Overall, we find that seedlings inoculated with 299 or 303 are distinct from all other seedling samples (Figure 3.2B), as well as no plant control samples (Figure 3.3A). Among the total detected metabolites, 104 matched verified compounds in the facility library with 19 verified compounds differing in normalized ion counts between inoculated and uninoculated seedlings (Figure 3.2C). Some metabolites appear to decrease with any inoculation, such as glycolate and pyroglutamic acid, (Figure 3.2C (I)) while allantoin ion counts decreased when 299, 303 or CL18 are inoculated onto seedlings (Figure 3.2C (II)). This result is congruent with the predicted compound flux from the metabolic modeling, which predicted that 299, 303, and CL18 could take up and utilize allantoin.

We also observed ion count increases for compounds in inoculated samples. For example, sulfolactate increases when 299, 303, or CL18 are inoculated onto seedlings (Figure 3.2C (III)). There are another two groups of metabolites that increased in seedlings inoculated with 303: 9 are shared when 299 is inoculated onto seedlings (Figure 3.2C (IV)) and 6 are unique to 303 inoculation (Figure 3.2C (V)). Because we fail to detect these differences in the no plant control samples (Figure 3.3A), we predict that the differences we observe in exudates of seedlings inoculated with 299 or 303 require the interaction between these isolates and Arabidopsis. While the majority of the identified compounds did not specifically mimic our metabolic modeling outputs, we hypothesize

this is due to modelling gaps, variation between steady-state (i.e., FBA) and dynamic biological systems (i.e., metabolomics). The subset of metabolites with increased normalized ion counts in 299 or 303 inoculated seedlings includes: defense related phytohormones (i.e., salicylate and jasmonate), multiple compounds involved in glyoxylate metabolism, and indole-3-carboxylate (Figure 3.2C (IV)). We hypothesized that the increase in defense phytohormones and glyoxylate metabolism are the result of increased seedling colonization and the subsequent interactions driven by these two isolates. Therefore, we decided to further investigate the ability of 299 and 303 to produce indole-3-acetic acid (IAA), a phytohormone, which is also a microbially produced compound associated with increased plant colonization (49) that can be degraded into the indole-3-carboxylate we detected (50).

IAA production by* Streptomyces *strains 299 and 303

As compared to control uninoculated seedlings and those inoculated with isolate CL18, seedlings grown with 299 and 303 appear to result in more lateral roots and less primary root length (Figure 3.1A, B). Interestingly, seedlings grown with 136 resulted in primary roots that were longer than those associated with 299 and 303 but had more lateral root growth than those associated with CL18 (Figure 3.1A, B). However, root biomass and phyllosphere biomass did not significantly differ between control and inoculated plants, even after 8 weeks of growth (19), suggesting that *Streptomyces* strains do not individually influence plant biomass accumulation in the conditions tested.

Plant- and microbe-derived auxins increase lateral root growth and inhibit primary root growth (51). Hence, the phenotype of plants colonized with 299 and 303 appeared to mimic the effects produced by auxin exposure (Figure 1A, B). To determine if our *Streptomyces* strains produce IAA, the colorimetric IAA assay described by Szkop *et al. (34)* was performed on the supernatant of each isolate grown in liquid media supplemented with tryptophan. Isolate 303 produced significantly more IAA than 299, CL18, and 136, and 299 produced significantly more IAA than CL18 and 136 cultures (Figure 1C). Together, these findings suggest 299 and 303 may produce IAA during

seedling colonization. To identify additional relevant metabolites that may be present during seedling microbiome assembly, it was necessary to compare the genomes of each *Streptomyces* isolate.

Secondary metabolic profiles of* Streptomyces *reveal differences between isolate potential and antibiosis capability

To explore potential *Streptomyces*-derived compounds, we used antiSMASH ((35), v5) to predict the secondary metabolites produced by each isolate. *Streptomyces* strains with higher levels of seedling colonization, 299 and 303, are predicted to encode 33 and 28 BGCs respectively, while CL18 and 136 are only predicted to encode 14 and 15 BGCs (Figure 3.4A). *Streptomyces* isolates 299 and 303 were predicted to possess 2 copies of melanin BGCs (Figure 3.4A), which was previously confirmed *in vitro (19)*. Interestingly, only 303 was predicted to have distinct phenazine clusters (Figure 3.4A), which can mediate antibiosis or antibiotic tolerance (52). Matches to other previously identified antimicrobial clusters were also present in each *Streptomyces* isolate, suggesting the possibility of antibiosis with other microbes. With the diverse metabolic potential of these four *Streptomyces* isolates and predicted products relevant to plant association, we hypothesized that they could shape microbial communities via direct microbial interaction.

In vitro co-culturing suggests* Streptomyces *strains influence and are influenced by other microbes directly

To determine if *Streptomyces* might influence the growth of bacteria from the other dominant plant colonizing phyla (i.e. Bacteroidetes, Firmicutes, and Proteobacteria), we co-cultured our four *Streptomyces* strains on 3 different agar types with 6 genome-sequenced bacterial isolates previously included in Arabidopsis colonization studies ((18, 37); Table 3.2, 3.3). Using perpendicular culture spots, isolates were grown 1cm apart from each other to limit the effect of nutrient acquisition and growth rate as the sole cause of observable interactions. While 303 and CL18 each inhibited four of the six tested bacterial strains, 299 only inhibited two, and 136 inhibited none (Figure 3.4B). Isolates

299, 303, and CL18 each inhibited the growth of proteobacterial strains *Rhizobium* sp. 2 and *Burkholderia* sp. CL11. Isolates 303 and CL18 each inhibited the growth of Bacteroidetes member *Flavobacterium* sp. 40 and Proteobacteria *Brevundimonas* sp. 374. Interestingly, 299 and 136 each promoted the growth of strain 374 (Figure 3.4B). Therefore, these *in vitro* co-culture assays demonstrated that these four *Streptomyces* isolates were capable of predicted antibiosis, but also growth promotion of particular non-*Streptomyces* strains.

Among the non-*Streptomyces* strains, *Paenibacillus* sp. 181 and *Pseudomonas* sp. 50 inhibited the growth of the most isolates, including all 4 *Streptomyces* isolates (Figure 3.4B). When we compared the genomes and biosynthetic potential of these 6 non-*Streptomyces* isolates, 181 had 25 BGCs and 50 had 13 BGCs (Figure 3.4A). *Burkholderia sp.* CL11 also had 13 BGCs (Figure 3.4A), but it only inhibited the growth of *Streptomyces* sp. CL18 (Figure 3.4B). *Brevundimonas* sp. 374, which is only predicted to encode a bacteriocin and a terpene (Figure 3.4A), was able to inhibit the growth of the Bacteriodetes isolate *Flavobacterium* sp. 40 (Figure 3.4B). Finally, although *Rhizobium sp.* 2 is predicted to encode 6 BGCs (Figure 3.4A), it did not instigate growth alterations for any of the other strains tests. Together, these data suggest that while the ability to influence the growth of other microorganisms generally positively correlates with genome-encoded BGCs, the types of BGCs require further investigation to more specifically identify the active compounds driving these phenotypes. Further, we do not know if any of these BGCs are expressed during seedling colonization or the mechanism behind those that may be conferring an advantage to one isolate over another. Therefore, we next investigated if our four *Streptomyces* isolates influenced the assembly of other bacteria into mature root microbiome communities.

Inoculum complexity affects microbial community membership more than* Streptomyces *initial inoculation

To determine the impact of our four *Streptomyces* strains on subsequent root microbiome assembly, we first inoculated sterile Arabidopsis seedlings with single *Streptomyces* strains. We then transferred seedlings into pots containing sterile calcined clay subsequently inoculated with nothing (No Bacteria, NB), a SynCom of 11 bacterial isolates (Table 3.3), or soil slurry supernatant (SoilSup) inoculum (Figure 3.5A). The composition of our SynCom included the 6 bacterial isolates characterized for their co-culturing *in vitro* in Figure 3.4 (i.e. 2, 50, CL11, 374, 181, and 40), as well as two poor plant colonizers (i.e. *E. coli* and *Deinococcus sp.* TN56), a *Pseudomonas* in addition to *Pseudomonas sp.* 50 (i.e. *Pseudomonas sp.* TN19), a *Burkholderia* in addition to *Burkholderia sp.* CL11 (i.e. *Burkholderia sp.* TN8), and a *Firmicute* in addition to *Paenibacillus* sp. 181 (i.e. *Bacillus sp.* A415) (Table 3.3). After 6-8 weeks of open-air growth in a common reach-in plant growth chamber, where microbes from the surrounding air could also be acquired by plants, the assembled root microbiome was determined using 16S rRNA gene amplicon sequencing. There was a total of 146 samples included in our analysis, grouped according to initial (e.g. no bacteria (NB), 299, 303, CL18, or 136) and subsequent (e.g. NB, SynCom, or SoilSup) inoculum, resulting in 15 different treatments (Figure 3.5A), as well as the SynCom and SoilSup inocula samples.

We examined the alpha diversity of assembled mature root microbiomes using a Hill numbers approach, which generates the effective number of species with increasing weight given to abundance as order of q increase. We observed that the SoilSup inoculum samples had the highest effective number of species at all orders of q (Figure 3.5B), which was significantly higher than most other sample types (Table 3.5). The only sample type that was not less diverse was root microbiome samples from plants that did not receive subsequent inoculum at q=0 (Table 3.5). When q=0, rare and common taxa are weighted equally. This suggests that SoilSup inoculum and root samples from plants that received no subsequent inoculum possess indistinguishable reads from low abundance taxa. Interestingly, the root microbiomes of several groups of samples that received NB as the secondary inoculum have higher alpha diversity than samples that received SoilSup at

q=0 (Table 3.5). However, as orders of *q* increase, and thus more abundant taxa are weighted more heavily, this phenotype inverts, and roots that receive SoilSup are more diverse than those that receive no subsequent inoculum (Figure 3.5B). We predict this phenotype reflects the number of low abundance taxa assembled into root samples when no subsequent inoculum is provided to seedlings. Together these results suggest that while fewer organisms assemble into root microbiomes from SoilSup than NB samples, the organisms that do assemble are more abundant.

We next used a weighted UniFrac distance matrix to generate a principal coordinate analysis (PCoA) for beta diversity comparisons to reveal differences between sample types. Notably, there is a clear impact of secondary inoculation (e.g. NB, SynCom, and SoilSup) on the assembled communities (Figure 3.5C). While root microbiome samples with no subsequent inoculum (NB, grey) were scattered, seedlings inoculated with SynCom and SoilSup formed distinct groups (Figure 3.5C). No obvious differences were observed when considering the primary inoculation with any *Streptomyces* strain for any subsequent inoculum group (Figure 3.6), suggesting that subsequent inoculation contributes more to the overall resulting mature root microbiome composition than initial *Streptomyces* inoculation.

In low complexity inoculum, *Streptomyces* spp. alter the ability of air-acquired taxa to assemble into root communities

At the phylum level, Actinobacteria and Proteobacteria dominated all assembled root communities, but we again did not observe differences between samples initially inoculated with a *Streptomyces* isolate (Figure 3.7A, D, E). When we looked at the abundance of each *Streptomyces* isolate in these samples, 299 had the highest relative abundance, which decreased as the complexity of subsequent inoculum increased from NB to SoilSup (Figure 3.8A)**.** Interestingly, 299 and 303 reads were present in more samples than CL18 and 136 in samples that received SynCom or SoilSup (Figure 3.6A), suggesting better persistence following subsequent inoculation.

We detected a number of ASVs that were not present in SynCom or SoilSup inoculum samples, which we inferred were assembled into the root microbiomes from the ambient air in their common plant reach-in chamber. Our Indicator Species Analysis identified a *Methylobacterium* ASV and a *Paenarthrobacter* ASV were more likely to be present in root samples that received no subsequent inoculum. We also identified 32 ASVs from the Microbacteriaceae family that were absent in the SynCom and SoilSup inoculum samples that were commonly found in root microbiome samples of all treatment groups (Figure 3.8B). From reads pooled for these 32 ASVs, we found that Microbacteriaceae abundance was higher in samples that received SoilSup compared to SynCom samples (Figure 3.7B), suggesting that a member (or members) of the SynCom may prevent colonization by these Microbacteriaceae. Samples that received no subsequent inoculum were too variable to observe any significant differences in Microbacteriaceae reads with the subsequent inoculum groups (Figure 3.7B). When we further investigated those plants that received no subsequent inoculum, we discovered that samples initially inoculated with 136 had significantly more Microbacteriaceae reads than any other initial inoculation group (Figure 3.7C) although this difference was not observed in SynCom or SoilSup samples. We do not predict decreased Microbacteriaceae colonization is caused by seedling colonization with 299, 303, or CL18 because samples initially inoculated with 136 are also higher than the NB initial inoculum controls. Thus, we suggest that 136 colonized seedlings produce a metabolite that increases the ability of these Microbacteriaceae ASVs to colonize Arabidopsis. While there were no metabolites from the compound library that increased in ion counts for seedling inoculated with 136 (Figure 3.2C), there are 4 compounds and 20 reactions predicted by our metabolic modeling that are unique to the 136 isolate (Table 3.1). Together, these data demonstrate that initial *Streptomyces* inoculation impacts the ability of microbes present in the ambient air to invade root microbiomes in the absence of SynCom or SoilSup communities.

Streptomyces *strains impact the ability of low abundant SynCom members to establish in a mature root microbiome*

When we examined the capability of the individuals in our 11-member SynCom to assemble into root microbiomes, *Burkholderia* sp. CL11 was present with the highest relative abundance for all samples that received the SynCom subsequent inoculum (Figure 3.9A). Several isolates were more abundant in the SynCom inoculum than in root samples, indicating that they did not colonize successfully during the experiment (Figure 3.9A). Among these isolates were *Flavobacterium* sp. 40 and *E. coli*, which were previously defined as "poor" colonizers (18). Surprisingly, another previously defined poor colonizer of alfalfa seedlings, *Deinococcus* sp. TN56, was present with different relative abundances between seedlings initially inoculated with different *Streptomyces* strains (Figure 3.9B). Specifically, plants initially inoculated with 303 had higher relative abundance of TN56 than plants that initially received 299 or 136, and plants that initially received CL18 had a higher relative abundance of TN56 than plants that initially received 136 (Figure 3.9B). These findings correspond to *in vitro* co-culturing of TN56 with these *Streptomyces*, which had the slowest growth when incubated with 136 (data not shown). Within this SynCom, *Rhizobium* sp. 2 abundance was significantly higher when seedlings were initially inoculated with 299 compared to those that were inoculated with 303 or CL18 (Figure 3.9C). Interestingly, when all four *Streptomyces* were included in a 38-member SynCom inoculated onto Arabidopsis, *Rhizobium* sp. 2 was the highest colonizing isolate (18). Together, these results indicate that *Streptomyces* strains positively or negatively impact subsequent colonization by particular low abundance bacterial isolates.

When we investigated the assembled root microbiome communities from plants that received the complex SoilSup as their subsequent inoculum, the majority of ASVs found in the inoculum were not present in root samples (Figure 3.10B). Interestingly, the most abundant ASV in these samples was another *Burkholderia* sp. the same genus as CL11, which was the most abundant ASV in samples that received the SynCom (Figure 3.9A). We failed to detect differences in assembled root microbiomes for samples that received different *Streptomyces* strain initial inocula, which may reflect the inability of

these *Streptomyces* to equally persist in mature root microbiome communities (Figure 3.8A). Collectively, our *in silico*, *in vitro*, and *in vivo* studies of these four *Streptomyces* strains provide evidence that while not the most abundant microbiome members, biosynthetically diverse *Streptomyces* species alter root exudate composition and when present, subsequent colonization potential of particular strains during root microbiome assembly.

DISCUSSION

Among microbes capable of agricultural applications, *Streptomyces* promote plant growth by producing auxins, mediating drought survival, and suppressing the growth of soil-borne pathogens (16, 17). *Streptomyces* are recognized as cosmopolitan organisms, colonizing internal root tissue of a wide variety of plant species (48, 53, 54) in geographically and geologically diverse soils (5, 6). Here, we provide evidence that inoculation of *Streptomyces* strains impacts Arabidopsis root exudate composition (Figure 3.2) and influences the ability of specific taxa from ambient air (Figure 3.7B, C) or an 11-member SynCom (Figure 3.9B, C) to assemble into mature root microbiomes.

Members of the *Streptomyces* genus are known for their diverse metabolisms and vast secondary metabolite production (17). When we measured the composition of seedling exudates inoculated with our 4 *Streptomyces* isolates, we observed that those inoculated with 299 and 303 are unique from the other metabolite samples, which was not observed in no plant control samples (Figure 3.2B and 3.3). Interestingly, inoculation with either isolate resulted in more salicylic acid (Figure 3.2C), which these particular isolates are more resistant to than CL18 or 136 (19). Further, salicylic acid is able to directly and indirectly shape root microbiome assembly (18). This seems to indicate that salicylic acid modulation may be mediated by the array of plant host defenses that get triggered depending on the *Streptomyces* strain present, which can subsequently affect other microbial community members.

When we investigated predicted *Streptomyces* strain encoded secondary metabolites, strains with higher colonization levels (i.e., 299 and 303) showed much higher predicted BGC profiles than the other strains (Figure 3.4A). However, any induced differences in subsequent *in vitro* co-culturing (Figure 3.4B) or root microbiome assembly (Figure 3.5,3.7,3.9) would have to be mediated by the specific compounds actually produced. Our investigation of non-*Streptomyces* isolates followed a similar trend and further suggests that secondary metabolism size alone is not sufficient to predict colonization capabilities. While isolates like *Paenibacillus* sp. 181 had as many predicted BGCs as 299 and 303 (Figure 3.4A), it does not effectively assemble into mature root communities when Arabidopsis is inoculated with an 11-member (Figure 3.9A) or a 38-member SynCom (18). Our characterization of root exudates and secondary metabolite potential is an exciting starting place for future research of the impact of particular metabolites, even those without matches to our initial compound library, on root microbiome assembly.

Our *in vitro* co-culture experiments reveal *Streptomyces* strains influence other strains both positively and negatively (Figure 3.4B), which is partially observed in our 16S rRNA amplicon community studies (Figure 3.7C, 3.9B, and C). For example, in co-culture experiments, 299, 303 and CL18 inhibited growth of *Rhizobium sp.* 2 (Figure 3.4B), yet relative abundance data actually saw an increase of Rhizobium reads in samples initially inoculated with 299 compared to 303 or CL18 (Figure 3.9C). Further, while our *in vitro* co-culturing indicated that CL11 could be inhibited by most of the other microbes in the SynCom, CL11 was the most abundant microbe in roots that received SynCom (Figure 3.9A), even when potential instigators of antibiosis were also present (Figure 3.4B). These findings highlight disparities between *in vitro* antibiosis and *in planta* colonization outcomes, potentially due to differences in the environment induced by a host plant or other surrounding microbes. Therefore, the observed differences cannot be entirely explained by direct inhibitory ability of specific *Streptomyces* and requires further exploration of more indirect effects of isolates in a community, potentially by using

iterations of SynComs with particular microbes removed as previously performed in Arabidopsis phyllosphere studies (29).

Our use of multiple orders of magnitude in inoculum complexity including monoinoculation (i.e., 1), low complexity SynCom (~10), medium complexity chamber air (~100), and high complexity SoilSup (~1,000) allowed us to observe that our *Streptomyces* strains impact particular microbes in the medium complexity range. Specifically, we found that *Streptomyces* initial inoculation only influenced the assembly of invading, presumably airbourne ASVs (Figure 3.7C) or low abundance isolates (Figure 3.9B, C). Interestingly, these particular taxa are diverse and include members of Actinobacteria, Deinococcus-Thermus, and Proteobacteria phyla. We did not observe that *Streptomyces* initial inoculation altered microbiome composition of roots that received subsequent SoilSup inoculum, which may be influenced by uneven persistence of *Streptomyces* in these samples (Figure 3.8A) or the high diversity SoilSup inoculum (Figure 3.5B, C). Instead, we observed that in SoilSup samples, the influence of subsequent inoculum community composition remains the primary root-microbiome determinant (55). We note here that while *Streptomyces* can carry large and diverse metabolic potentials, their influence on the community may be subtle and heavily influenced by inoculum complexity (Figure 3.5B, C). Together, these data indicate *Streptomyces* isolate colonization of Arabidopsis seedlings positively and negatively influence the ability of particular, diverse bacteria to assemble into mature root microbiomes. Root microbiome assembly is a complex set of plant-microbe and microbe-microbe interactions that has impacts on host physiology and overall microbial community assembly. Therefore, future experiments can now investigate the mechanisms behind *Streptomyces* influence and the overall outcome of plant hosts by community alterations by *Streptomyces*.

ACKNOWLEDGEMENTS

The four strains of *Streptomyces* as well as several SynCom isolates were originally isolated in the laboratory of Jeffery Dangl at the University of North Carolina. This work is supported by the National Science Foundation grant IOS-1750717 to S. Lebeis and DEB-1638922 to S. Lebeis and J. Fordyce. This material is partially based upon work supported by the National Science Foundation Graduate Research Fellowship Program under Grant No. DGE-1938092 awarded to B.S.O. Any opinions, findings, and conclusions or recommendations expressed in this material are those of the author(s) and do not necessarily reflect the views of the National Science Foundation.

REFERENCES

1. Compant S, Samad A, Faist H, Sessitsch A. 2019. A review on the plant microbiome: Ecology, functions, and emerging trends in microbial application. J Advert Res 19:29–37.
2. Fierer N, Jackson RB. 2006. The diversity and biogeography of soil bacterial communities. Proc Natl Acad Sci U S A 103:626–631.
3. Hassani MA, Durán P, Hacquard S. 2018. Microbial interactions within the plant holobiont. Microbiome 6:58.
4. Gopal M, Gupta A, Thomas GV. 2013. Bespoke microbiome therapy to manage plant diseases. Front Microbiol 4:355.
5. Lundberg DS, Lebeis SL, Paredes SH, Yourstone S, Gehring J, Malfatti S, Tremblay J, Engelbrektson A, Kunin V, Rio TG del, Edgar RC, Eickhorst T, Ley RE, Hugenholtz P, Tringe SG, Dangl JL. 2012. Defining the core Arabidopsis thaliana root microbiome. Nature 488:86–90.
6. Bulgarelli D, Rott M, Schlaeppi K, Ver Loren van Themaat E, Ahmadinejad N, Assenza F, Rauf P, Huettel B, Reinhardt R, Schmelzer E, Peplies J, Gloeckner FO, Amann R, Eickhorst T, Schulze-Lefert P. 2012. Revealing structure and assembly cues for Arabidopsis root-inhabiting bacterial microbiota. Nature 488:91–95.
7. Bonaldi M, Chen X, Kunova A, Pizzatti C, Saracchi M, Cortesi P. 2015. Colonization of lettuce rhizosphere and roots by tagged Streptomyces. Front Microbiol 6:25.
8. Niu B, Paulson JN, Zheng X, Kolter R. 2017. Simplified and representative bacterial community of maize roots. Proc Natl Acad Sci U S A 114:E2450–E2459.
9. Gottel NR, Castro HF, Kerley M, Yang Z, Pelletier DA, Podar M, Karpinets T, Uberbacher E, Tuskan GA, Vilgalys R, Doktycz MJ, Schadt CW. 2011. Distinct microbial communities within the endosphere and rhizosphere of Populus deltoides roots across contrasting soil types. Appl Environ Microbiol 77:5934–5944.
10. Fitzpatrick CR, Copeland J, Wang PW, Guttman DS, Kotanen PM, Johnson MTJ. 2018. Assembly and ecological function of the root microbiome across angiosperm plant species. Proc Natl Acad Sci U S A 115:E1157–E1165.

11. Tringe SG, von Mering C, Kobayashi A, Salamov AA, Chen K, Chang HW, Podar M, Short JM, Mathur EJ, Detter JC, Bork P, Hugenholtz P, Rubin EM. 2005. Comparative metagenomics of microbial communities. Science 308:554–557.
12. Pascale A, Proietti S, Pantelides IS, Stringlis IA. 2019. Modulation of the Root Microbiome by Plant Molecules: The Basis for Targeted Disease Suppression and Plant Growth Promotion. Front Plant Sci 10:1741.
13. Seipke RF, Kaltenpoth M, Hutchings MI. 2012. Streptomycesas symbionts: an emerging and widespread theme? FEMS Microbiology Reviews.
14. Schlatter D, Kinkel L, Thomashow L, Weller D, Paulitz T. 2017. Disease Suppressive Soils: New Insights from the Soil Microbiome. Phytopathology® 107:1284–1297.
15. Poudel R, Jumpponen A, Schlatter DC, Paulitz TC, Gardener BBM, Kinkel LL, Garrett KA. 2016. Microbiome Networks: A Systems Framework for Identifying Candidate Microbial Assemblages for Disease Management. Phytopathology 106:1083–1096.
16. Xu L, Naylor D, Dong Z, Simmons T, Pierroz G, Hixson KK, Kim Y-M, Zink EM, Engbrecht KM, Wang Y, Gao C, DeGraaf S, Madera MA, Sievert JA, Hollingsworth J, Birdseye D, Scheller HV, Hutmacher R, Dahlberg J, Jansson C, Taylor JW, Lemaux PG, Coleman-Derr D. 2018. Drought delays development of the sorghum root microbiome and enriches for monoderm bacteria. Proc Natl Acad Sci U S A 115:E4284–E4293.
17. Viaene T, Langendries S, Beirinckx S. 2016. Streptomyces as a plant's best friend? FEMS microbiology.
18. Lebeis SL, Paredes SH, Lundberg DS, Breakfield N, Gehring J, McDonald M, Malfatti S, Glavina del Rio T, Jones CD, Tringe SG, Dangl JL. 2015. PLANT MICROBIOME. Salicylic acid modulates colonization of the root microbiome by specific bacterial taxa. Science 349:860–864.
19. Chewning SS, Grant DL, O'Banion BS, Gates AD, Kennedy BJ, Campagna SR, Lebeis SL. 2019. Root-Associated Streptomyces Isolates Harboring melC Genes Demonstrate Enhanced Plant Colonization. Phytobiomes Journal 3:165–176.

20. Berendsen RL, Vismans G, Yu K, Song Y, de Jonge R, Burgman WP, Burmølle M, Herschend J, Bakker PAHM, Pieterse CMJ. 2018. Disease-induced assemblage of a plant-beneficial bacterial consortium. ISME J 12:1496–1507.
21. Mello BL, Alessi AM, McQueen-Mason S, Bruce NC, Polikarpov I. 2016. Nutrient availability shapes the microbial community structure in sugarcane bagasse compost-derived consortia. Sci Rep 6:38781.
22. Castrillo G, Teixeira PJPL, Paredes SH, Law TF, de Lorenzo L, Feltcher ME, Finkel OM, Breakfield NW, Mieczkowski P, Jones CD, Paz-Ares J, Dangl JL. 2017. Root microbiota drive direct integration of phosphate stress and immunity. Nature 543:513–518.
23. Moccia K, Willems A, Papoulis S, Flores A, Forister ML, Fordyce JA, Lebeis SL. 2020. Distinguishing nutrient-dependent plant driven bacterial colonization patterns in alfalfa. Environ Microbiol Rep 12:70–77.
24. Yuan Y, Brunel C, van Kleunen M, Li J, Jin Z. 2019. Salinity-induced changes in the rhizosphere microbiome improve salt tolerance of Hibiscus hamabo. Plant Soil 443:525–537.
25. Lucaciu R, Pelikan C, Gerner SM, Zioutis C, Köstlbacher S, Marx H, Herbold CW, Schmidt H, Rattei T. 2019. A Bioinformatics Guide to Plant Microbiome Analysis. Front Plant Sci 10:1313.
26. Regalado J, Lundberg DS, Deusch O, Kersten S, Karasov T, Poersch K, Shirsekar G, Weigel D. 2020. Combining whole-genome shotgun sequencing and rRNA gene amplicon analyses to improve detection of microbe–microbe interaction networks in plant leaves. ISME J 14:2116–2130.
27. Vorholt JA, Vogel C, Carlström CI, Müller DB. 2017. Establishing Causality: Opportunities of Synthetic Communities for Plant Microbiome Research. Cell Host Microbe 22:142–155.
28. O'Banion BS, O'Neal L, Alexandre G, Lebeis SL. 2020. Bridging the Gap Between Single-Strain and Community-Level Plant-Microbe Chemical Interactions. Mol Plant Microbe Interact 33:124–134.
29. Carlström CI, Field CM, Bortfeld-Miller M, Müller B, Sunagawa S, Vorholt JA. 2019.

Synthetic microbiota reveal priority effects and keystone strains in the Arabidopsis phyllosphere. Nat Ecol Evol 3:1445–1454.

30. Chen I-MA, Markowitz VM, Chu K, Palaniappan K, Szeto E, Pillay M, Ratner A, Huang J, Andersen E, Huntemann M, Varghese N, Hadjithomas M, Tennessen K, Nielsen T, Ivanova NN, Kyrpides NC. 2017. IMG/M: integrated genome and metagenome comparative data analysis system. Nucleic Acids Res 45:D507–D516.
31. Arkin AP, Cottingham RW, Henry CS, Harris NL, Stevens RL, Maslov S, Dehal P, Ware D, Perez F, Canon S, Sneddon MW, Henderson ML, Riehl WJ, Murphy-Olson D, Chan SY, Kamimura RT, Kumari S, Drake MM, Brettin TS, Glass EM, Chivian D, Gunter D, Weston DJ, Allen BH, Baumohl J, Best AA, Bowen B, Brenner SE, Bun CC, Chandonia J-M, Chia J-M, Colasanti R, Conrad N, Davis JJ, Davison BH, DeJongh M, Devoid S, Dietrich E, Dubchak I, Edirisinghe JN, Fang G, Faria JP, Frybarger PM, Gerlach W, Gerstein M, Greiner A, Gurtowski J, Haun HL, He F, Jain R, Joachimiak MP, Keegan KP, Kondo S, Kumar V, Land ML, Meyer F, Mills M, Novichkov PS, Oh T, Olsen GJ, Olson R, Parrello B, Pasternak S, Pearson E, Poon SS, Price GA, Ramakrishnan S, Ranjan P, Ronald PC, Schatz MC, Seaver SMD, Shukla M, Sutormin RA, Syed MH, Thomason J, Tintle NL, Wang D, Xia F, Yoo H, Yoo S, Yu D. 2018. KBase: The United States Department of Energy Systems Biology Knowledgebase. Nature Biotechnology.
32. Lu W, Bennett BD, Rabinowitz JD. 2008. Analytical strategies for LC-MS-based targeted metabolomics. J Chromatogr B Analyt Technol Biomed Life Sci 871:236–242.
33. Hammer Ø, Harper DAT, Ryan PD, Others. 2001. PAST: Paleontological statistics software package for education and data analysis. Palaeontol Electronica 4:9.
34. Szkop M, Sikora P, Orzechowski S. 2012. A novel, simple, and sensitive colorimetric method to determine aromatic amino acid aminotransferase activity using the Salkowski reagent. Folia Microbiol 57:1–4.
35. Blin K, Medema MH, Kottmann R, Lee SY, Weber T. 2017. The antiSMASH database, a comprehensive database of microbial secondary metabolite

biosynthetic gene clusters. Nucleic Acids Res 45:D555–D559.
36. Vargas-Bautista C, Rahlwes K, Straight P. 2014. Bacterial competition reveals differential regulation of the pks genes by Bacillus subtilis. J Bacteriol 196:717–728.
37. Finkel OM, Salas-González I, Castrillo G, Conway JM, Law TF, Teixeira PJPL, Wilson ED, Fitzpatrick CR, Jones CD, Dangl JL. 2020. A single bacterial genus maintains root growth in a complex microbiome. Nature 587:103–108.
38. Paredes SH, Gao T, Law TF, Finkel OM, Mucyn T, Paulo José Pereira, González IS, Feltcher ME, Powers MJ, Shank EA, Jones CD, Jojic V, Dangl JL, Castrillo G. 2018. Design of synthetic bacterial communities for predictable plant phenotypes. PLOS Biology.
39. Klindworth A, Pruesse E, Schweer T, Peplies J, Quast C, Horn M, Glöckner FO. 2013. Evaluation of general 16S ribosomal RNA gene PCR primers for classical and next-generation sequencing-based diversity studies. Nucleic Acids Res 41:e1.
40. Caporaso JG, Kuczynski J, Stombaugh J, Bittinger K, Bushman FD, Costello EK, Fierer N, Peña AG, Goodrich JK, Gordon JI, Huttley GA, Kelley ST, Knights D, Koenig JE, Ley RE, Lozupone CA, McDonald D, Muegge BD, Pirrung M, Reeder J, Sevinsky JR, Turnbaugh PJ, Walters WA, Widmann J, Yatsunenko T, Zaneveld J, Knight R. 2010. QIIME allows analysis of high-throughput community sequencing data. Nat Methods 7:335–336.
41. Callahan BJ, McMurdie PJ, Rosen MJ, Han AW, Johnson AJA, Holmes SP. 2016. DADA2: High-resolution sample inference from Illumina amplicon data. Nat Methods 13:581–583.
42. Callahan BJ, McMurdie PJ, Holmes SP. 2017. Exact sequence variants should replace operational taxonomic units in marker-gene data analysis. ISME J 11:2639–2643.
43. Quast C, Pruesse E, Yilmaz P, Gerken J, Schweer T, Yarza P, Peplies J, Glöckner FO. 2013. The SILVA ribosomal RNA gene database project: improved data processing and web-based tools. Nucleic Acids Res 41:D590–6.
44. Dickey JR, Fordyce JA, Lebeis SL. 2020. Bacterial communities of the Salvia lyrata rhizosphere explained by spatial structure and sampling grain. Microb Ecol 80:846–

858.
45. Ma Z (sam). 2018. Measuring Microbiome Diversity and Similarity with Hill Numbers. Metagenomics.
46. Jost L. 2007. Partitioning diversity into independent alpha and beta components. Ecology 88:2427–2439.
47. De Cáceres M, Legendre P. 2009. Associations between species and groups of sites: indices and statistical inference. Ecology 90:3566–3574.
48. Yeoh YK, Paungfoo-Lonhienne C, Dennis PG, Robinson N, Ragan MA, Schmidt S, Hugenholtz P. 2016. The core root microbiome of sugarcanes cultivated under varying nitrogen fertilizer application. Environmental Microbiology.
49. Naveed M, Qureshi MA, Zahir ZA, Hussain MB, Sessitsch A, Mitter B. 2015. L-Tryptophan-dependent biosynthesis of indole-3-acetic acid (IAA) improves plant growth and colonization of maize by Burkholderia phytofirmans PsJN. Ann Microbiol 65:1381–1389.
50. Böttcher C, Chapman A, Fellermeier F, Choudhary M, Scheel D, Glawischnig E. 2014. The Biosynthetic Pathway of Indole-3-Carbaldehyde and Indole-3-Carboxylic Acid Derivatives in Arabidopsis. Plant Physiol 165:841–853.
51. Fu S-F, Wei J-Y, Chen H-W, Liu Y-Y, Lu H-Y, Chou J-Y. 2015. Indole-3-acetic acid: A widespread physiological code in interactions of fungi with other organisms. Plant Signal Behav 10:e1048052.
52. Schiessl KT, Hu F, Jo J, Nazia SZ, Wang B, Price-Whelan A, Min W, Dietrich LEP. 2019. Phenazine production promotes antibiotic tolerance and metabolic heterogeneity in Pseudomonas aeruginosa biofilms. Nature Communications.
53. Bulgarelli D, Garrido-Oter R, Münch PC, Weiman A, Dröge J, Pan Y, McHardy AC, Schulze-Lefert P. 2015. Structure and function of the bacterial root microbiota in wild and domesticated barley. Cell Host Microbe 17:392–403.
54. Araújo JM de, Silva AC da, Azevedo JL. 2000. Isolation of endophytic actinomycetes from roots and leaves of maize (Zea mays L.). Braz Arch Biol Technol 43:0–0.
55. Yeoh YK, Dennis PG, Paungfoo-Lonhienne C, Weber L, Brackin R, Ragan MA,

Schmidt S, Hugenholtz P. 2017. Evolutionary conservation of a core root microbiome across plant phyla along a tropical soil chronosequence. Nat Commun 8:215.

56. Krzywinski M, Schein J, Birol I, Connors J, Gascoyne R, Horsman D, Jones SJ, Marra MA. 2009. Circos: an information aesthetic for comparative genomics. Genome Res 19:1639–1645.

APPENDIX: TABLES

Table 3. 1:Seedling exudate metabolites that were altered with *Streptomyces* inoculation.

Select metabolites that significantly differ between uninoculated seedlings and those inoculated with strains 299, 303, CL18, 136, or 374 strains. The discovery of metabolites that differ from the NB controls was performed by using an unpaired *t*-test for each inoculated sample type followed by a two-stage Benjamini, Krieger, and Yekutili False Discovery Rate procedure for compounds with lower (top, blue) and higher (bottom, pink) ion counts. 5 replicates per treatment type, degrees of freedom 832, n.s.= no significance.

	299 inoculation			303 inoculation			CL18 inoculation			136 inoculation			374 inoculation		
Decreased metabolites	P value	t ratio	q value	P value	t ratio	q value	P value	t ratio	q value	P value	t ratio	q value	P value	t ratio	q value
Glycolate	<0.000000000000001	8.294	6E-15	3.629E-12	7.055	3.4617E-11	<0.000000000000001	12.56	<0.000000000000001	9.00615E-09	5.808	4.63907E-07	7.00389E-08	5.44	3.6077E-06
Pyroglutamic acid	<0.000000000000001	18.96	<0.000000000000001	<0.000000000000001	17.69	<0.000000000000001	<0.000000000000001	31.88	<0.000000000000001	<0.000000000000001	13.26	<0.000000000000001	6.04742E-08	5.467	3.6077E-06
Allantoin	6.94263E-05	3.998	0.000531747	0.00269434	3.659	0.001285049	5.62883E-07	5.043	1.42128E-05	n.s.			n.s.		
Increased metabolites															
Sulfolactate	8.7E-14	7.588	1.001E-12	<0.000000000000001	12.42	<0.000000000000001	4.4091E-11	6.679	1.4844E-09	n.s.			n.s.		
Salicylate	<0.000000000000001	9.094	<0.000000000000001	1.58769E-05	4.342	9.73596E-05	n.s.			n.s.			n.s.		
Jasmonate	<0.000000000000001	9.129	<0.000000000000001	<0.000000000000001	16.81	<0.000000000000001	n.s.			n.s.			n.s.		
Indole-3-carboxylate	<0.000000000000001	14.56	<0.000000000000001	<0.000000000000001	38.21	<0.000000000000001	n.s.			n.s.			n.s.		
Citrate/isocitrate	<0.000000000000001	13.4	<0.000000000000001	<0.000000000000001	24.25	<0.000000000000001	n.s.			n.s.			n.s.		
Allantoate	2.16467E-05	4.272	0.000180868	1.205E-12	7.216	1.2934E-11	n.s.			n.s.			n.s.		
2-Hydroxy-2-methylsuccinate	2.20279E-07	5.225	2.21765E-06	1.68923E-08	5.697	1.31837E-07	n.s.			n.s.			n.s.		
2-hydroxyglutaric acid	2.41285E-07	5.208	2.21765E-06	1.8924E-08	5.677	1.35385E-07	n.s.			n.s.			n.s.		
Glyoxylate	<0.000000000000001	9.944	<0.000000000000001	8E-15	7.917	1.11E-13	n.s.			n.s.			n.s.		
D-Gluconate	0.000200736	3.735	0.001419206	4.63E-13	7.353	5.673E-12	n.s.			n.s.			n.s.		
D-Glucarate	n.s.			7.31268E-05	3.986	0.000392371	n.s.			n.s.			n.s.		
Pantothenate	n.s.			9.93962E-05	3.911	0.000501951	n.s.			n.s.			n.s.		
N-Acetylglutamate	n.s.			3.98188E-05	4.131	0.000227897	n.s.			n.s.			n.s.		
Citraconate	n.s.			0.000627454	3.433	0.002835102	n.s.			n.s.			n.s.		
2-Isopropylmalate	n.s.			1.29594E-06	4.876	8.55819E-06	n.s.			n.s.			n.s.		
myo-Inositol	n.s.			1.3424E-11	6.86	1.15249E-10	n.s.			n.s.			n.s.		

Table 3. 2: Genome overview of bacterial strains.

Available genomes of isolates used in this study were analyzed on a number of criteria. Isolates were compared by genome size (bp), GC % content, scaffold number, gene number, biosynthetic gene clusters (BGC) and number of genes associated in BGCs. Data generated from antiSMASH outputs. Actinobacteria (blue), Bacteroidetes (yellow), Firmicutes (purple), and Proteobacteria (orange).

Strain	IMG Genome ID	Size (bp)	GC %	Scaffolds	# of genes	BGC	# of genes in BGC	% genes in BGC
299	2521172643	10479972	70.32	116	9710	33	822	8.47
303	2521172626	9550898	71.4	77	8480	28	726	8.56
CL18	2521172643	7336835	72.26	49	6677	14	311	4.66
136	2636416059	7836607	69.83	31	6991	15	288	4.12
40	2563366720	5577194	33.68	11	4820	7	189	3.92
181	2639762524	5602441	45.54	35	5066	26	400	7.9
2	2517572231	6550409	61.06	44	6365	5	137	2.15
374	2596583649	2971437	66.26	9	2934	2	34	1.16
CL11	2546825541	8471422	62.32	31	7562	13	13	0.17
50	2228664007	6455262	59.3	32	5920	13	72	1.22

Table 3. 3: Bacterial strains used in these experiments.

In these studies, we characterize several Actinobacteria (blue), Bacteroidetes (yellow), Deinococcus-Thermus (grey), Firmicutes (purple), and Proteobacteria (orange) strains.

Phylum	Genus	Strain name	Label	Figures
Actinobacteria	*Streptomyces*	*Streptomyces sp.* 303MFCol5.2	**299**	**1-5, SF 1-5**
		Streptomyces canus 299MFChir4.1	**303**	**1-5, SF 1-5**
		Streptomyces sp. UNC401CLCol	**CL18**	**1-5, SF 1-5**
		Streptomyces sp. 136MFCol5.1	**136**	**1-5, SF 1-5**
Bacteroidetes	*Flavobacterium*	*Flavobacterium sp.* 40S8	**40**	**2-5, SF3**
Deinococcus-Thermus	Deinococcus	*Deinococcus sp. TN56*	**TN56**	**3-5, SF3**
Firmicutes	*Bacillus*	*Bacillus sp.* A415	**A415**	**3-5, SF3**
	Paenibacillus	*Paenibacillus sp.* 181MFCol5.1	**181**	**2-5, SF3**
Proteobacteria	*Rhizobium*	*Rhizobium sp.* 2MFCol3.1	**2**	**2-5, SF3**
	Brevundimonas	*Brevundimonas sp.* 374	**374**	**2-5, SF2-3**
	Burkholderia	*Burkholderia* CL11	**CL11**	**2-5, SF2-3**
	Burkholderia	*Burkholderia sp.* TN8	**TN8**	**2-5, SF2-3**
	Escherichia	*Escherichia coli* DH5a	**E.coli**	**2-5, SF2-3**
	Pseudomonas	*Pseudomonas sp.* KD5	**50**	**2-5, SF2-3**
	Pseudomonas	*Pseudomonas sp.* TN19	**TN19**	**2-5, SF2-3**

Table 3. 4: Replicate numbers in each treatment group for the two-step inoculation experiment.

Distribution of sample numbers (N) as well as mean, minimum and maximum read number for each treatment group in the two-step inoculation experiment. Sample types were organized by inoculum alone: SynCom (blue) and SoilSup (brown); and by post-treatment: No bacteria (NB) (grey), SynCom (blue), SoilSup (brown).

Sample Type	Replicate #	Mean Read #	Min. Read #	Max. Read #
NB->NB	9	88375.44	23861	17640
299->NB	6	107704.6	61047	208813
303->NB	9	104922.67	39464	176113
CL18->NB	8	78786.67	28494	147048
136->NB	5	101045.75	47954	156785
SynCom Inoc	3	78187.67	62150	98170
NB->SynCom	11	109765.36	38600	2432323
299->SynCom	15	71306.33	13781	140184
303->SynCom	14	67878.43	11852	199865
CL18->SynCom	13	65215.29	38643	144613
136->SynCom	16	79271.31	17790	167139
SoilSup Inoc	3	10005	4399	15335
NB->SoilSup	6	53561.2	24147	95046
299->SoilSup	11	66037.58	55353	96046
303->SoilSup	3	54455.67	49313	60953
CL18->SoilSup	5	40904.8	13176	74089
136->SoilSup	8	57556.13	10259	147136

Table 3. 5: Alpha diversity comparison by treatment group.

Hill numbers were generated between samples for the two-step inoculation experiment using alpha diversity at exponents of *q*=0, *q*=1, and *q*=2. Samples are grouped by treatment group, as determined by the initial and subsequent inoculum on the x and y-axis. Color indicates p-value changes from dark orange p<0.01 to lighter orange values p<0.05 (adjusted p-values reported, single step method).

q=0

	NB->NB	299->NB	303->NB	CL18->NB	136->NB	SynCom Inoc	NB->SynCom	299->SynCom	303->SynCom	CL18->SynCom	136->SynCom	SoilSup Inoc	NB->SoilSup	299->SoilSup	303->SoilSup	CL18->SoilSup	136->SoilSup
NB->NB																	
299->NB	1																
303->NB	1	1															
CL18->NB	1	0.9994	0.9997														
136->NB	1	1	1	1													
SynCom Inoc	0.9967	0.9917	0.994	0.9999	0.9998												
NB->SynCom	1	1	1	1	1	0.9969											
299->SynCom	0.9649	0.9046	0.9147	1	1	1	0.9849										
303->SynCom	0.9927	0.9686	0.956	1	1	1	0.9779	1									
CL18->SynCom	0.8379	0.7384	0.6344	0.9997	0.9998	1	0.6808	1	1								
136->SynCom	0.9949	0.9737	0.98	1	1	1	0.992	1	1	1							
SoilSup Inoc	0.1281	0.1896	0.1561	0.056	0.0765	**<0.01**	0.1231	**0.0221**	**0.0299**	**0.0143**	**0.0323**						
NB->SoilSup	0.0733	0.0514	0.0779	0.4613	0.5824	1	0.1522	0.8621	0.7707	0.9665	0.7233	**<0.01**					
299->SoilSup	**0.0184**	**<0.01**	**0.0136**	0.3265	0.4793	1	0.0605	0.7901	0.6561	0.9533	0.5927	**<0.01**	1				
303->SoilSup	0.3303	0.2062	0.2474	0.8086	0.8345	1	0.4234	0.9697	0.9381	0.9951	0.9202	**<0.01**	1	1			
CL18->SoilSup	**0.0131**	**<0.01**	**<0.01**	0.1764	0.2626	1	**0.0342**	0.5171	0.3956	0.7535	0.3431	**<0.01**	1	1	1		
136->SoilSup	**0.0145**	**<0.01**	0.0153	0.2231	0.3561	1	**0.047**	0.6618	0.5246	0.8779	0.4653	**<0.01**	1	1	1	1	

q=1

	NB->NB	299->NB	303->NB	CL18->NB	136->NB	SynCom Inoc	NB->SynCom	299->SynCom	303->SynCom	CL18->SynCom	136->SynCom	SoilSup Inoc	NB->SoilSup	299->SoilSup	303->SoilSup	CL18->SoilSup	136->SoilSup
NB->NB																	
299->NB	1																
303->NB	1	1															
CL18->NB	1	0.9999	1														
136->NB	1	1	1	1													
SynCom Inoc	1	1	1	1	1												
NB->SynCom	1	1	1	1	1	1											
299->SynCom	1	1	1	1	1	1	1										
303->SynCom	1	1	1	1	1	1	1	1									
CL18->SynCom	1	1	1	0.9999	1	1	1	1	1								
136->SynCom	1	1	1	0.9988	1	1	1	1	1	1							
SoilSup Inoc	**<0.01**	**<0.01**	**<0.01**	**<0.01**	**<0.01**	**<0.01**	**<0.01**	**<0.01**	**<0.01**	**<0.01**	**<0.01**						
NB->SoilSup	0.587	0.2994	0.2627	0.8665	0.6873	0.9028	0.393	0.1814	0.2283	0.171	0.909	**<0.01**					
299->SoilSup	0.9646	0.7492	0.7068	0.9991	0.9779	0.998	0.8677	0.588	0.6748	0.5631	0.3525	**<0.01**	0.9999				
303->SoilSup	0.9992	0.98	0.9811	1	0.9987	0.9998	0.9959	0.9801	0.9865	0.9735	0.9439	**<0.01**	1	1			
CL18->SoilSup	0.9699	0.8122	0.7996	0.9983	0.9746	0.9959	0.9113	0.754	0.8045	0.7235	0.5784	**<0.01**	1	1	1		
136->SoilSup	0.9174	0.6562	0.6176	0.9944	0.9447	0.9923	0.7835	0.5042	0.5848	0.4786	0.303	**<0.01**	1	1	1	1	

q=2

	NB->NB	299->NB	303->NB	CL18->NB	136->NB	SynCom Inoc	NB->SynCom	299->SynCom	303->SynCom	CL18->SynCom	136->SynCom	SoilSup Inoc	NB->SoilSup	299->SoilSup	303->SoilSup	CL18->SoilSup	136->SoilSup
NB->NB																	
299->NB	1																
303->NB	1	1															
CL18->NB	1	0.9886	0.9998														
136->NB	1	1	1	0.9997													
SynCom Inoc	1	0.9998	1	1	1												
NB->SynCom	1	0.9951	1	1	0.9999	1											
299->SynCom	1	1	1	0.9996	1	1	0.9998										
303->SynCom	1	0.9805	0.9993	1	0.9995	1	1	0.998									
CL18->SynCom	1	0.9996	1	1	1	1	1	1	1								
136->SynCom	1	1	1	0.9844	1	0.9999	0.9863	1	0.9366	0.9991							
SoilSup Inoc	**<0.01**	**<0.01**	**<0.01**	**<0.01**	**<0.01**	**<0.01**	**<0.01**	**<0.01**	**<0.01**	**<0.01**	**<0.01**						
NB->SoilSup	**0.0325**	**<0.01**	**0.0163**	0.19	0.0279	0.9185	0.1544	**0.0114**	0.1705	0.0626	**<0.01**	**<0.01**					
299->SoilSup	0.3485	**0.04**	0.1511	0.8642	0.2809	0.9998	0.7764	0.142	0.8151	0.5092	**0.0388**	**<0.01**	0.9923				
303->SoilSup	0.9601	0.6253	0.8521	0.9998	0.8709	1	0.9963	0.8599	0.9981	0.9801	0.6799	**<0.01**	0.9994	1			
CL18->SoilSup	0.1041	**0.0114**	**0.0409**	0.42	0.0793	0.9735	0.3316	0.0384	0.3956	0.1682	**0.0108**	**<0.01**	1	0.9997	1		
136->SoilSup	0.3971	0.0691	0.22	0.8603	0.3051	0.9996	0.7922	0.1884	0.366	0.5541	0.0635	**<0.01**	0.9977	1	1	1	

APPENDIX: FIGURES

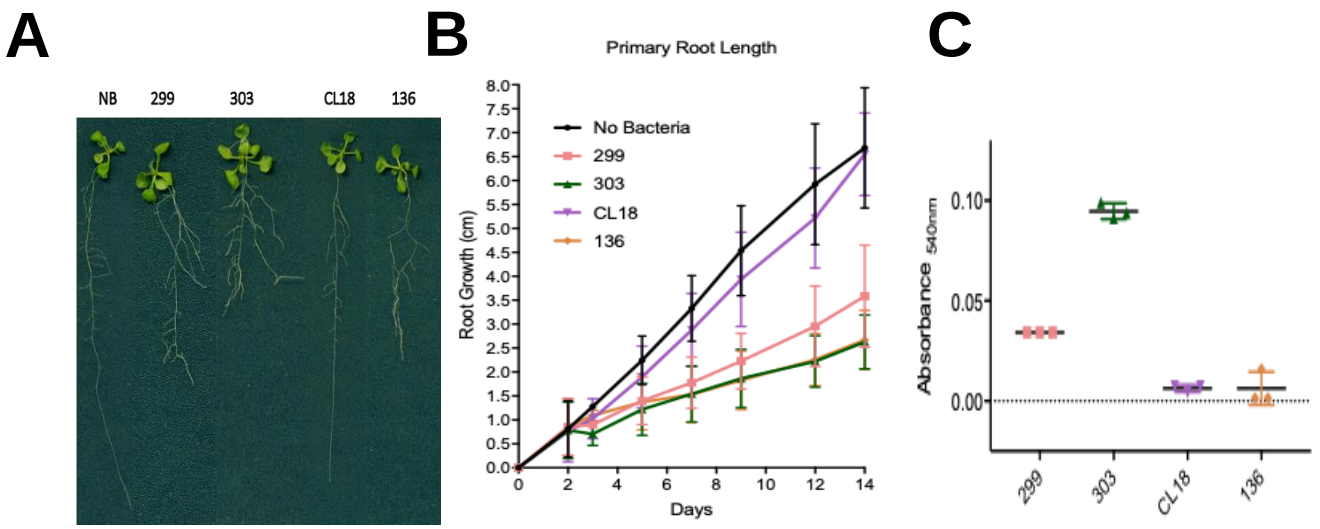

Figure 3. 1: Arabidopsis root morphology following *Streptomyces* inoculation and indole-3-acetic acid (IAA) quantification.

A) Axenic 7-day old Arabidopsis seedlings were inoculated on ¼ MS plates with each of the four *Streptomyces* isolates and grown vertically for 14 days. An example of each Arabidopsis seedling root morphology is shown. B) Primary root length over the 14 days of seedling growth. A 1-Way ANOVA with a *post hoc* Dunnett's multiple comparisons of the mean of 9 replicates was performed. * indicates significantly different than no bacteria (NB) control ($\boldsymbol{\alpha}$=0.05, $F_{4,39}$=43.46). C) Colorimetric IAA quantification of *Streptomyces* isolate cultures from medium with tryptophan added (299 (pink), 303 (green), CL18 (purple), and 136 (orange)). Following the addition of Salkowski reagent, absorbance was measured at 540nm after 30 minutes with uninoculated medium control values subtracted from the measurement. A 1-way ANOVA with *post hoc* Tukey's multiple comparison test was performed ($\boldsymbol{\alpha}$=0.05, $F_{3,8}$= 238.5). Letters indicate significantly different groups.

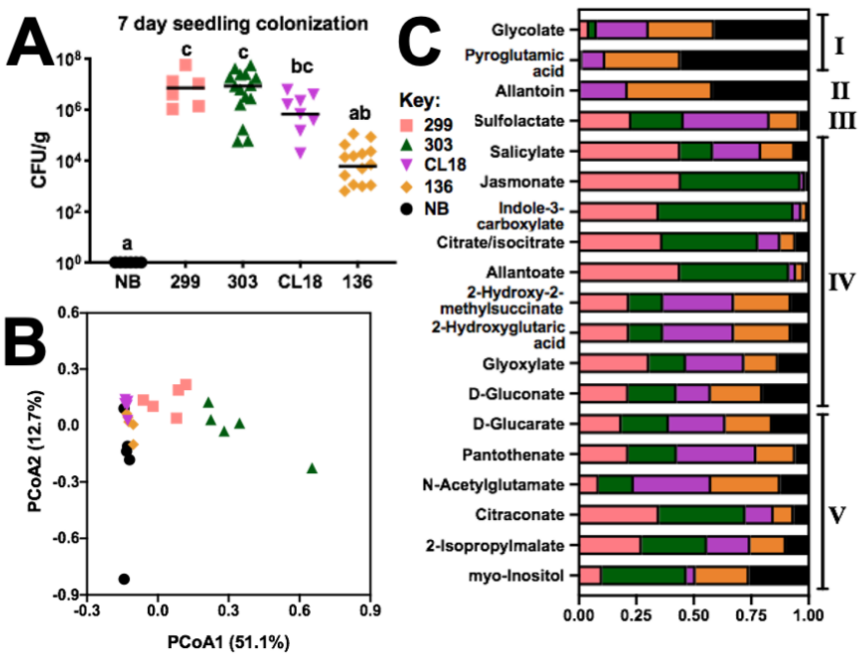

Figure 3. 2: *Streptomyces* strains show different colonization phenotypes and alter metabolic profiles of Arabidopsis seedling root exudates.

A) Arabidopsis seedling colonization 7 days after inoculation was determined by counting colony forming units and normalized by gram of plant tissue (CFU/g). Horizontal line represents the mean value. A Kruskal-Wallis with *post hoc* Dunn's multiple comparisons was performed (n=6-16 , $p<0.05$, z-score=38.79). Letters indicate significantly different groups. B) Metabolomics data from Arabidopsis seedling exudates. Principal Coordinate Analysis (PCoA) based on Euclidean distances results were generated from ion counts for 5 replicate samples each normalized by mass. For A and B, *Streptomyces* strains are represented by pink squares for 299, green upward triangles for 303, purple downward triangles from CL18, and orange diamonds for 136, as well as no bacteria (NB) controls represented by black circles. C) A subset of 19 metabolites detected in B were differentially abundant between at least 1 inoculated set of samples and the NB controls 7 days after inoculation. Results of multiple *t*-tests are found in Table S2. Metabolites that decrease with inoculation of all *Streptomyces* (I), metabolites that decrease with 303, 299, and CL18 inoculation (II), metabolites that increase with 303 and 299 inoculation (III), and metabolites that increase with only 303 inoculation (IV).

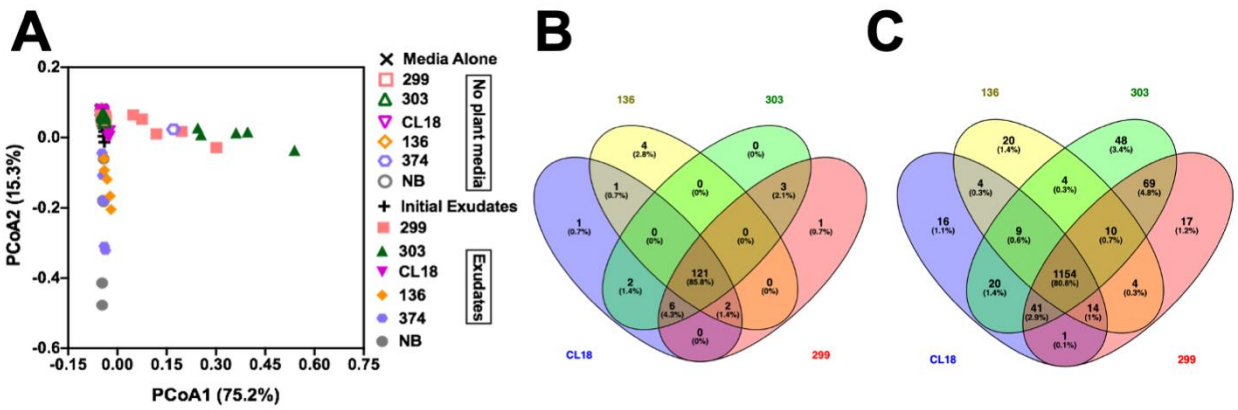

Figure 3. 3: Detected metabolites and predicted metabolisms were compared between each *Streptomyces* isolate.

A) A PCoA of Euclidean distances was generated using metabolomics of media alone controls (open symbols) and with inoculated plant root exudates (closed symbols). *Brevundimonas* sp. 374 (blue hexagon) is included with *Streptomyces* isolates 299 (pink square), 303 (green circle), CL18 (purple triangle), and 136 (orange diamond) as an unrelated bacterial control. No bacteria (NB, grey circles) controls were also included. B-C) Venn diagram of predicted compounds taken up by strains (B) and metabolic pathways encoded by strain genomes (C) using metabolic modelling to show overlap between isolates.

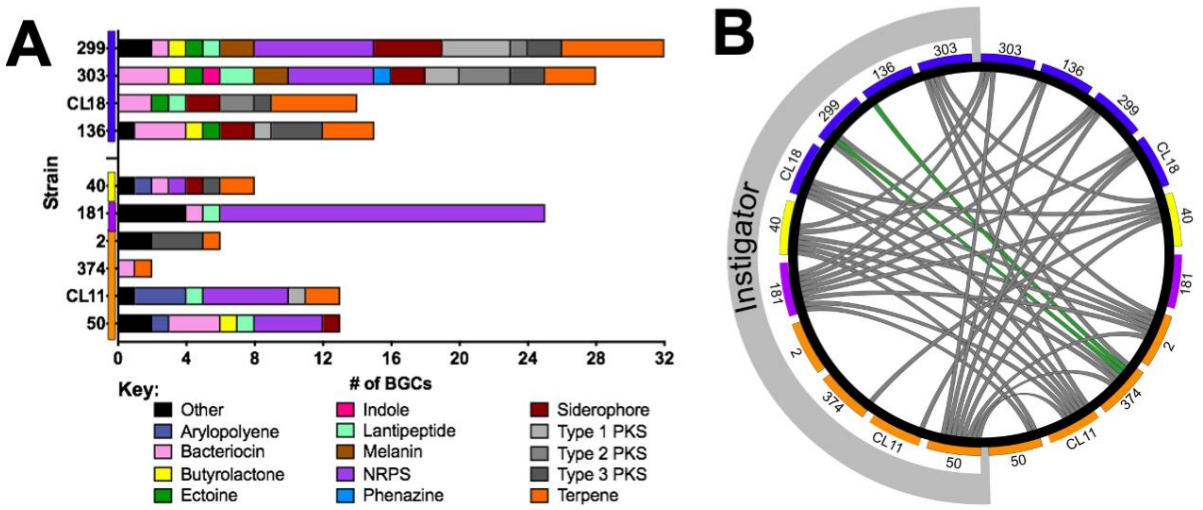

Figure 3. 4: *Streptomyces* strains show different predicted biosynthetic gene clusters and microbial interactions in vitro.

A) Predicted biosynthetic gene clusters (BGCs) were classified using antiSMASH version 5 for the genomes of *Streptomyces* (blue) and representative non-*Streptomyces* strains representing the other major phyla found in plant microbiomes; Bacteroidetes (yellow), Firmicutes (purple), and Proteobacteria (orange). Clusters are shown by class of predicted compound. B) Microbial *in vitro* co-culture assays between *Streptomyces* and non-*Streptomyces* isolates on the left side of the Circos plot (56) instigated either negative (grey lines) or positive (green lines) changes in the growth of the isolates on the right of the plot on at least one of the three media types tested.

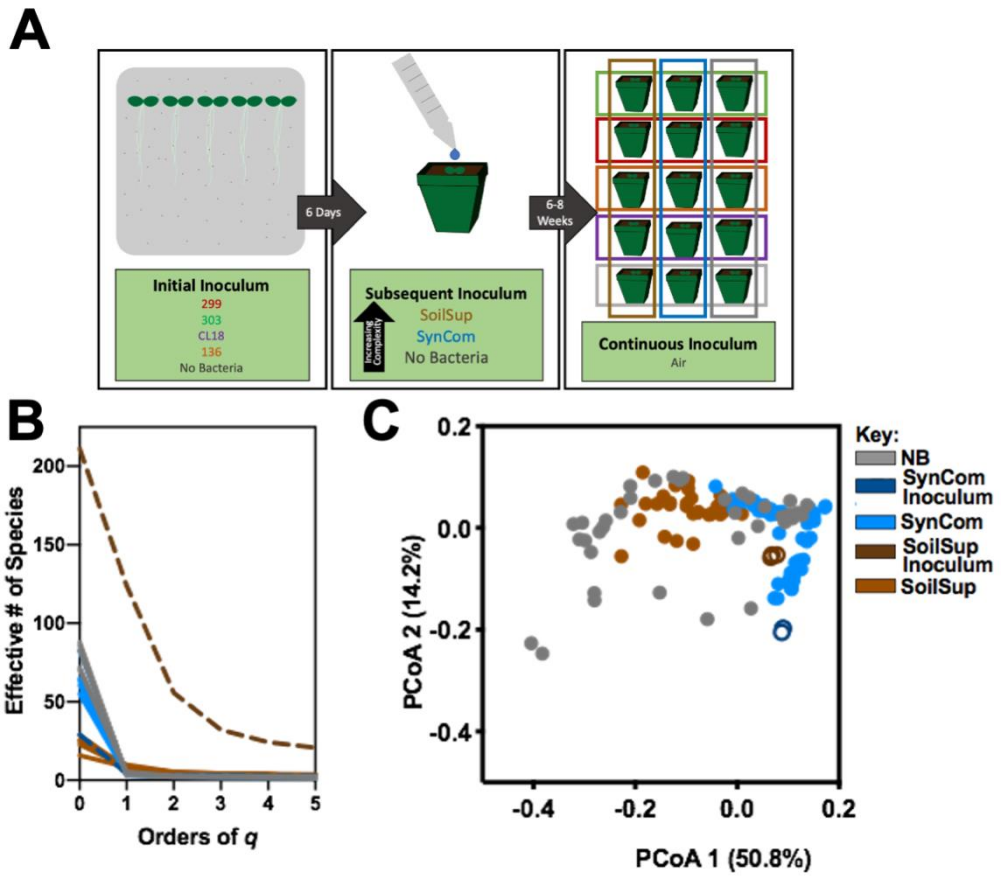

Figure 3. 5: In a two-step seedling inoculation experiment, assembled root microbiome samples cluster by subsequent inoculum.

A) An overview of experimental design to generate 15 different types of treatment groups based on 5 initial inoculum types and 3 subsequent inoculum types. B) A Hill numbers approach to observe alpha diversity calculated the effective number of species in each treatment group for all non-singleton, microbial ASVs. Root samples that received subsequent inoculum SynCom (light blue) and SoilSup (light brown), as well as no bacteria (NB; grey) were compared with SynCom inoculum (dashed dark blue) and SoilSup inoculum (dashed dark brown). C) Weighted UniFrac distances based on all non-singleton, ASVs were used to generate Principal Coordinates Analysis (PCoA) for NB (closed, grey), SynCom (closed, light blue), and SoilSup (closed, light brown) root samples, as well as SynCom (open, dark blue) and SoilSup (open, dark brown) inoculum samples.

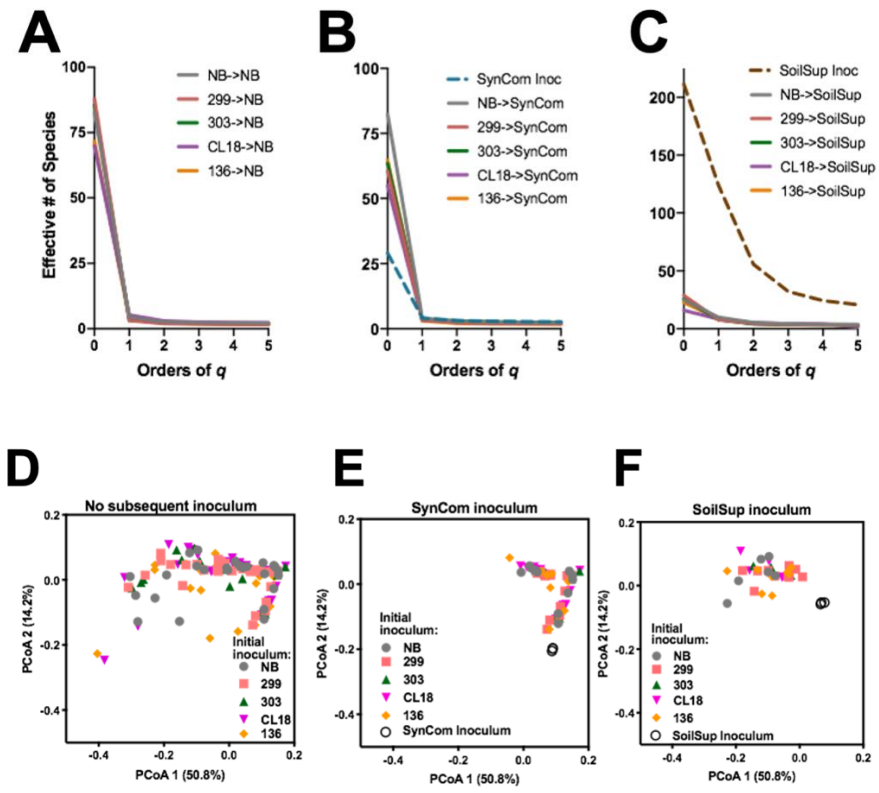

Figure 3. 6: Alpha and beta diversity comparisons show differences in effective number of species and composition of the community following different initial and subsequent inoculum treatments.

A-C) Effective number of species using alpha diversity across orders of *q* to detect changes in rare and abundant ASVs initially inoculated with no bacteria (NB, grey) or *Streptomyces* strain 299 (pink), 303 (green), CL18 (purple), 136 (orange) for samples subsequently inoculated with NB (A), SynCom with SynCom inoculum control (dashed blue line) (B), and SoilSup with SoilSup inoculum control (dashed brown line) (C). D-F) PCoA plots generated from weighted UniFrac distances showing assembled root community composition. Initial inoculum include NB (grey, circle), 299 (pink, upwards triangle), 303 (green, downwards triangle), CL18 (purple, diamond), and 136 (orange, square) are shown for NB subsequent inoculum (D), SynCom subsequent inoculum with Inoculum alone composition (open circle) (E) and SoilSup subsequent inoculum with Inoculum alone composition (open circle). PCoA axis labels PCoA 1 (50.8%) and PCoA 2 (14.2%).

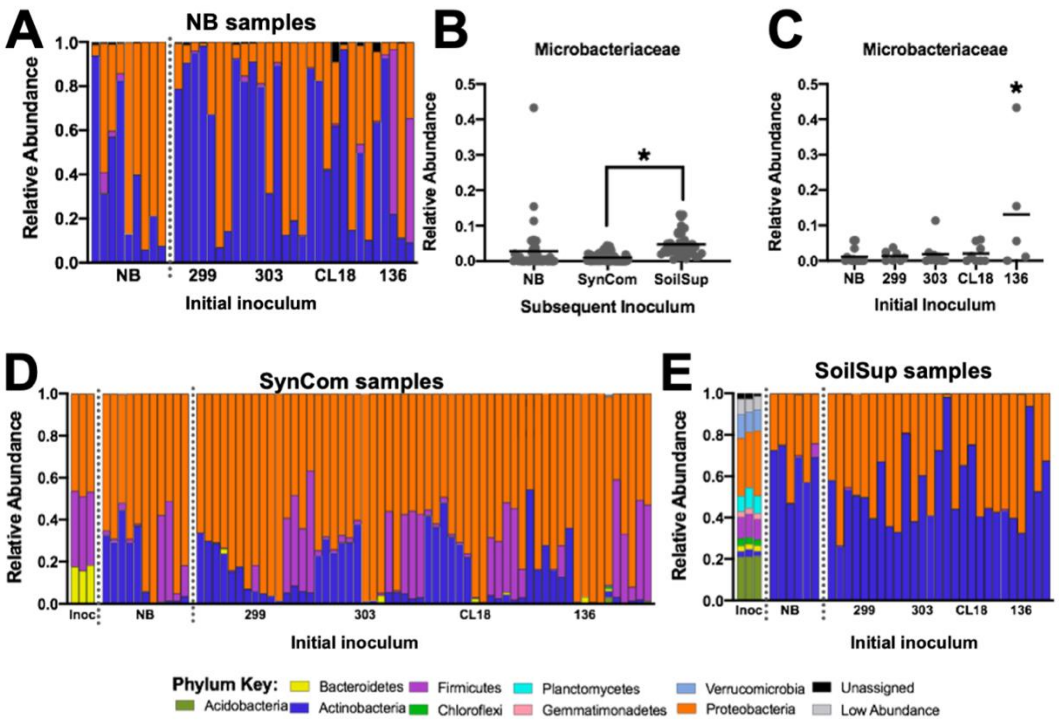

Figure 3. 7: Phyla distributions of assembled root microbiomes highlight only particular taxa from air, SynCom, and SoilSup inocula assemble.

A) Relative abundance of phyla in No Bacteria (NB) subsequent-inoculation root samples (n=4-9). B) Pooled relative abundance of the 32 Microbacteriaceae ASVs absent in SynCom and SoilSup inoculum in root samples from NB plants (n=38), SynCom (n=69), and SoilSup (n=33). * indicates significantly different as identified by a 1-way ANOVA with *post hoc* Tukey's multiple comparisons (α=0.05, $F_{2,143}$=8.786). C) Among samples that received no subsequent inoculum, relative abundance of pooled 32 Microbacteriaceae ASVs. Samples are separated by their initial inoculation with NB (n=9), 299 (n=7), 303 (n=9), CL18 (n=8), and 136 (n=5). * indicates higher abundance than all other sample types as identified by a 1-way ANOVA with *post hoc* Tukey's multiple comparisons was performed (α=0.05, $F_{4,39}$=3.842). D) Relative abundance of phyla in SynCom subsequent-inoculation samples with NB, 299, 303, CL18, and 136 initial-inoculation root samples (n=11-16) and SynCom inoculum composition (Inoc) (n=3). E) Relative abundance of phyla in SoilSup subsequent-inoculation root samples with NB, 299, 303, CL18, and 136 initial-inoculation (n=3-11) and SoilSup inoculum composition (Inoc, n=3).

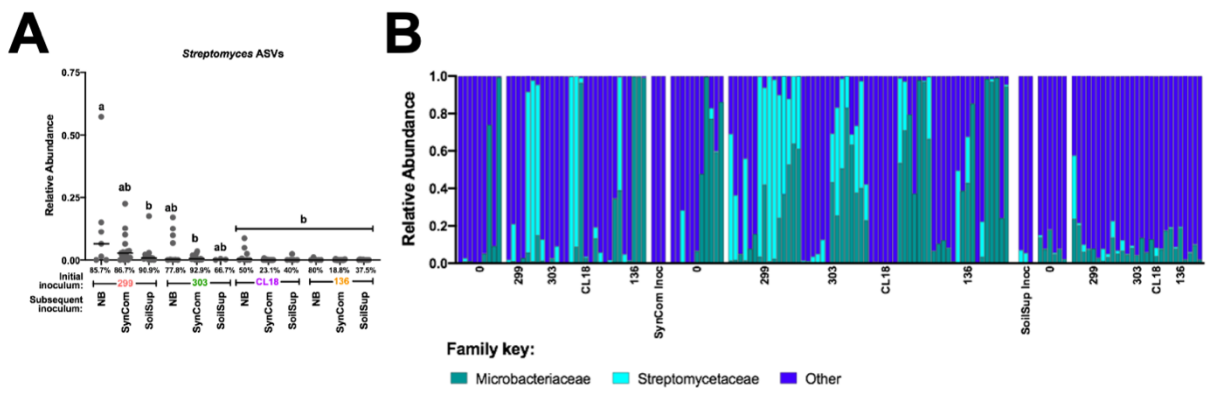

Figure 3. 8: Distributions of Actinobacteria across all treatment groups showing family level relative abundances highlight differences in composition of Actinobacteria.

A) For each *Streptomyces* isolate, the relative abundance of its ASV is shown across the subsequent inocula treatments. A 1-way ANOVA with *post hoc* Tukey's multiple comparison was run (α=0.05, $F_{11,102}$=3.694). Letters indicate significantly different abundances. B) Resulting community relative abundances are shown for samples given subsequent inoculum of no bacteria (NB), SynCom inoculum, and SoilSup inoculum paired with initial inoculum of *Streptomyces* isolates 299, 303, CL18, and 136 and NB. Light blue indicates *Streptomyces* ASVs, blue-green indicates the 32 Microbacteriaceae ASVs not present in SynCom or SoilSup inoculum samples, and dark-blue indicates all other Actinobacteria phyla ASVs.

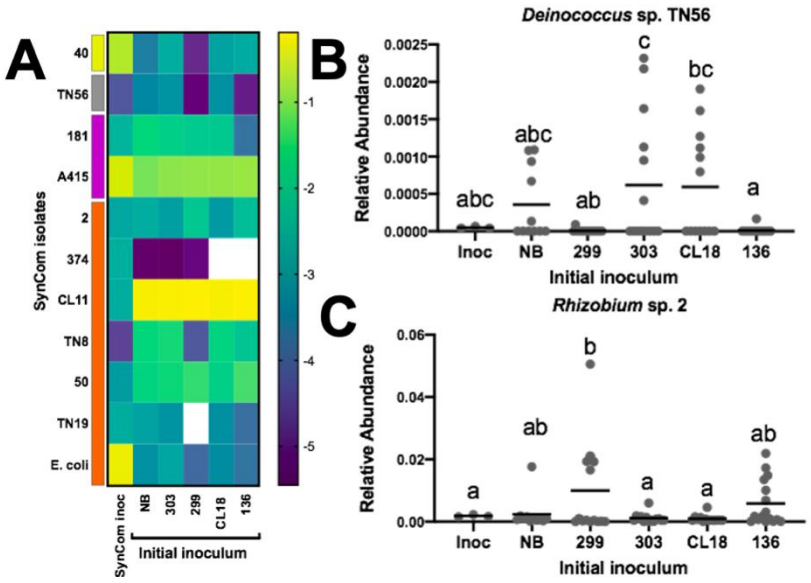

Figure 3. 9: *Streptomyces* pretreatment alters the abundance of individual SynCom members.

A) Heat map of SynCom isolates degree of colonization. The log-transformed abundance of each SynCom member (left label) is shown with the phylum it belongs to denoted by a color block (Bacteroidetes in yellow, Deinococcus-Thermus in grey, Firmicutes in purple, and Proteobacteria in orange). The initial inoculum treatment is shown on the bottom label. White indicates no reads were observed. B-C) Relative abundance of *Deinococcus* sp. TN56 (B) and *Rhizobium* sp. 2 (C) in the SynCom inoculum (n=3) and in assembled root microbiomes from samples initially inoculated with NB (n=11) or with each *Streptomyces* (299 (n=15), 303 (n=14), CL18 (n=13), and 136 (n=16)). A 1-way ANOVA with *post hoc* Tukey's multiple comparison test was performed (α=0.05, $F_{5,66}$=3.857 for B and $F_{5,66}$=2.828 for C). Letters indicate significantly different groups.

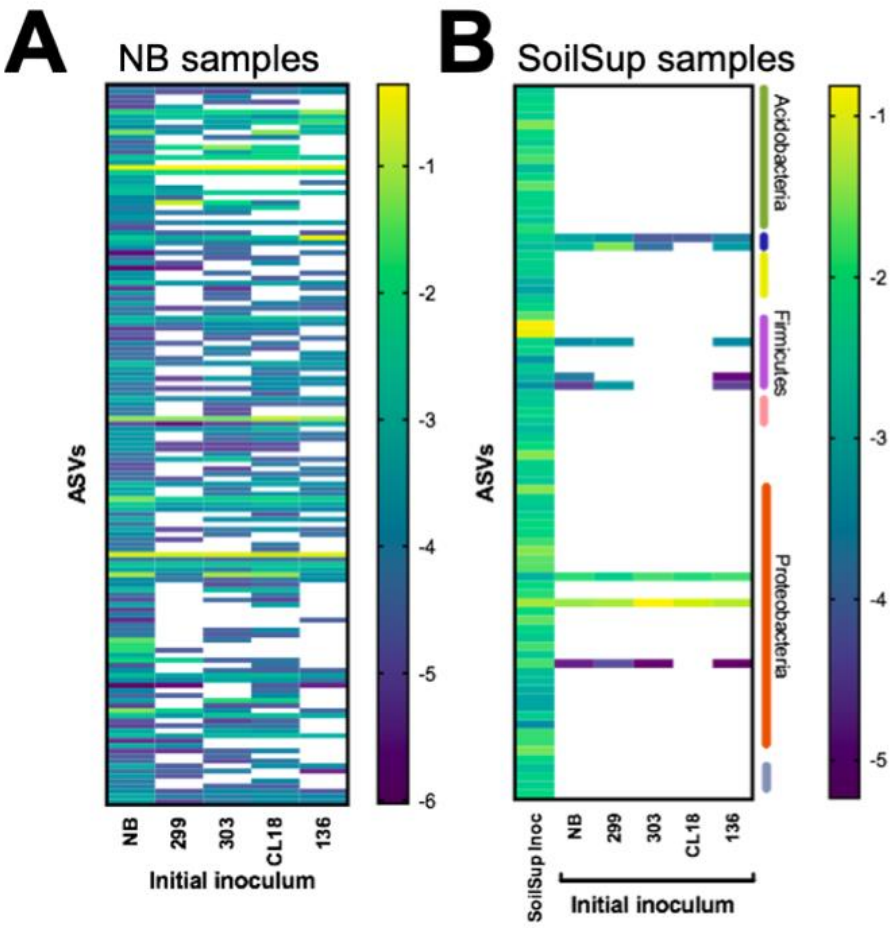

Figure 3. 10: ASV abundance in NB and SoilSup subsequent inoculum samples. A) The log-transformed abundance of each ASV present in samples that received no subsequent inoculum (left label) is shown for each sample treatment group for each initial inoculum (bottom label). B) The log-transformed abundance of each ASV present in the SoilSup inoculum (left label) is shown in the inoculum, as well as mature root microbiomes for samples from each initial inoculum treatment group (bottom label). White indicates no reads were observed for that ASV in that sample type for both heat maps.

CHAPTER FOUR: INVESTIGATING THE IMPACT OF INDIVIDUAL BACTERIAL STRAINS ON *LEMNA MINOR* MICROBIOME AND ITS SURROUNDING WASTEWATER MICROBIAL COMMUNITIES

A VERSION OF THIS MANUSCRIPT IS IN PREPARATION FOR SUBMISSION.

David L. Grant, Jyotirmoy Mondal, Bridget S. O'Banion, Andrew Willems, Barry Bruce, Sarah L. Lebeis

AUTHOR CONTRIBUTIONS

Duckweed wastewater collection was performed by DG and JM. Duckweed maintenance and growth was performed by JM. Duckweed and DAB association experiment was performed by DG and JM. DNA extraction was performed by DG with the assistance of JM. BSO and AW performed analysis of duckweed 16S data. Experiments were conceived by DG, JM, BSO, and SLL.

ABSTRACT

Duckweed is an aquatic plant that is gaining recognition for wastewater remediation by removing excess nutrients. Duckweed is a potential candidate to help alleviate the harmful effects of fertilizer runoff and eutrophication of water sources. Here we explore how bacteria isolated from duckweed tissue, Duckweed Associated Bacteria (DAB), impact duckweed physiology. In this study, DAB representatives from phyla Actinobacteria, Firmicutes, and Proteobacteria with variable Biosynthetic Gene Clusters (BGC) ranging from 4-12 BGCs in an individual isolate were inoculated with duckweed to observe their individual impacts on duckweed microbial communities. Duckweed was grown in wastewater liquid with water and duckweed tissue collected over time to highlight dynamic changes in microbial community with the presence or absence of duckweed. We observed that the addition of duckweed and DAB changes the microbial community of the ambient water. The presence of duckweed along with at least one DAB alters wastewater microbiomes and impacts microbial membership. However, we did not see an additive effective of combing multiple DAB together on duckweed efficiency. We also see a selective process of duckweed with a low diversity in tissue-associated samples. Overall, we investigate the ability of duckweed to make changes to the microbial membership of a wastewater environment and the impact that DAB have on this ability. These studies provide a critical baseline for our future RNA-sequencing results to explore gene expression differences in plant and DABs following colonization.

INTRODUCTION

Agricultural advances drastically improved the human population's ability to sustain itself. Crop yield enhancement through the use of chemical fertilizers and pesticides during the green revolution in the 19th and 20th centuries provided humanity with the means to feed an ever-growing population [1-3]. Specifically, agricultural industrialization helped sustain healthy human diets by improving vegetable and fruit yields by protecting them from disease and via promoting their growth [2]. In this way, fertilizers and pesticides are critical in our ability to maintain food supply and their role cannot be underestimated in utility. However, the cost of sustaining the human population through these means has caused a dramatic increase in environmental pollution and damage that warrants changes in their usage and for alternatives to be considered [2].

Runoff of chemical fertilizers and pesticides can contaminate freshwater sources and without remediation can be toxic to humans and other natural life [2]. These chemicals often end up accumulating in waste-water reservoirs, and if not appropriately managed will return to natural water sources. Furthermore, the use of nitrogen in fertilizer is currently in excess of that which is necessary, resulting in extra nitrogen that winds up in these water reservoirs [4]. The runoff of fertilizer with high nitrogen and phosphorous concentrations can stimulate immense microbial growth, causing a depletion of available oxygen in water sources for other organisms. For instance, harmful algal blooms can be the result of fertilizer runoff into water sources where algae reside, depleting oxygen for other microbes and fish organisms [5]. These issues highlight the need for new alternatives to chemicals that are harmful to people and to the environment. Furthermore, it is equally important to remediate current waste generated from these practices.

One proposed method for the bioremediation of wastewater uses the aquatic plant duckweed. Duckweed is a fast growing, fast replicating, aquatic monocot that grows just beneath water surfaces [6-8]. Beyond these characteristics, duckweed is also

a well-studied organism due to its small size and simple architecture that makes it an easy system to work with for plant experiments [9-11]. Furthermore, it can take up phosphorus and nitrogen from its environment, making it ideal for handling the byproducts from fertilizer runoff [8]. Therefore, these reasons make duckweed an ideal organism to test clean ways of bioremediation. However, the potential of duckweed to bioremediate largely depends on the conditions of its environment [12]. Temperature, light, and nutrient supply are factors beyond duckweed control that the plant must have mechanisms in place for handling to be efficient even in non-optimal environments.

To help handle changing environmental conditions, duckweed can use the metabolisms of present bacteria and its surrounding water microbiome to stabilize its own metabolic efficiency [13]. For instance, the role of indoles from bacteria, including aquatic bacteria, has been connected to increased plant growth promotion [14]. Bacterial products that can affect plant physiology, like the phytohormone indole-3-acetic acid, highlight the impact that microbial communities can have on a plant host. Likewise, these products highlight the need for investigation into the mechanisms they employ in manipulating microbiomes to increase host efficiency. A bacterial isolates from duckweed tissue, called Duckweed Associated Bacteria (DAB), include strains that impact plant physiology by interacting with the plant via signal production, such as indole [13]. Here, we look to manipulate a microbial community to observe shifts in duckweed physiology, with potential downstream effects on its ability to uptake excess phosphorus and nitrogen from its environment, as well as to filter pathogens and other toxic compounds from local Knoxville wastewater sources.

Placing duckweed in wastewater not only provides an alternate means for bioremediation but also provides insight into plant-microbe and microbe-microbe interactions. By investigating the interactions between DAB and duckweed, we can better understand the complex mechanisms that promote certain bacteria association over others. Furthermore, we can observe how the inclusion of DAB affects duckweed physiology and the impact on other organisms found in wastewater from those changes.

Ultimately, the goal of this work is to help uncover the effects of DAB on microbiome assembly and duckweed bioremediation efficiency.

MATERIALS AND METHODS

Duckweed and Culture Maintenance

Duckweed, Lemna-370, was grown for 30 days using 1L of Schenk and Hildebrandt (SH) media in 2000mL Fernbach flasks [15]. Bacterial, DAB, cultures were grown for 1-2 days in 10mL LB broth with 1:5 headspace in 50mL falcon tubes at 30°C with shaking. Prior to inoculation of Duckweed, DAB were grown individually in LB for 2 days at 30°C before being suspended in 1X PBS. DAB investigated here include 370.1, RRCA, 9509.4, 2C, and 38E (Table 1).

Wastewater Retrieval

Wastewater was obtained from Hallsdale Powell Utility District (HPUD) in Knoxville, Tennessee. During the treatment process, wastewater arrives as influent and gets filtered to remove large solids from the water. Water then passes through treatment and becomes clarifier effluent once all solids are removed and just before being chlorinated and returned to nature. For these experiments, clarifier effluent taken before the chlorination treatment step was collected as wastewater. Wastewater was retrieved at two timepoints in early Fall (September) 2018 for replicate 1 and in Spring (March) 2019 for replicate 2.

Wastewater microbial community experiment sample collection and processing

Fourteen 2000mL Fernbach flasks of Lemna-370 and DAB cultures were incubated as described above. When Duckweed plants were grown, 100mL of SH media was removed from seven flasks and replaced with 100mL of collected wastewater. The concentration of bacteria in wastewater for each flask was ~1 x 10^4 CFU/mL. Each individual DAB was inoculated into a flask with wastewater and without wastewater. A flask with wastewater and one without were inoculated with a mix of all DAB together. Controls with wastewater and without wastewater were created for

Duckweed without DAB. Controls were also created for wastewater with DAB and no Duckweed in 50mL Falcon tubes. DABs were inoculated at an OD_{600} of 0.005 in respective tubes and the mix of all DAB was made so all DAB together added up to OD_{600} 0.005.

Samples were collected at three timepoints: 4 days, 10 days, and 15 days post-inoculation. For the second replicate, only the timepoints at 4 days and 10 days were used for analysis. To harvest samples, 50mL of liquid was extracted from each flask and 5mL from each control Falcon tube. Approximately 0.25g of Duckweed tissue was also collected from each flask using a flame-sterilized spatula. Tissue and liquid samples were separated from one another and tissue samples were immediately flash frozen in liquid nitrogen and stored at -80°C. Liquid samples were filtered using Millipore 0.22um MCE Membrane filters (ref. GSWP02500) and a Pharmacia FH225V 10 place filter manifold (ref. 80-6024-14). Filters were then placed into microcentrifuge tubes and flash frozen to be stored at -80°C. Qiagen DNeasy Powerwater kits (ref. 14900-100-NF) were used to extract DNA from liquid samples collected on membrane filters. Qiagen DNeasy Powersoil kits (ref. 12888-100) were used to extract DNA from Duckweed tissue samples. Each extraction was performed in triplicate for each sample.

RNAseq and metatranscriptome generation

Arabidopsis thaliana (Arabidopsis) seed were surface sterilized and germinated in the dark at 4°C for 3 days. After germination, axenic seedlings were transferred on to ½ Murashige and Skoog Basal Medium with Gamborg's Vitamins (MS) (MP Biomedicals ref. 2623220) with sucrose media (2.22g/L MS, 8g/L Phytoagar (PlantMedia ref. 9002-18-0), 10g/L Sucrose) and incubated for 7-days in a diurnal 22°C light for 10 hours and 18°C night for 14 hours cycles. After 7 days, DAB isolates *Microbacterium* sp. RU370.1, *Azospirillum* sp. RU38E, and the all-DAB mix (*Microbacterium* sp. RU370.1, *Azospirillum* sp. RU38E, *Microbacterium* sp. RURRCA19A, *Bacillus* sp. 9509.4, *Bacillus* sp. RU2C) were inoculated onto square 100mm x 100mm ¼ MS (1.11g/L MS, 10g/L Phytoagar) with no sucrose plates at an

OD_{600} of 0.01. Five seedlings were then transferred to each square plates and Parafilm was wrapped around the plate. Plates were incubated vertically at the same diurnal cycle for 7 days.

Seedlings were harvested off square plates, transferred to 5mL centrifuge tubes with flame-sterilized tweezers, and water washed 3 time with sterile dH_2O. Seedlings were then transferred to pre-filled 2mL acid washed bead tubes (100um + 4mm Silica, 1.7mm Zirconium, OPS Diagnostics PFMM 4000-100-28). 0.75mL of Ambion TRIzol reagent (15596026) was added to each bead tube and tubes were placed in a Spex Sample Prep Geno/grinder 2010. Samples were homogenized for 2 minutes, then placed on ice for 1 minute until a total of 10 minutes was reached of homogenization at 1000rpm. Once homogenized, liquid was transferred to an Invitrogen Phasemaker tube (A33248) and 200ul of Chloroform was added. Samples were spun down, and the aqueous phase was then transferred to a new microcentrifuge tube. Samples were then run through the Zymo RNA clean and concentrator kit (R1015). Extracted RNA was flash frozen with liquid nitrogen and stored at -80°C until shipped to JGI on dry ice.

Data Analysis

The first duckweed replicate experiment was analyzed using Qiime2 for 16S rRNA gene amplicon sequencing for microbial analysis. Data was imported using the .qza file format using the qiime tools import command. FastQC was used for quality metrics and reads were trimmed by the first 15bp and truncated at 250bp. Metrics that were created include Weighted and Unweighted UniFrac along with ASV abundances across sample type. The SILVA database was used to assign taxonomy for reported ASVs. The second duckweed replicate experiment was analyzed using R packages Dada2, phyloseq, and ggplot. An indicator species analysis was performed using relative abundances of ASVs in each sample, comparing samples by timepoint, wastewater presence, and duckweed presence. 50,000 permutations were run using the R package indicspecies [16]. The analysis identified which ASVs were associated with each specific treatment type. Metatranscriptomes were generated by JGI following

RNA extraction and submission. Metatranscriptomes are included in Proposal 1779 at JGI under the title “Uncovering the composition and function of the aquatic microbiome for duckweeds”.

RESULTS

DAB isolates have varying potentials and identities

The five DAB isolates (370.1, 38E, RRCA, 9509.4, 2C) were obtained from duckweed tissue and were chosen as representatives of phyla commonly found associated with duckweed. Included in the five isolates are 2 Actinobacteria, 2 Firmicutes, and 1 Proteobacteria (Table 4.1). The isolates also have varying GC content, and a variable range of BGCs from 4-12 (Table 4.1, Figure 4.1). Of interest in secondary metabolic potential, isolate 38E contained 3 bacteriocins, more than any other isolate, which are predicted antimicrobial compounds. Also, isolates 9509.4 and 2C both contained a siderophore, iron-chelating compounds for iron sequestration, within their predicted secondary metabolites. Bacteriocins and siderophores both highlight possible compounds involved in microbe-microbe interactions. Isolates 370.1 and RRCA are both predicted to produce the phytohormone IAA (Indole-3-acetic acid), while 9509.4, 2C, and 38E all do not. In this way, each isolate has unique potentials and identifiers to investigate the differences in how they affect duckweed phenotypes and microbiome assembly.

Consistently associated duckweed microbes show changes in plant tissue association

Microbes that consistently associate with duckweed were investigated for changes in relative abundance between? samples. Microbes that are consistently associated with duckweed include members from Actinobacteria, Bacteroidetes, Firmicutes, and Proteobacteria phyla [11]. Water and tissue samples were separated for comparison of abundances of microbes in the bulk media and those that associate with the plant host (Figure 4.2). Replicate 1 and 2 were analyzed separately due to the different seasonal collection times. In replicate 1, Proteobacteria showed higher relative

abundances in tissue samples than surrounding water samples and dominated both sample types (Figure 4.3). Interestingly, Actinobacteria appeared in higher relative abundances in surrounding wastewater than in tissue samples. Bacteroidetes also followed this trend, with the highest relative abundance in samples without DAB. Firmicutes did not show a trend between tissue and water samples but had the highest relative abundances in wastewater samples that contained all DAB (Figure 4.3).

In replicate 2, Actinobacteria and Proteobacteria displayed higher relative abundances overall within plant tissue as compared to the surrounding water across all treatments with and without DAB inclusion (Figure 4.4). This result is in support of previous work that shows these two phyla are often associated within plant species [17]. Conversely, Bacteroidetes and Firmicutes showed higher relative abundances in surrounding water samples and was variable based on DAB inoculum (Figure 4.4). At the family level, Intrasporangiaceae (Actinobacteria) had the highest relative abundances in tissue samples. Members of Azospirillaceae (Proteobacteria) were present in samples inoculated with 38E or all DAB. Bacillaceae (Firmicutes) trended higher relative abundances in water samples, except when inoculated with DAB 38E and no DAB (Figure 4.4). Across the phyla that consistently associate with duckweed, we see variability between tissue and water samples in bacterial relative abundance, indicating some level of selection by the plant for certain bacterial isolates. Furthermore, there is variability between these taxa with different DAB inoculum requiring investigation into what role these isolates are playing in microbial assembly.

Duckweed microbial community shifts are driven by DAB and other factors

While not the major driver of microbial community shifts, DAB do seem to play some role in the community assembly process. Throughout the experiment, duckweed microbial communities were sampled in plant tissue and in surrounding water environments using 16S rRNA gene amplification sequencing on both types of samples at each time point. Numerous factors were identified within each sample that appeared to have an impact on community assembly, including tissue compared to water sample

type, timepoint, and duckweed and DAB presence. In samples with wastewater, there was an expected increase in microbial diversity using Shannon's diversity index (Figure 4.4). Interestingly, in samples with wastewater, the diversity was only higher in tissue when a DAB isolate was also present. In samples without added DAB, the diversity between tissue and water samples is even. This is an interesting result, as we would expect tissue samples to have a lower overall abundance than the surrounding water sample. However, it highlights some effect that the DABs appear to have on the duckweed community assembly process.

Community establishment and membership showed changes across each of the timepoints studied here. Three different timepoints at 4-days, 10-days and 15-days were used to observe community shift over time. These times have been used in previous duckweed community experiments and were chosen with consideration to community establishment, where the minimum incubation time required for DAB is longer than 2 days, and large shifts in community have been observed around 7-days post inoculation [11]. Therefore, using these timepoints allows us to capture these shifts. Interestingly, some species were found to disappear between 4-day and 15-day time points, including all Actinobacterial ASVs. Actinobacteria appear higher in abundance at the 4-day timepoint but gradually decrease, especially in wastewater samples (Figure 4.3). Likewise, Bacteroidetes were generally higher in abundance in 4-day water samples but decrease over time until the 15-day timepoint. Burkholderiaceae also saw decreases in abundance over the course of the experiment for all inoculated samples. In this way, time appears to impact the presence of certain bacterial isolates. However, the mechanisms that drive these community dynamics require further investigation.

The membership of the microbial community in water samples was impacted largely by whether duckweed was present or absent within the system. Similarly, this impact was affected by the presence or absence of the DAB isolate. Proteobacteria, that are high in abundance across most sample types dominated the most in day-15 tissue samples that contained a DAB member, while Proteobacteria was less abundant

in day-15 water samples that contained no DAB or duckweed (Figure 4.3). Firmicutes were found in higher abundances in samples that contained no duckweed. Similarly, Chlamydiae were found in higher abundances in day-15 with no duckweed or DAB present. At day 15, tissue samples with DAB appeared to exclude Bacteroidetes that were present in 4-day wastewater samples. While the presence of DAB appeared to shift community assembly, there was no noticeable change with all DAB together compared to individual strains. Across individual DAB samples, the presence of DAB 2C seemed to impact microbiome composition of tissue and water samples compared to the other DAB isolates across all time points (Figure 4.5). Thus, showing an isolate specific effect on community assembly that depends on DAB isolate and a potential for community control using microbial inoculum.

Indicator species analysis

An indicator species analysis was performed on the second replicate to compare the effects of different treatments and identify which ASVs were indicators of a given treatment. Of interest, Rhizobiaceae ASVs (were identified as indicators (p-value 0.0003) in 4-day and 10-day samples with duckweed. Pseudomondaeae (*Pseudomonas*) ASVs (p-value 0.0031) and Flavobacteriazeae (*Flavobacterium*) ASVs (p-value 0.0206) were indicator species at 4-days but not indicators at 10-days when duckweed was present in the sample. Without duckweed, Pseudomonadaceae was still an indicator organism (p-value 0.0004). Also, at 10-days without Duckweed, Yersiniaceae (*Serratia*) was highlighted as an indicator organism (p-value 0.0039). The changes in which organisms were identified as indicator species throughout the experiment highlights the impact that Duckweed has on microbial members within the community.

DISCUSSION

Here we investigate the impact of duckweed along with DAB in a wastewater environment to alter microbial community structure and in bioremediation. Further, we see that multiple different factors influence the assembly of microbes in duckweed

tissue and in the surrounding water. Of note, timepoint, the presence of duckweed, and the presence of DAB all appear to be factors that affect microbiome structure. Differences were noted between tissue communities and the surrounding wastewater environment, highlighting some level of selection within duckweed for bacterial members within its community. Tissue samples showed a decreased level of diversity compared to water samples. Therefore, it appears as though duckweed is able to exert control over its microbiome and be selective of its membership. And by extension, exert some impact on the surrounding water microbiome.

Across the different time points of samples taken, there are detectable shifts in microbiome composition. Both Actinobacteria and Bacteroidetes showed decreases in relative abundance from day 4 to day 15 samples, indicating an inability on their part to establish themselves as predominant members of the community. This is interesting as both of these taxa are commonly found associated with terrestrial plant species. Proteobacteria grew in abundance from day 4 to day 15, indicating an ability to better establish themselves within the community. The similarity between plant species' microbial communities, such as with duckweed, rice, and other terrestrial plants, have highlighted a role of host tissue in the assembly process. Furthermore, these studies have identified core microbiome assemblies and genetic commonalities such as auxin production for plant growth promotion [11, 18]. Therefore, we wanted to further investigate this assembly and what factors could create shifts in community composition.

The presence of Duckweed along with at least one DAB seemed to carry a large impact on what taxa were able to establish themselves. For instance, Firmicutes seemed to only establish themselves in the absence of duckweed, with increases in relative abundance when across timepoints. Likewise, Chlamydiae showed higher relative abundances at day-15 only in the absence of duckweed and DAB. While Chlamydiae may be symbiotic, due to the potential pathogenic capabilities of these organisms, it is beneficial for duckweed to bioremediate wastewater of organisms like

these in many cases. Thus, indicating duckweed is having some active role in microbial establishment given the differences noted in its presence or absence within the system.

The DAB isolates showed an impact on duckweed microbial community assembly across all time points and sample types. By comparing each community post-inoculation by DAB, there is a shift in community composition in the communities where one of the *Bacillus* strain, 2C, is the inoculum compared to the other DAB inocula. DAB 2C, while not large in secondary metabolite potential, makes a predicted carotenoid terpene that may play a role in microbe-plant association. Overall, this result indicates that the community of microbes that can assemble is in part dependent on microbial inoculum influence.

Duckweed shows a potential to alleviate the presence of potentially pathogenic bacteria within the water samples. Using the indicator species analysis, potentially pathogenic *Pseudomonas* and *Flavobacterium* species were indicators of early 4-day wastewater and later 10-day wastewater samples but not in 10-day wastewater samples with Duckweed present. *Pseudomonas* strains can be pathogenic to human and plant species while *Flavobacterium* can be pathogenic for fish [19, 20]. However, *Pseudomonas* strains can also be beneficial for plants and due to the limitations of this 16S rRNA gene amplicon sequencing, to know if these ASVs are pathogens would require further experimentation. The presence of *Serratia* as an indicator in 10-day wastewater samples only when Duckweed is absent indicates some effect duckweed has on *Serratia* presence. *Serratia* includes species of human pathogens, including *Serratia marcescens* [21]. In this way, Duckweed appears to have a bioremediation effect on wastewater via a decrease in pathogenic bacteria within the community.

The work here focuses two replicates of wastewater data collected in the Fall 2018 and Spring of 2019 separately. Further work is necessary to compare both replicates together and better understand the impact that duckweed can have in bioremediation. Wastewater collected from different seasons also provides an

interesting avenue in observing changes in wastewater composition depending on the time of year. Furthermore, liquid samples were collected from each timepoint and stored to be used for chemical analysis. Thus, allowing us to observe the impact that Duckweed and DAB have on environment chemistry and in the bioremediation of toxic compounds within wastewater.

Future work will investigate the metatranscriptomic data that was generated for specific DAB grown with *Arabidopsis thaliana.* This data, which will include both plant and bacterial transcripts, requires analysis to look at gene expression of these organisms when they are plant associated. Arabidopsis was used for the host organism due to its ease of use in the laboratory setting and the already troubleshot and designed RNA extraction protocols. Also, Arabidopsis phyllosphere and duckweed both have similar bacterial assemblies and further provides a bridge linking the two organisms together for commonalities in plant microbiome assembly across plant species [11].

Overall, this work is an important progression in microbiome research as well as uncovering new bioremediation methods. By utilizing duckweed, we observe changes in microbial community structure of wastewater with the addition of certain growth promoting DAB. While some microbes maintain higher abundances, like Proteobacteria species, others seem to decrease over time, like actinobacterial ASVs. Similarly, the decrease in abundance of Chlamydiae and Firmicutes ASVs highlights a promising bioremediation ability of duckweed to eliminate pathogenic bacteria from wastewater. We also note the selectivity of duckweed with its closely associated microbiome, with drops in microbiome diversity in tissue samples compared to surrounding water. Therefore, duckweed does appear to carry some level of control in microbiome composition that can be affected by the presence of DAB, that could allow it to bioremediate water sources and help to remove harmful organisms within water sources.

REFERENCES

1. Pingali, P.L., *Green Revolution: Impacts, limits, and the path ahead.* PNAS, 2012. **109**(31): p. 12302-12308.
2. Aktar, M.W., D. Sengupta, and A. Chowdhury, *Impact of pesticides use in agriculture: their benefits and hazards.* Interdisciplinary Toxicology, 2009. **2**(1): p. 1-12.
3. Russel, D.A. and G.G. Williams, *History of Chemical Fertilizer Development.* Soil Science of America Journal, 1977. **41**(2): p. 260-265.
4. Good, A.G. and P.H. Beatty, *Fertilizing Nature: A Tragedy of Excess in the Commons.* PLOS Biology, 2011. **9**(8).
5. Heisler, J., et al., *Eutrophication and Harmful Algal Blooms: A Scientific Consensus.* Harmful Algae, 2008. **8**(1): p. 3-13.
6. Smith, M.D. and I. Moelyowati, *Duckweed based wastewater treatment (DWWT) design guidlines for hot climates.* Water Science and Technology, 2018. **43**(11): p. 291-299.
7. Iqbal, J., A. Javed, and M.A. Baig, *Growth and nutrient removal efficiency of duckweed (lemna minor) from synthetic and dumpsite leachate under artificial and natural conditions.* PLOS One, 2019.
8. Paterson, J.B., M.A. Camargo-Valero, and A. Baker, *Uncoupling growth from phosphorus uptake in Lemna: Implications for use of duckweed in wastewater remediation and P recovery in temperate climates.* Food and Energy Security, 2020. **9**.
9. Laird, R.A. and P.M. Barks, *Skimming the surface: duckweed as a model system in ecology and evolution.* American Journal of Botany, 2018. **105**(12): p. 1962-1966.
10. Hillman, W.S., *The Lemnaceae, or duckweeds: a review of the descriptive and experimental literature.* Botanical Review, 1961. **27**: p. 221-287.
11. Acosta, K., et al., *Duckweed hosts a taxonomically similar bacterial assemblage as the terrestrial leaf microbiome.* PLOS ONE, 2020.

12. Hashimi, M.A.A.-. and R.A. Joda, *Treatment of Domestic Wastewater Using Duckweed Plant.* Journal of King Saud University - Engineering Sciences, 2010. **22**(1): p. 11-18.
13. Ishizawa, H., et al., *Community dynamics of duckweed-associated bacteria upon inoculation of plant growth-promoting bacteria.* FEMS Microbiology Ecology, 2020. **96**(7).
14. Gilbert, S., et al., *Bacterial Production of Indole Related Compounds Reveals Their Role in Association Between Duckweeds and Endophytes.* Frontiers in Chemistry, 2018. **6**(265).
15. Yu, C., et al., *Comparative Analysis of Duckweed Cultivation with Sewage Water and SH Media for Production of Fuel Ethanol.* PLOS ONE, 2014.
16. Cáceres, M.D. and P. Lgendre, *Associations between species and groups of sites: indices and statistical inference.* Ecology, 2009. **90**: p. 3566-3574.
17. Lundberg, D.S., et al., *Defining the core Arabidopsis thaliana root microbiome.* Nature, 2012. **488**(7409): p. 86-90.
18. Huang, W., et al., *Host-specific and tissue-dependent orchestration of microbiome community structure in traditional rice paddy ecosystems.* Plant Soil, 2020. **452**: p. 379-395.
19. Barreteau, H., et al., *Human- and Plant-Pathogenic Pseudomonas Species Produce Bacteriocins Exhibiting Colicin M-Like Hydrolase Activity towards Peptidoglycan Precursors.* Applied and Environmental Microbiology, 2009. **191**(11): p. 3657-3664.
20. Nicolas, P., et al., *Population Structure of the Fish-Pathogenic Bacterium Flavobacterium psychrophilum.* Applied and Environmental Microbiology, 2008. **74**(12): p. 3702-3709.
21. Kurz, C.L., et al., *Virulence factors of the human opportunistic pathogen Serratia marcescens identified by in vivo screening.* The EMBO Journal, 2003. **22**(7): p. 1451-1460.

APPENDIX: TABLES

Table 4. 1: Strains used in this study.

Genomes were characterized using IMG to obtain size, GC%, Scaffold number, and secondary metabolic information.

Strain Name	Number	IMG Number	Size (bp)	GC %	Scaffolds	# of genes	BGC	# of genes in BGC	% genes in BGC	Gram Stain
Microbacterium sp. RU370.1	370.1	2608642165	3389976	70.7	10	3224	4	127	3.94	Positive
Azospirillum sp. RU38E	38E	2708742412	3895001	63.55	70	5228	9	164	3.14	Negative
Microbacterium sp. RURRCA19A	RRCA	2710264756	3671865	70.32	15	3507	6	167	4.76	Positive
Bacillus sp. RU9509.4	9509.4	2606217744	3706009	41.18	44	3868	12	324	8.38	Positive
Bacillus sp. RU2C	2C	2708742419	3903958	37.9	53	4189	7	140	3.34	Positive

APPENDIX: FIGURES

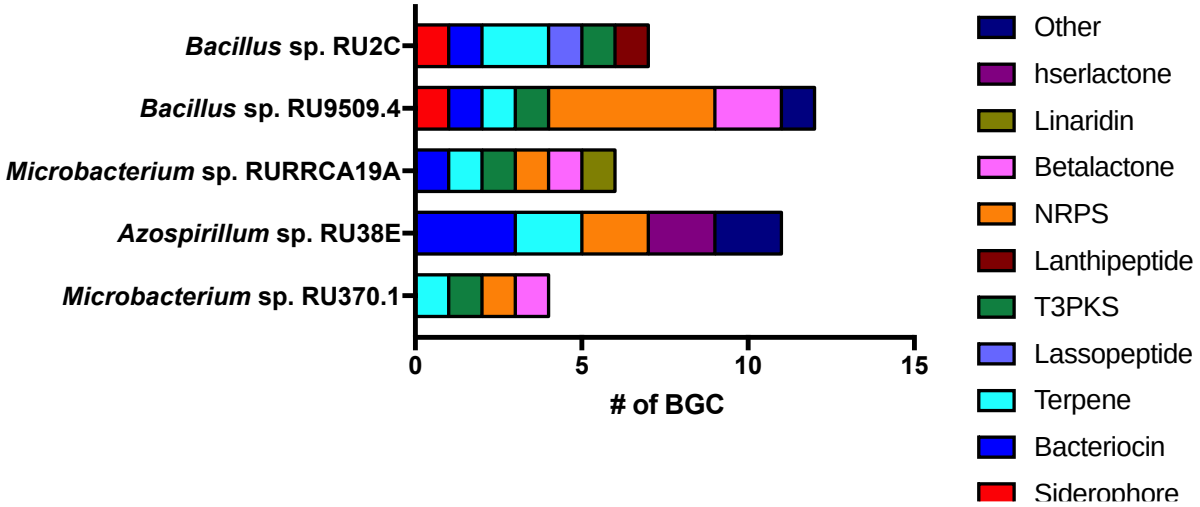

Figure 4. 1:Predicted Biosynthetic Gene Clusters in each DAB.

BGC's predicted using antiSMASH, clusters are shown by predicted compound.

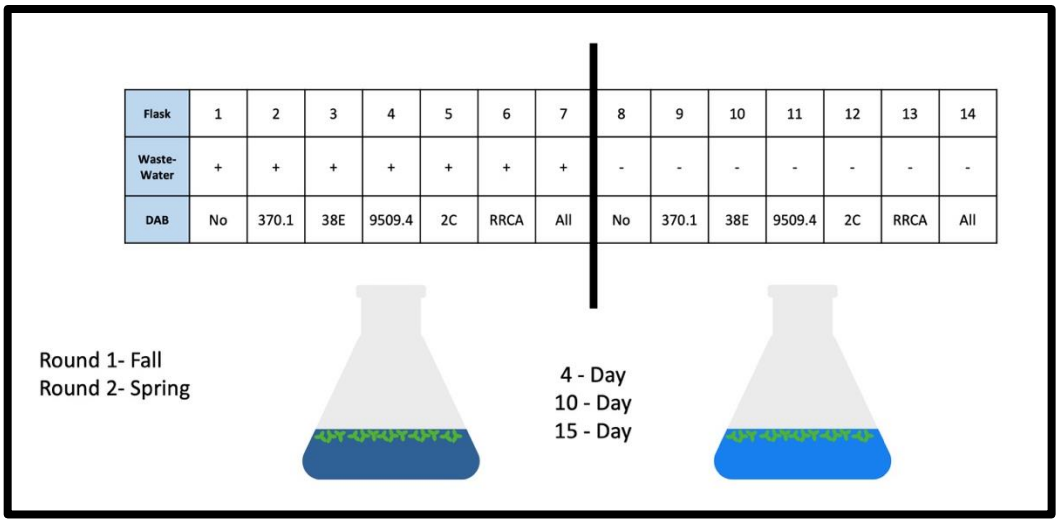

Figure 4. 2:Experimental design of Duckweed experiment.

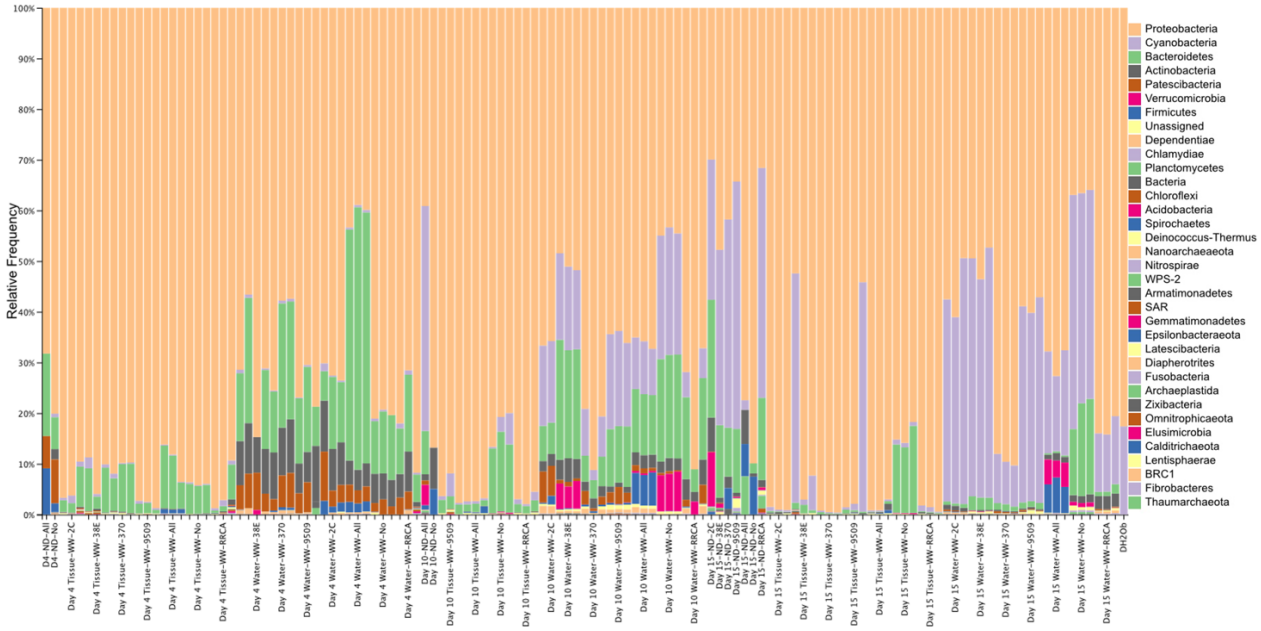

Figure 4. 3: Qiime output of ASVs in each Duckweed sample for replicate 1.

Relative abundance is generated for each sample, using ASVs that are characterized by phylum level.

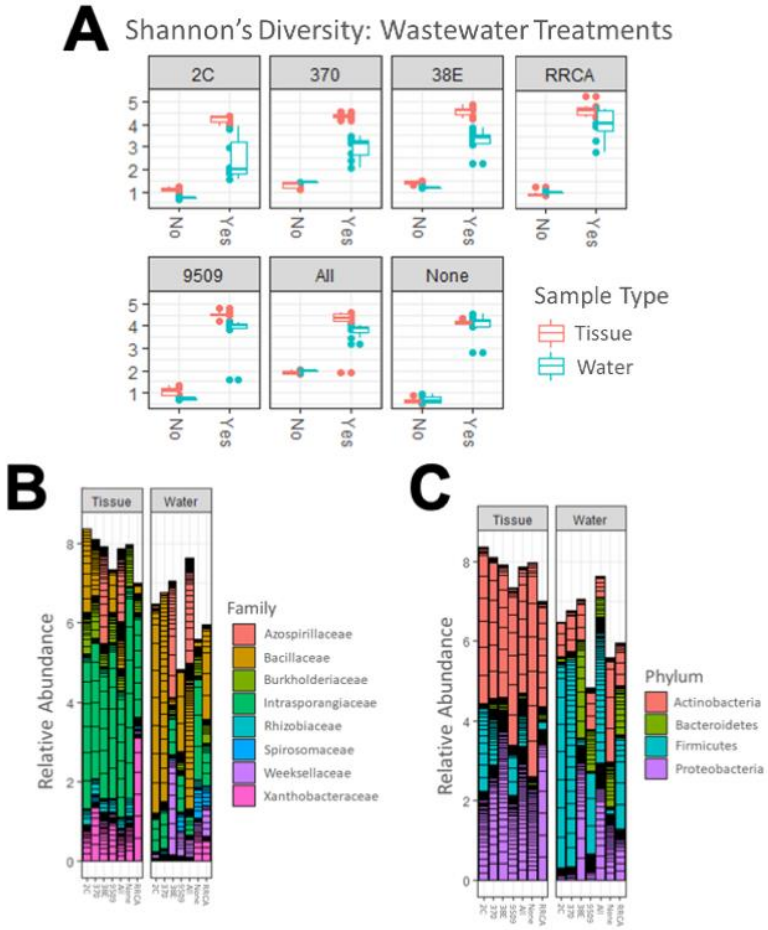

Figure 4. 4: Results from Duckweed experiment replicate 2.

A) Shannon's diversity across all samples, split into different frames based on the isolate treatment. "Yes" and "No" refer to whether Wastewater was added or not. Red/pink represents samples from duckweed tissue, while blue represents samples from the bulk water/media. B-C) The relative abundance of the Top 20 most abundant ASVs across the samples at phylum level (B) and family level (C).

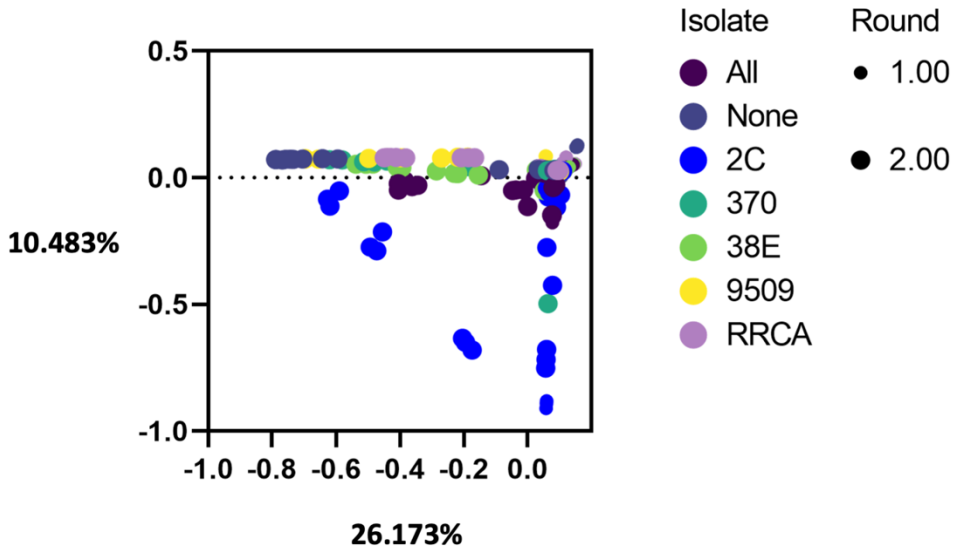

Figure 4. 5: PCoA of tissue and water samples at all timepoints for both duckweed experimental runs.

All DABs (dark purple), no DABs (light purple), and DAB isolates 2C (blue), 370 (green), 38E (light green), 9509 (yellow), and RRCA (pink) were plotted against one another, comparing microbial members within each sample. Small circles indicate the first replicate, large circles indicate the second replicate. X-axis is 26.173% and Y-axis 10.483%.

CHAPTER FIVE: CONCLUSIONS AND FUTURE DIRECTIONS

Importance of Microbiomes

Root microbiome studies constitute a large and consistently growing area of research due to their important ecological roles and functions in plant health and development. Advances in sequencing technology now allow researchers to obtain a much more accurate picture of what bacterial communities look like beyond culturing microbes in the lab [1]. However, microbial membership alone does not tell the whole story of the intricacies involved inside a microbiome. There is still much that remains unknown about the functional aspect within a microbiome and how microbes interact with one another to individually contribute to a community. The microbiomes that associate with a host organism have an additional layer of complexity to understand how their activities impact host health. Thus, numerous studies aimed to characterize the composition and functionalities of microbiomes across a variety of host organisms, including humans, fruit flies, and plants [2-4] with many noting positive effects on the environment and on host organisms, leading to questions of what factors determine the benefits of a microbiome [5, 6]. A better understanding of these beneficial bacterial traits opens the door for new agricultural and industrial systems while obtaining healthier alternatives to current farming practices. However, the functions and intricacies of microbiomes are largely not understood within the context of host-microbe and microbe-microbe relationships that are instrumental in ultimate host benefit.

Host-Microbe Interactions

Understanding how microbes interact with a host organism is critical to establishing the groundwork for enhancing the benefits provided by a microbial community to a plant host. Plants are constantly exposed to new microbes as roots travel through soil environments that host a diverse array of bacterial inhabitants. With bacterial exposure, plants are impacted by metabolic potentials and can have dramatic impacts on the plant including pathogenic or beneficial bacteria. For these reasons, it is necessary for a plant to have some level of control over a microbial community [7]. Therefore, plants possess important systems in place to control rhizosphere community

assembly via direct and indirect methods [8]. For instance, the plant innate immune system and root exudates each display microbiome structuring capabilities, recruiting some microbial members over others within the community [9, 10]. Plants can secrete high amounts of carbon via root exudates into the rhizosphere as nutrients for its microbial members [11]. Studies using roots of tomato, cucumber, and sweet pepper show that they secrete high amounts of organic acid and its rhizosphere community corresponded to organisms that could use those acids as a sole carbon source [11]. Alternatively, plants can secrete inhibitory compounds like benzoxazinoids that inhibit certain microbes [11]. In this way, we see that plants maintain some level of control over community assembly. The goal for this research is to take that understanding of plant microbiome assembly and use it to enhance plant health by assembling a community of beneficial bacteria, providing an alternative to current chemicals in use. To do this requires an understanding of not only the plant's effects on the microbes, but also the many impacts that a plant host receives from its microbiome.

Microbial interactions with a host that can be classified as pathogenic, commensal, or symbiotic based on host health outcomes. Most studied interactions between microbes and plants have focused on either pathogenic behavior of microbes or in a microbe's ability to be beneficial and alleviate abiotic stress [12]. In beneficial bacteria, microbes within a plant community can aid in pathogen defense, remediation, plant growth, and drought tolerance [13]. Other beneficial bacteria, including some *Pantoea* spp., secrete phytohormones, including the auxin compound Indole Acetic Acid (IAA), that are growth promoting for plant hosts [10]. Pathogenic bacteria, such as *Pseudomonas syringae*, secrete phytotoxic compounds that result in plant disease [10]. While there are many defined positive and negative impacts of microbial interactions with a plant, there are also many subtle effects that microbes can have on their plant hosts, including effects on other microbial members. A recent study on plant microbiome diversity found that the loss of even rare microbial taxa decreased plant productivity [14]. Therefore, it is well established that microbiomes can have a large range of impacts on plant host health and overall productivity. However, the complexity

and intricacies of these interactions are largely not understood in a community context which is necessary when attempting to maximize plant efficiency and health with beneficial bacteria.

To address the complexity present in plant-host interactions, I investigated specific genes present in Arabidopsis-associated *Streptomyces* species and in Proteobacteria. Interestingly, organisms harboring pigment producing genes for melanin and a carotenoid showed enhanced plant association. We see that genes encoding pigment producing enzymes provide enhanced survivability against phenolic compounds, many of which are found in soil environments. Therefore, it makes sense that soil-dwelling organisms harboring these genes are provided some advantage. By enhancing survival, we predict that these organisms can therefore interact with a plant host, setting up plant-microbe interactions. Highlighting microbial characteristics that lead to establishing microbe-host interactions. However, being able to associate with a plant host only provides a subset of the interactions, and further work was needed to address how microbes can influence the plant host.

To investigate the direct impact of microbes on a host organism, plant hosts were matched up with their respective associated microbes. *Streptomyces* strains were grown with Arabidopsis to observe changes in root exudates based on strain presence. Depending on the *Streptomyces* strain, different exudate compositions were found, indicating a direct impact of microbial presence on plant phenotype. Furthermore, an aquatic plant system using duckweed and duckweed associated bacteria (DAB) was utilized to investigate the impact of microbes on plant host remediation capability in a waste-water environment. The DAB member present showed alterations in waste-water composition, imparting some effect of microbial member on duckweed phenotype. Members of both *Streptomyces* and DAB can produce the plant phytohormone IAA, which may act as a signal between plant hosts and microbes [15]. Highlighting the impact of host-microbe interactions and the requirement of investigating microbial genes

that enhance association to make more efficient the establishment of beneficial bacteria with a plant host.

Microbe-Microbe Interactions

Beyond host-microbe relationships, there are also numerous interactions between microbes within a community. Microbial communities are often competitive environments where the survival of an organism depends on establishing itself into its desired niche and to have access to required nutrients [16]. While the basis of this is competitive in nature, microbes as individuals may not be competitive and are in many circumstances beneficial to one another [17]. Therefore, highlighting the complexity of a microbial community beyond just interactions with their host and requiring investigation into microbe-microbe dynamics to understand community assembly. Not every community member will act the same in every environment and understanding the relationships of microbes with one another to maximize the efficiency of a microbiome is critical [18].

To address how microbes impact each another in a community, I utilized synthetic communities (SynCom) of microbes in taxa common to soil environments and investigated how they individually interact with one another and in a community setting. SynComs provide us an intermediate level of microbial complexity between bulk soil and single microbe mono-associations to investigate systems with a more informative resolution. SynComs also allow us to control for microbial membership within the system and target specific hypotheses [19]. Setting up *in vitro* microbe-microbe interactions provided a look into the potential of what microbes could either inhibit or benefit others based on nutrient availability, and is a way to help untangle community dynamics [20]. Furthermore, investigation into the genomes of SynCom members highlighted genes to predict potential microbial interactions. By assembling these data together, it provides a functional look into the potential of microbial members to interact with one another that could greatly impact microbiome structure. While focusing on

microbial members together identifies potential, it is equally important to contextualize these interactions in a relevant environment with a plant host.

To further understand how microbial members may interact with each other in a relevant system with a plant host allows for investigation into indirect methods of microbe-microbe interaction. Using duckweed and DAB, we were able to observe how using certain bacterial members can ultimately impact the overall microbial community around the plant host. Thus, highlighting how one microbe can affect the presence or absence of another by affecting plant phenotype. Therefore, we observe that microbiome establishment is a complex web of indirect and direct interactions among microbial members and microbes with the host organism. For this reason, I my work helped untangle these different threads and reveal key interactions so that we might understand the mechanisms behind community assembly and further our knowledge of microbiomes. The ultimate goal that increasing the benefits imparted to a plant host from microbial assemblies will increase plant efficiencies in growth and metabolism for industrial and agriculture purposes.

Importance and Future Directions

As the human population continues to grow and we search for ways to sustain it, we must be mindful of the steps taken to reduce waste and harmful byproducts of our actions while increasing food production [21]. Climate change, human population growth, and higher waste production are all challenges that we will face as we approach the mid-century mark [21]. One such path that shows promise in alleviating the effects of population increase is using microbial organisms to both improve in crop yield and in bioremediation of current waste. Microbes contain a high diversity of metabolic potential that if understood and harnessed effectively, would help to keep food sources sustainable for human life.

The next steps to tackle the compounding issues we are facing will integrate microbes into advancements in agricultural processes as well as in remediation efforts

to clean waste already accumulated. Here, I investigate approaches for tackling each of these problems using the capability of microbial communities with their respective hosts. In order to enhance agricultural yield in sustainable and clean ways for the environment, it is necessary to transition away from chemical fertilizers and pesticides that show toxic effects on the environment and the organisms residing there. A recent study on tea orchards found that chemical fertilizers can leave heavy metals in soil environments and have effects on soil degradation and quality [22]. One such alternative to chemical fertilizers uses bioinoculants comprised of beneficial microbes to enhance host health and increase crop production [23]. However, the benefits of bioinoculants are often inconsistent due to the complexity of interactions that occur between hosts and microbes and between microbial community members. Therefore, it is of benefit to look for ways to enhance bioinoculant efficiency to make it a more viable option for common agricultural products.

For microbial members in bioinoculants to be effective, they must accomplish a few important tasks. First, they must be able to establish themselves with close proximity to the plant host so that any benefit they may impart will be credited to the host. Also, they must impart some benefit to the plant. The most common and easiest to observe is through plant growth promotion. Lastly, they must be able to survive and be metabolically active within a microbial community and ideally impart some control or effect on the community assembly. Understanding all of these characteristics requires a deep dive into both host-microbe and microbe-microbe interactions occurring and understanding the intricacies at play.

Plant growth promoting characteristics within microbes has been largely studied and has identified auxin production among other mechanisms as growth promoting for plant hosts [24]. While genetic determinants have been identified, including the presence of carbohydrate metabolism functionality and the absence of mobile elements, genes that result in effective colonization with a plant host is still largely unknown [25]. To uncover additional factors, I sought to identify genes within *Streptomyces* organisms

that show enhanced levels of colonization. Interestingly, we identified genes encoding tyrosinases that confer melanin-production as potential markers for enhanced association with Arabidopsis hosts. To further investigate this potential mechanism, we will need to generate *Streptomyces* mutants with targeted knockouts and observe root colonization. Establishing this pipeline would further provide a pipeline to test other identified microbial predictors of root microbiome colonization success and how microbe-microbe interactions contribute to successful bioinoculant colonization, both necessary parts of bioinoculant efficiency. While this work benefits the replacement of toxic chemical fertilizers, there is still the issue of already present waste generated by fertilizer and pesticide use.

To help alleviate the waste accumulation caused by toxic chemical fertilizers and pesticides, bioremediation using duckweed and associated bacteria was also investigated. Duckweed has been used in municipal sources and as wastewater treatments in many developing countries as an inexpensive and clean way of handling toxic compounds [26, 27]. However, its effectiveness is inconsistent and reliant on environmental factors, including nutrients, temperature and aeration to maximize growth and Nitrogen and Phosphorus uptake [28, 29]. Therefore, finding ways to enhance duckweed efficiency would make large strides towards bioremediation efforts. Future work using duckweed may focus on the application of a more robust bioinoculant comprised of a larger community rather than single DAB. Furthermore, work will be needed in characterizing the mechanisms behind duckweed remediation and investigating complementary genes in bacteria for inclusion.

Streptomyces and DAB provides a two-way approach at handling the coming issues associated with human population increases. First, to enhance crop production by finding genes associated with enhanced plant colonization and associating. Second, by increasing the effectiveness of a bioremediation approach using duckweed and its DAB community. These approaches harness the incredible capabilities of microbial communities and microbial members to offer clean alternatives for sustainability.

Conclusions

The results outlined in this Thesis highlight the need for future research focusing on *Streptomyces,* and other plant-associating microbes, genetics and performing high throughput techniques to evaluate the necessity of genes for effective Arabidopsis colonization. While *Streptomyces* are hearty organisms and difficult to manipulate genetically, they have a wealth of metabolic potential that remains to be explored, making them an intriguing reservoir of scientific research. Also, their ability to consistently colonize plants and to be found in soil raises questions as to what genes are responsible for these phenotypes. By investigating their genomes, I believe there is an abundance of knowledge to be uncovered that would be useful in bioinoculant tuning. However, future work to establish and employ more molecular biology tools is still required to answer these questions about microbial genetics.

The goal of this work is to help unravel root microbiome dynamics between hosts and microbes and between microbial members of a community. By unraveling these dynamics in this work, we may better equip ourselves to enhance the efficiency of bioinoculants to replace current chemical fertilizer and pesticide use. My hope is to enhance crop yield in clean and effective ways that leverage natural microbial products and to more away from toxic chemicals currently in use. Furthermore, I hope to help clean up the waste that has built up over generations and provide tools to developing regions. In doing so, creating a greater level of sustainability for future generations and safeguarding food resources for human populations.

REFERENCES

1. Koskella, B., L.J. Hall, and C.J.E. Metcalf, *The microbiome beyond the horizon of ecological and evolutionary theory.* Nature Ecology and Evolution, 2017. **1**: p. 1606-1615.
2. Lloyd-Price, J., G. Abu-Ali, and C. Huttenhower, *The healthy human microbiome.* Genome Medicine, 2016. **8**(51).
3. Lundberg, D.S., et al., *Defining the core Arabidopsis thaliana root microbiome.* Nature, 2012. **488**(7409): p. 86-90.
4. Ludington, W.B. and W.W. Ja, *Drosophila as a model for the gut microbiome.* PLOS Pathogens, 2020.
5. Gould, A.L., et al., *Microbiome interactions shape host fitness.* PNAS, 2018. **115**(51): p. E11951-E11960.
6. Martin, A.M., et al., *The Influence of the Gut Microbiome on Host Metabolism Through the Regulation of Gut Hormone Release.* Frontiers in Physiology, 2019. **10**(428).
7. Chisholm, S.T., et al., *Host-Microbe Interactions: Shaping the Evolution of the Plant Immune Response.* Cell, 2006. **124**(4).
8. Qu, Q., et al., *Rhizosphere Microbiome Assembly and Its Impact on Plant Growth.* Journal of Agricultural and Food Chemistry, 2020. **68**: p. 5024-5038.
9. Bulgarelli, D., et al., *Revealing structure and assembly cues for Arabidopsis root-inhabiting bacterial microbiota.* Nature, 2012. **488**: p. 91-95.
10. Compant, S., et al., *A review on the plant microbiome: Ecology, functions, and emerging trends in microbial application.* Journal of Advanced Research, 2019. **19**: p. 39-37.
11. Berendsen, R.L., C.M.J. Pieterse, and P.A.H.M. Bakker, *The rhizosphere microbiome and plant health.* Trends in Plant Science, 2012. **17**(8).
12. Jacoby, R., et al., *The Role of Soil Microorganisms in Plant Mineral Nutrition—Current Knowledge and Future Directions.* Frontiers in Plant Science, 2017. **8**(1617).

13. Jones, P., et al., *Plant Host-Associated Mechanisms for Microbial Selection.* Frontiers in Plant Science, 2019. **10**(862).
14. Hol, W.H.G., et al., *Context dependency and saturating effects of loss of rare soil microbes on plant productivity.* Frontiers in Plant Science, 2015. **6**(485).
15. Gilbert, S., et al., *Bacterial Production of Indole Related Compounds Reveals Their Role in Association Between Duckweeds and Endophytes.* Frontiers in Chemistry, 2018. **6**(265).
16. Bauer, M.A., et al., *Microbial wars: Competition in ecological niches and within the microbiome.* Microbial Cell, 2018. **5**(5): p. 215-219.
17. Boon, E., et al., *Interactions in the microbiome: communities of organisms and communities of genes.* FEMS Microbiology Reviews, 2014. **38**(1): p. 90-118.
18. Pacheco, A.R. and D. Segré, *A multidimensional perspective on microbial interactions.* FEMS Microbiology Letters, 2019. **366**(11).
19. Vorholt, J.A., et al., *Establishing Causality: Opportunities of Synthetic Communities for Plant Microbiome Research.* Cell Host and Microbe, 2017. **22**(2): p. 142-155.
20. Moccia, K., et al., *Distinguishing nutrient-dependent plant driven bacterialcolonization patterns in alfalfa.* Environmental Microbiology Reports, 2020. **12**(1): p. 70-77.
21. Godfray, H.C.J. and T. Garnett, *Food security and sustainable intensification.* Philosophical Transactions of the Royal Society B, 2014. **5**(369).
22. Lin, W., et al., *The effects of chemical and organic fertilizer usage on rhizosphere soil in tea orchards.* PLOS ONE, 2019. **14**(5).
23. Owen, D., et al., *Use of commercial bio-inoculants to increase agricultural production through improved phosphrous acquisition.* Applied Soil Ecology, 2015. **86**: p. 41-54.
24. Tsukanova, K.A., et al., *Effect of plant growth-promoting Rhizobacteria on plant hormone homeostasis.* South African Journal of Botany, 2017. **113**: p. 91-102.
25. Levy, A., et al., *Genomic features of bacterial adaptation to plants.* Nature Genetics, 2018. **50**(1): p. 138-150.

26. Hashimi, M.A.A.-. and R.A. Joda, *Treatment of Domestic Wastewater Using Duckweed Plant.* Journal of King Saud University - Engineering Sciences, 2010. **22**(1): p. 11-18.
27. Iqbal, J., A. Javed, and M.A. Baig, *Growth and nutrient removal efficiency of duckweed (lemna minor) from synthetic and dumpsite leachate under artificial and natural conditions.* PLOS One, 2019.
28. Zirschky, J. and S.C. Reed, *The use of duckweed for wastewater treatment.* Water Pollution Control Federation, 1988. **60**(7): p. 1253-1258.
29. Bonomo, L., G. Pastorelli, and N. Zambon, *Advantages and limitations of duckweed-based wastewater treatment systems.* Water Science and Technology, 1997. **35**(5): p. 239-246.

VITA

David Grant was born in Escondido, California to his parents Greg and Tressia Grant on September 1st, 1995. When he was 7 years old, his family moved to middle Tennessee where they currently reside. He has three older sisters, Lindsey, Jessica, and Jennifer. His interest in science stemmed from interest in the health care field which developed into an interest in microbiology and chemistry.

He attended the University of Tennessee Knoxville and graduated in 2017 with majors in Microbiology and Chemistry. Even then, he had a hard time making a decision between two great choices and his instinct was to just do both. He found his microbiology labs incredibly interesting and the independent work in some of them as fuel to pursue scientific research. In the Spring of 2016, he stared working in the Lebeis lab as an Undergraduate researcher. He loved getting to do independent science and the people he got to work with in the lab. It was a major growing experience and by the time he graduated in 2017 he wasn't sure what was next but new he enjoyed research and wanted to keep it up. He continued working in the lab as a research specialist where he got to develop more lab workflow skills and responsibilities that he enjoyed.

After enough time had passed, Sarah proposed turning all of the knowledge and experience gained into a degree. So, David stayed in the lab for a couple more years to work on his Masters and continue getting to do research. With his degree, he hopes to return to healthcare in some capacity.